



This is to certify that the
dissertation entitled

NEURODYNAMICS OF EPISODIC MEMORY
CONSOLIDATION

presented by

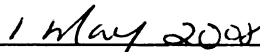
JEREMY LEE SMITH

has been accepted towards fulfillment
of the requirements for the

PH.D. degree in NEUROSCIENCE



Major Professor's Signature



Date

MSU is an affirmative-action, equal-opportunity employer

PLACE IN RETURN BOX to remove this checkout from your record.
TO AVOID FINES return on or before date due.
MAY BE RECALLED with earlier due date if requested.

DATE DUE	DATE DUE	DATE DUE

508 K:\Proj\Acc&Pres\CIRC\DateDue.indd

NEURODYNAMICS OF EPISODIC MEMORY CONSOLIDATION

By

Jeremy Lee Smith

A DISSERTATION

**Submitted to
Michigan State University
in partial fulfillment of the requirements
for the degree of**

DOCTOR OF PHILOSOPHY

Neuroscience

2008

ABSTRACT

NEURODYNAMICS OF EPISODIC MEMORY CONSOLIDATION

By

Jeremy Lee Smith

The present study endeavored to implement conventional fMRI analyses and two novel approaches to BOLD signal characterization with consolidation – Shannon entropy and voxel-response cross-correlation with task (VTCC) – to assess the brain's ability to optimize memory network assemblies with consolidation. In this dissertation the current state of the episodic consolidation literature is reviewed. These concepts are then related to the anatomy and functional architecture of episodic memory systems. Past and present fMRI and electrophysiological methodologies are also discussed and related to the study of physiological changes in the memory system with consolidation.

A paired-associate task was used to examine changes in functional modularity and connectivity with episodic memory consolidation. This task required subjects to learn to associate visually presented words with abstract pictures, then identify correctly-matched, incorrectly-matched, and control pairings during a testing session. A hypothesized improvement subject recall performance with consolidation was not substantiated, but instead remained level between pre- and post-consolidation subjects, suggesting that access to the memory traces remained approximately constant over the consolidation interval despite network changes. Improvements in performance were correlated with decreased recruitment of premotor cortex and visual areas V2, V3, and V4, but not

medial temporal, primary motor, or primary visual cortices. Changes in activation volume, BOLD signal magnitude, the mean correlation between activated voxels and the paired-associate task, and BOLD signal Shannon entropy, were also assessed. The present findings indicate that neurons still participatory in trace retrieval were individually more active than their pre-consolidation counterparts, that BOLD signal entropy increased with consolidation in perirhinal cortex and in components of the ventral visual stream, and, moreover, that BOLD signal response rates increased significantly with consolidation in all areas except left hemisphere primary motor cortex. These findings are discussed in the context of basic scientific research in memory network dynamics, as well as the methodological contributions to neuroscience.

Copyright by
JEREMY LEE SMITH
2007

ACKNOWLEDGEMENTS

The author wishes to thank Mrs. Katey Smith, Mr. William Smith, Ms. Barbara Parker Smith, Mr. and Mrs. Donald and Marcia Brown, Mr. Kenneth M. Cobb, and Dr. Craig Branch for their ongoing support during the writing of this dissertation; Drs. Alessandra M. Passarotti, Laura Symonds, Sue Barman, Christine Larson, David Zhu, Jerry Gebber, and Cheryl Sisk for indispensable advice and guidance; Dr. David Zhu, Mr. Jeremy Grounds, and Mr. Dave McFarlane for unrelenting patience and assistance with daily technical issues; Dr. Matt Hoptman, for critical feedback on this manuscript; and the students and faculty of the Neuroscience Program, without whose encouragement and helpful comments this work would likely have suffered exceedingly.

TABLE OF CONTENTS

LIST OF TABLES	VIII
LIST OF FIGURES	X
LIST OF FIGURES	X
EPISODIC MEMORY AND MEMORY CONSOLIDATION	1
Connectivity and Functional Architecture in Episodic Retrieval.....	4
Declarative memory: the semantic and episodic systems	5
Role of other memory systems in episodic retrieval.....	10
REGIONS OF INTEREST	13
Premotor cortex as a visuospatial attention area	17
Visual areas	18
Primary motor cortex: a control area	20
FMRI SPATIAL AND TEMPORAL SPECIFICITY	21
BOLD signal physiology	21
Spatiotemporal resolution of FMRI.....	23
Modeling the hemodynamic response functions	26
AIMS AND THEORETICAL TREATMENT OF CONSOLIDATION	
NEURODYNAMICS	27
Consolidation as an optimizing process.....	28
Evidence for interim physiological changes in retrieval substrates	30
Computational efficiency and cortical demands: activation volume and entropy	32
Cortical reinstatement and retrieval orientation effects in visual and medial-temporal areas	35
HYPOTHESES	38
METHODOLOGY	43
Subject pool and participants	43
Paradigm	44
Data acquisition	47
Behavioral analysis	48
Modular analysis	49

Deconvolution	49
Percent BOLD signal change from baseline	52
Activation volume.....	53
Voxel-task cross-correlation.....	54
Shannon entropy of the voxel time series	55
 MEMORY CONSOLIDATION AND RETRIEVAL PERFORMANCE: EFFECTS OF STIMULUS MODALITY AND PAIR CONCORDANCE	 59
Behavioral results	61
Reaction time.....	62
Accuracy.....	63
Changes in BOLD Physiology with Consolidation.....	71
ROI analysis of metabolic demand.....	71
ROI analysis of cortical recruitment	73
ROI analysis of BOLD response rate.....	75
Retrieval orientation and cortical reinstatement: Interpretation of Physiological Findings in the Context of Signal Entropy.....	78
 NEURODYNAMICS OF EPISODIC MEMORY CONSOLIDATION: CONCLUSIONS AND DISCUSSION	 85
Effects of stimulus modality and testing interval on task performance.....	87
Disparity between behavioral predictions and findings.....	87
Theoretical reconsolidative basis for the non-Kamin Ebbinghaus exception	89
Interpretation of Metabolic Demand, Recruitment, and Signal Response Rate.....	93
Disparity between physiological predictions and findings	93
Caveats of the entropy metric	100
Theory: Cortical reinstatement and Retrieval Orientation.....	101
Possible cortical reinstatement effects	103
Closing remarks.....	105
 APPENDIX A: ANOVA TABLES FOR BEHAVIORAL DATA.....	 107
 APPENDIX B: MAIN-EFFECT ANOVA AND POST-HOC RESULTS FOR PHYSIOLOGICAL STATISTICS.....	 109
 APPENDIX C: DECONVOLUTION COMMAND LINE	 134

LIST OF TABLES

Table 1 Projections to the perihippocampal regions (Lavenex and Amaral 2000). Abbreviations: <i>PPC</i> , posterior parietal [association] cortex; <i>SSC</i> , somatosensory cortex; <i>OFC</i> , orbitofrontal cortex; <i>PFC</i> , prefrontal cortex; <i>STS</i> , superior temporal sulcus; <i>TE</i> , <i>V4</i> , visual areas TE and V4.	8
Table 2 Regions typically involved in episodic retrieval tasks. <i>LH</i> , left hemisphere; <i>RH</i> , right hemisphere; <i>BL</i> , bilateral. Several of these regions will be used as target ROIs in the present study (see next chapter).	12
Table 3 Summary of the <i>hypotheses</i> for the present study.	41
Table 4 Summary of the <i>predictions</i> for the present study with respect to subject performance (reaction time and accuracy), as well as physiological descriptions of the shape and temporal characteristics of the BOLD signal on the delayed match-to-sample portions of the paired associates task. Both behavioral and physiological findings are represented as being greater (+), less (–), or equal (no change, N/C) in post-consolidation subjects relative to pre-consolidation subjects. Abbreviations: <i>HC</i> , hippocampus, <i>ERC</i> , entorhinal cortex, <i>EcRC</i> , ectorhinal cortex, <i>PRC</i> , perirhinal cortex, <i>V1</i> , <i>V2</i> , <i>V3</i> , visual areas 1-3, <i>FUSI</i> , fusiform gyrus, <i>MI</i> , primary motor cortex, <i>PMC</i> , premotor cortex; <i>RT</i> , subject reaction time, <i>Acc</i> , accuracy; <i>BOLD mag.</i> , percent BOLD signal change from baseline, <i>recruitment</i> , cortical recruitment (activation volume), <i>BOLD rate</i> , BOLD signal response rate (evaluated by the voxel-task cross-correlation, VTCC). Hypothesis 4 (H4), which predicts a predominance of right hemisphere activation in post-consolidation subjects, is not included in the table.	41
Table 5 A qualitative review of the results presented in the present chapter and the conclusions drawn from them. “Per-neuron activity” was determined by dividing the metabolic demand (PC) of an ROI by the extent of its recruitment (AV) to obtain a rudimentary $\Delta P/\text{mm}^3$ estimate. Abbreviations: <i>N/C</i> , no change; <i>fusi.</i> , fusiform gyrus; <i>Vx</i> , visual area x.	84
Table 6 Summary of the predictions (“Predicted”) and findings (“Actual”) for the present study with respect to subject performance (reaction time and accuracy), as well as physiological descriptions of the shape and temporal characteristics of the BOLD signal on the delayed match-to-sample portions of the paired associates task. Both behavioral and physiological findings are represented as being greater (+), less (–), or equal (no change, N/C) in post-consolidation subjects relative to pre-consolidation subjects. Abbreviations: <i>HC</i> , hippocampus, <i>ERC</i> , entorhinal cortex, <i>EcRC</i> , ectorhinal cortex, <i>PRC</i> , perirhinal cortex, <i>V1</i> , <i>V2</i> , <i>V3</i> , visual areas 1-3, <i>FUSI</i> , fusiform gyrus, <i>MI</i> , primary motor cortex, <i>PMC</i> , premotor cortex; <i>RT</i> , subject	

reaction time, *Acc*, accuracy; *BOLD mag.*, percent BOLD signal change from baseline, *recruitment*, cortical recruitment (activation volume), *BOLD rate*, BOLD signal response rate (voxel-task cross-correlation).....86

LIST OF FIGURES

- Figure 1 Connections of the rhinal and perihippocampal cortices. PHC, perihippocampal cortex; PRC, perirhinal cortex; EcRC, ectorhinal cortex; ERC, entorhinal cortex; HC, hippocampus. Adapted from (Lavenex and Amaral 2000) and (Save, Nérard and Poucet 2000).....7
- Figure 2 (A) Interconnections among constituent regions of the MTL and other areas of interest in the present study. Blue arrows indicate neuronal projections between areas as determined by anatomical studies of the cortex and temporal lobe. Arrow locations do not accurately reflect the anatomical location of interregional projections (Sources: Deacon, Eichenbaum, Rosenberg and Eckmann 1983; Schacter, Buckner, Koutstaal, Dale and Rosen; Burwell and Amaral; Burwell and Amaral; Lavenex and Amaral; Save and Poucet 2000a; Save and Poucet 2000b). (B) The anatomical locations of MTL areas in the Talairach-Tourneaux template brain, obtained from the AFNI suite's Talairach Daemon. *Abbreviations: LH*, left hemisphere; *RH*, right hemisphere; *ctx.*, cortex; *BA*, Brodmann area.16
- Figure 3 The training/testing paradigm for the present study. Stimuli consisted of 20 non-rehearsable, non-generalizable abstract pictures paired with animal nouns. Word stimuli were presented either audibly (computer-based training/testing) or visually (fMRI training/testing). Following a training session, during which the correct pairings of stimuli were learned, subjects were tested on their recall either immediately (pre-consolidation time point; 50% of subjects) or 7 days after training (post-consolidation time point; 50% of subjects). For the purposes of testing, subjects were presented with 33 correctly-matched, 33 incorrectly-matched, and 34 control (scrambled) stimulus pairs, and subjects were required to identify each type correctly by button press.44
- Figure 4 (A) Example of a paired associate as presented for the fMRI version of the training/testing paradigm: note that the word component of fMRI training and testing associates was presented below the abstract visual component. The centroid of the presented paired associate was positioned in the center of the subjects' field of view. (B) A schematic of a single run from the fMRI testing paradigm: match, mismatch, and control-condition stimuli were presented with a constant interstimulus interval of 12.5 seconds. Presentation order was randomized across the three types of stimuli; *x*-axis represents TR (1 TR = 2.5 seconds).46
- Figure 5 Mean reaction times for the paired-associate task by testing group (computer-based, CBT, versus fMRI subjects), pair concordance (matched, mismatched, or control), and time point (pre- versus post-consolidation). fMRI subjects, who were given unimodal (visual) training and testing stimulus pairs, were slower at identifying both correctly-matched and mismatched stimulus pairs than CBT subjects, who were given dual-modal (visual and auditory) training and testing

stimulus pairs. This effect was seen at both pre- and post-consolidation time points. However, neither fMRI nor CBT subjects were significantly faster at identifying correctly-matched stimulus pairs after one week. Neither group improved with respect to reaction time with consolidation for control stimuli, nor did CBT and fMRI subjects differ significantly with respect to reaction time for control stimuli at either time point. Error bars represent standard errors of the means. * $p < .05$62

Figure 6 Mean subject accuracy for the paired-associate task by testing group (computer-based, CBT, versus fMRI subjects), pair concordance (matched, mismatched, or control), and time point (pre- versus post-consolidation). fMRI subjects, who were given unimodal (visual) training and testing stimulus pairs, were more likely to identify mismatched associates as matched associates (exhibited more false positives) than CBT subjects, who were given dual-modal (visual and auditory) training and testing stimulus pairs. However, neither fMRI nor CBT subjects improved with respect to the number of false positives over the putative memory consolidation period, nor did either group improve with respect to accuracy with consolidation for matched associates (false negatives) or control stimuli. CBT and fMRI subjects did not differ significantly with respect to accuracy for correctly-matched associates or control stimuli at either time point. Symbols (light grey) indicate individual data points; error bars represent standard errors of the means. * $p < .05$; ** $p < 0.01$65

Figure 7 Group statistical parametric maps (SPMs) of voxel BOLD signal correlation with presentation of match, mismatch, and control-condition stimuli by region of interest. Voxel BOLD signal changes shown are significant at a full-model $F = 3.786$ ($p = 0.001$, corrected); colors represent whether changes are positive (yellow) or negative (blue) relative to the baseline. Group SPMs were obtained by studentizing individual BOLD datasets and registering them to a common Talairach-Tourneaux coordinate system (Talairach and Tourneaux, 1988). Datasets were then subjected to cluster analysis using a minimal 5mm, 10µl Gaussian kernel (to correct for type II error: see Salmond, Ashburner, et al. 2002; Geissler, Lanzenberger, et al. 2005) and averaged by condition. The location of the calcarine fissure (visual area V1) is shown on an axial slice in each case for reference (yellow boxes). Hemodynamic response functions for representative subjects were also obtained for ectorhinal area 36 (red box) and visual area V3/19 (green box) and are shown in Figure 9. *Abbreviations:* *Fus*, fusiform gyrus; *Ins*, *AIC*, anterior insular complex; *STG*, superior temporal gyrus; *IPL*, inferior parietal lobule; *SPL*, superior parietal lobule; *DG*, dentate gyrus; *pul*, pulvinar nucleus of the thalamus, *Ver*, cerebellar vermis, *Cal*, calcarine fissure. *Numbers* represent Brodmann areas: *3a*, digit somatosensory area; *4*, digit motor area; *31*, posterior cingulate cortex.....67

Figure 8 Estimated event-related average hemodynamic response functions (HRFs) for pre- (dotted line) and post- (solid line) consolidation right hemisphere ectorhinal cortex (EcRC, Brodmann area 36) and visual area V3 (Brodmann area 19) seed locations indicated in Figure 7. HRFs were obtained from the same studentized representative subject data as in Figure 7. Talairach-Tourneaux coordinates for each region are also given (see Talairach and Tourneaux, 1988).....69

Figure 9 Percent BOLD signal change from baseline (BOLD signal magnitude) in significantly task-correlated voxels constituting regions of interest at pre- and post-consolidation for matched associates. Analysis by main effect ANOVA indicated a significant difference in BOLD magnitude between pre- (T1) and post- (T2) consolidation subjects ($p < 0.001$) overall, however, post-hoc analysis by Tamhane T2 failed to indicate any differences in per-region signal change with consolidation. These findings suggest that the BOLD response magnitude is not affected by consolidation in significantly task-correlated voxels in these regions. Error bars indicate standard errors.72

Figure 10 Activation volume of significantly task-correlated voxels at pre- and post-consolidation for matched associates. Analysis by main effect ANOVA indicated a significant difference in activation volume between pre- and post-consolidation subjects overall ($p < 0.001$). Post-hoc analysis by Tamhane T2 further indicated significant reductions in cortical recruitment in the fusiform gyrus, premotor cortex, and visual areas V2 and V3. These findings suggest that the number of significantly task-correlated voxels is affected by consolidation in premotor areas, area V2, and ventral visual areas, but not in medial temporal, primary motor, or primary visual areas. Error bars indicate standard errors; *indicates a significant difference in activation volume, $p < 0.05$. ROI significances computed by post-hoc Tamhane T2.74

Figure 11 Mean voxel BOLD response-stimulus presentation covariance (voxel-task cross-correlation, VTCC) in significantly task-correlated voxels constituting regions of interest at pre- (T1) and post- (T2) consolidation for matched associates. Analysis by main effect ANOVA indicated a significant difference in VTCC between pre- and post-consolidation subjects overall ($p < 0.001$), and post-hoc analysis by Tukey HSD revealed significant differences in VTCC in all areas ($p < 0.05$). These findings suggest that the BOLD-task covariance is affected by consolidation in significantly task-correlated voxels in medial temporal, motor, premotor, and visual regions. Error bars indicate standard errors; *indicates a significant difference in VTCC, $p < 0.05$. ROI significances computed by post-hoc Tukey HSD unequal-N test.76

Figure 12 Mean BOLD signal Shannon entropy (TSE) in significantly task-correlated voxels constituting regions of interest at pre- and post-consolidation for matched associates. Analysis by main effect ANOVA indicated a significant difference in BOLD TSE between pre- and post-consolidation subjects overall ($p < 0.001$). Post-hoc analysis by Tamhane T2 further indicated significantly greater signal entropy in the fusiform gyrus and visual areas V2 and V3 ($p < 0.01$). These findings suggest that the BOLD signal entropy is affected by consolidation in significantly task-correlated voxels in extrastriate ventral visual areas, but not in medial temporal, premotor, or primary motor or visual cortex. Error bars indicate standard errors; *indicates a significant difference in TSE, $p < 0.01$. ROI significances computed by Tamhane T2.81

KEY TO SYMBOLS AND ABBREVIATIONS

Acc	Accuracy	RH	Right hemisphere
ANOVA	Analysis of variance	ROI	Region of interest
AV	Activation volume	RT	Response time
BA	Brodmann area	Sh	Shannon bits
BOLD	Blood oxygenation level dependent	SNR	Signal-to-noise ratio
CBF	Cerebral blood flow	SPM	Statistical parametric map
CBT	Computer-based testing	T	Tesla
CMRO₂	Cerebral metabolic rate of oxygen	TSE	Shannon entropy of the time series
DMTS	Delayed match to sample	V1	Visual area V1 (etc.)
DNMS	Delayed nonmatch to sample	VTCC	Voxel-to-task cross-correlation (indicative of BOLD signal rate)
dVS	Dorsal visual stream	vVS	Ventral visual stream
EcRC	Ectorhinal cortex	x	Denoised BOLD signal response vector
EEG	Electroencephalography	y	Raw BOLD signal (EPI) response vector
EPI	Echo-planar imaging		
ERC	Entorhinal cortex		
EVVS	Extrastriate ventral visual stream		
FMRI	Functional magnetic resonance imaging		
Hb/dHb	Hemoglobin/deoxyhemoglobin		
HC	Hippocampal formation		
HRF	Hemodynamic response function		
IRF	Impulse response function		
LFP	Local field potential		
LH	Left hemisphere		
LTD	Long-term depression		
LTP	Long-term potentiation		
M1	Primary motor cortex		
MT/V5	Visual area V5/MT		
MTL	Medial temporal lobe		
PC / ΔP	Percent BOLD signal change over baseline		
PET	Positron emission tomography		
PHC	Parahippocampal gyrus		
PHG	Perihippocampal cortex		
PMC	Premotor cortex		
PRC	Perirhinal cortex		
PRS	Perceptual representation subsystem		
R	Pearson product-moment correlation		

EPISODIC MEMORY AND MEMORY CONSOLIDATION

Consolidation refers to the process by which short-term memories are gradually indexed, transferred to cortex, and made permanent (Abel and Lattal 2001; Eichenbaum 2001; Haist, Bowden Gore and Mao 2001). Episodic memories are quite labile until stabilized through this process, which results in stronger connections among the elements (nodes) that are relevant to the memory and weaker connections among elements that are irrelevant to the memory. Neuroimaging and neuropsychological studies have provided reasonable evidence that the consolidation mechanism proceeds in two stages. In the first stage, short-term memory traces are encoded in the hippocampal CA3 region and linked by long-term potentiation to form stable networks. In the second stage, the medial temporal lobe (MTL) and association cortex backprojections, which are Hebb-modifiable by entorhinal θ rhythm entrainment (firing rate coherence: Treves and Rolls 1994; Chrobak and Buzsaki 1998b) are reactivated and reinforced. It is believed that the backprojections themselves drive the “repositioning” of the index of a memory from the hippocampal complex to the frontal lobe over a period of several years (Treves and Rolls 1994; Rolls 2000). The present study encompasses seven days between training on an association task and subsequent testing. Consequently, only Stage I consolidation effects – long-term potentiation of the short-term memory traces, evinced by increased association strength (retrieval efficiency, discussed in a later chapter) between the hippocampus and primary, secondary, and association areas – are expected.

Electrophysiological studies have produced reasonable evidence that particular spectral (frequency-related) changes in the interactions of neural populations occur at this stage, particularly with respect to *coherence* (the correlation between the timing and amplitude of population responses) and spectral power (Bodizs, Bekesy, Szucs, Barsi and Halasz 2002; Cantero, Atienza, Salas and Dominguez-Marin 2002b). At least one neuroimaging study has also demonstrated an overall decrease in the recruitment of brain areas after a period of consolidation (Buchel, Coull and Friston 1999). Both findings corroborate the intuitive prediction of changes due to Hebbian processes: brain regions necessary for learning, such as executive, attentional, and working memory regions, are recruited at the pre-consolidation (encoding) time point, as are regions involved in the perception of peripheral (distractor) stimuli; connections between these regions and the memory network undergo long-term depression, however, and are not activated at the post-consolidation recall time point (Alvarez and Squire 1994; Chrobak and Buzsaki 1998b; Chrobak and Buzsaki 1998a). Electrophysiological studies cannot unambiguously resolve signal sources, however, and thus cannot be used to create a final, systems-level interpretation of mnemonic binding; nor has any functional magnetic resonance (fMRI) study, to the knowledge of the author, attempted to operationalize changes in retrieval efficiency with these measures. The present study therefore endeavors to assess changes in cortical recruitment, metabolic demands, and fMRI signal complexity¹ and rate of change as correlates of memory consolidation.

¹ The terms *complexity*, *entropy*, and *chaoticity* are used interchangeably in the present dissertation, but it should be pointed out that all three terms are used in a *technical* (as opposed to *lay*) sense to refer to the Shannon (information-theoretic) entropy of a signal. More specifically, the Shannon entropy is a quantification for the degree of a vector's unstable aperiodicity. The BOLD time series Shannon entropy (TSE) is described in depth in the "Shannon entropy of the voxel time series (TSE)" section of the *Methodology* chapter; the reader is also referred to Shannon's seminal 1948 paper, *A Mathematical Theory of Communication* (Shannon, C. E. (1948). A mathematical theory of communication. *Bell Sys Tech J* 27:

The consolidation period has been shown to result in the decreased lability of memory traces, increased long-term potentiation (LTP) and firing rate coherence among mnemonic network constituents, and increased long-term depression (LTD) with decreased recruitment among peripheral networks (Bailey, Montarolo, Chen, Kandel and Schacher 1992; Alvarez and Squire 1994; Zhang, Endo, Cleary, Eskin and Byrne 1997; Chrobak and Buzsaki 1998b; Chrobak and Buzsaki 1998a; Buchel, Coull *et al.* 1999; Eichenbaum 2001; Bodizs, Bekesy *et al.* 2002; Cantero, Atienza *et al.* 2002b). Thus, one might expect the memory consolidation interval to serve as a temporal window during which binding and synaptic integration among memory traces are “tuned” to optimal efficiency (see McClelland, McNaughton and O'Reilly 1995; Squire and Alvarez 1995; Chrobak and Buzsaki 1998b; Abel and Lattal 2001; Eichenbaum 2001; Haist, Bowden Gore *et al.* 2001; Ross and Eichenbaum 2006; Wang, Hu and Tsien 2006). This does in fact appear to be the case, as previously-stored memory traces in medial temporal cortex and isocortex are reactivated and entrained to so-called sharp wave-ripple complex oscillations during the presumptive consolidation period of sleep, thus reenforcing synaptic weights (Buzsaki 1998; Siapas and Wilson 1998; Stickgold, Scott, Rittenhouse and Hobson 1999; Datta 2000; Maier, Nimmrich and Draguhn 2003; Gais and Born 2004; Walker and Stickgold 2004).

Conventional wisdom holds that, in spite of this putative consolidation-related mnemonic network optimization, recall performance declines with time, except when the items to be encoded are repeatedly presented; yet research into the neurodynamic consequences of the consolidation phenomenon at the whole-brain level have only recently been undertaken, and many of the published studies on the subject have focused

on the hippocampal, rather than cortical and medial-temporal, contributions to recall. Furthermore, recent experimental manipulations of encoding depth have indicated that subjects who are well-trained to remember specific memory items may exhibit an improved proficiency in *cortical reinstatement*, the reactivation of previously-encoded memory traces, and an improved capacity, or *retrieval orientation*, for processing stimulus features so as to better match them with stored representations, which suggests that the strength of sensory and retrieval-mode binding processes may differentially influence recall performance (Weldon, Roediger and Challis 1989; Rugg and Wilding 2000; Robb and Rugg 2002; Wheeler and Buckner 2003). However, these phenomena have not yet been studied in the context of a between-subjects paired associates task, nor in the context of episodic memory consolidation.

CONNECTIVITY AND FUNCTIONAL ARCHITECTURE IN EPISODIC RETRIEVAL

Demarcations of the various memory systems have classically been established through neuropsychological observation of human patients, notably through experiments with the amnesic patient H.M., and lesion studies in animals (Eichenbaum 1996; Eichenbaum, Dusek, Young and Bunsey 1996; Eichenbaum, Schoenbaum, Young and Bunsey 1996). These data have helped to establish the idea that memory can be dissociated into several cognitive networks, each of which is responsible for a particular type of mental representation of the past. At least five such networks are commonly referred to in the literature: two declarative memory systems (episodic and semantic memory) and the procedural, perceptual, and working memory systems.

Schacter and Tulving have proposed three criteria that a network should meet in order to be considered an independent and complete memory system (Schacter and Tulving 1994). First, the network should be composed of regions that perform interrelated tasks that permit the storage and retrieval of a particular class of information. Second, the network can be characterized in terms of operational qualities that are, as a whole, unique to that network. And third, the operations of the network can be dissociated from those of other networks through ablative or neuropsychological studies.

Based on these criteria, at least five major memory systems have been identified. These include *semantic memory* (long-term memory for facts and concepts, including associative memory for objects and words, independent of an episode in memory), the *perceptual representation system* (long-term, non-associative memory for objects and words), *procedural memory* (long-term habit learning, classification skills, grammatical rules, and sequence memory), *working memory* (short-term retention of information for cognitive problem solving), and *episodic memory* (long-term retention of events: Eichenbaum 1996; long-term retention of events: Eichenbaum, Dusek *et al.* 1996; long-term retention of events: Eichenbaum, Schoenbaum *et al.* 1996; Gabrieli 1998). Many of these five systems can be further dissociated into subsystems, as discussed below.

Declarative memory: the semantic and episodic systems

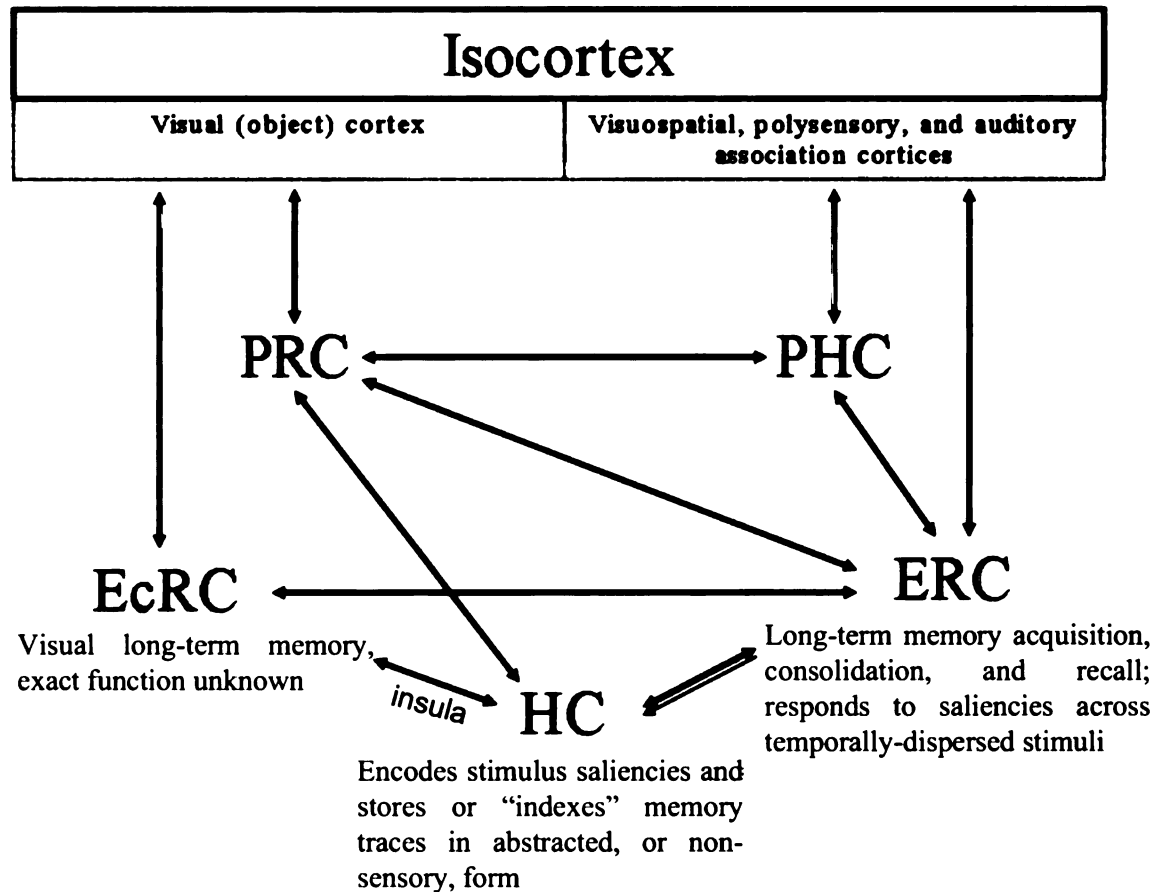
Semantic memory is memory for information in the abstract: factual memory, such as memory about historical events in which the subject did not participate. It is dependent on the medial temporal lobes (MTL; including rhinal cortex and the hippocampal and perihippocampal areas), and the fact that this anatomical division is shared with episodic

memory (discussed below) incorporates semantic and episodic memory into the descriptive heading “declarative memory.” In addition, semantic memory seems to recruit anterior and lateral regions of the temporal lobe in the left hemisphere (Eichenbaum *et al.*, 1996; Gabrieli, 1998).

Episodic memory itself is perhaps the most complex and best understood of the five memory systems. It is involved in memory for events that are the personal experience of the subject, and which are imbued with “warmth and intimacy,” as characterized by William James (James 1893). Like semantic memory, episodic memory has been linked with the MTL, which is comprised by the entorhinal cortex, perirhinal cortex, perihippocampal cortex, perihippocampal gyrus, and the hippocampal formation. The connections of the MTL are extensive; the hippocampus is connected to various unimodal and polymodal association areas through the perihippocampal gyrus and to the thalamus (see Figure 1). Furthermore, prefrontal areas (particularly the ventrolateral prefrontal cortex, precentral sulcus and inferior frontal gyrus; the dorsolateral prefrontal cortex, posterior middle frontal gyrus; and the left anterior prefrontal cortex are engaged during the recall *effort* (ecphory: Buckner, Koutstaal, Schacter, Dale, Rotte and Rosen 1998a; Buckner, Koutstaal, Schacter, Wagner and Rosen 1998b; Ranganath, Johnson and D'Esposito 2003), whereas the hippocampal formation itself is recruited during actual *recall* (Eichenbaum *et al.*, 1996). Right prefrontal cortex, which is involved in attention, has also been disambiguated from episodic retrieval (Cabeza, Locantore and Anderson 2003).

The medial temporal areas have traditionally been classified as subserving novelty detection (recognition: perirhinal and entorhinal cortices and the posterior

Figure 1 Connections of the rhinal and perihippocampal cortices. PHC, perihippocampal cortex; PRC, perirhinal cortex; EcRC, ectorhinal cortex; ERC, entorhinal cortex; HC, hippocampus. Adapted from (Lavenex and Amaral 2000) and (Save, Nerad and Poucet 2000).



hippocampus²), recency judgements (posterior hippocampus), visuospatial learning (medial entorhinal, anterior hippocampus), as well as the association of salient simultaneous or temporally-dispersed stimulus features (declarative associative learning and contextual learning: perirhinal, perihippocampal, entorhinal and ectorhinal cortices and posterior hippocampus) (Winters and Bussey 2005c; Witter and Moser 2006;

2 The functional neuroarchitectural divisions in question differ from quadrupeds to bipeds. The functional differentiation of the hippocampus, originally cited as following a “dorsoventral” axis, has more recently been retooled as following a “septotemporal” axis, since the rodent dorsal hippocampus corresponds to the primate posterior hippocampus, whereas the rodent ventral hippocampus corresponds to the primate anterior hippocampus. See Moser, M. B. and E. I. Moser (1998). Functional differentiation in the hippocampus. *Hippocampus* 8(6): 608-19.

Dudukovic and Wagner 2007; Kerr, Agster, Furtak and Burwell 2007; Kumaran and Maguire 2007). The individual medial temporal areas elude ascription to particular computational operations, however, due not only to the difficulty of constructing tasks that dissociate suppositional functions from each other, but also by the intricate interconnectivity, and therefore interdependence, of these areas (Preston and Gabrieli 2002).

The structure of the perihippocampal region consists of the entorhinal cortex, Brodmann areas 28 and 34; medial (area 35) and lateral (area 36) perirhinal cortex; and the parahippocampal cortex. Information flows from isocortex to the perirhinal and parahippocampal cortex, to the ERC, dentate gyrus, CA3 field, and subiculum, and back to isocortex. Information is initially processed in isocortex and then passed through the entorhinal (ERC), perirhinal (PRC), and parahippocampal (PHC) cortices to the hippocampal complex, where it is presumably optimized. After this optimization, the information is returned to the isocortical area of origin, resulting in long-term memory consolidation. Parahippocampal lesions cause deficits as severe as hippocampal lesions alone, yet the role of areas surrounding the hippocampus, such as the entorhinal cortex, is

Table 1 Projections to the perihippocampal regions (Lavenex and Amaral 2000). Abbreviations: *PPC*, posterior parietal [association] cortex; *SSC*, somatosensory cortex; *OFC*, orbitofrontal cortex; *PFC*, prefrontal cortex; *STS*, superior temporal sulcus; *TE*, *V4*, visual areas TE and V4.

Modality	Projection
TE (visual object information)	PRC
PPC and V4 (visuospatial)	PHC
SSC	Both
Ventrolateral cortex, OFC, cingulate, retrosplenial cortex, PFC, dorsal STS (polysensory cortices)	Both
Auditory association cortex	PHC

distinct from the role of the hippocampus itself. For example, ERC+PRC lesions prevent the formation of mnemonic representations of visually paired associates in the inferotemporal cortex. However, different *areas* of isocortex have different projections to the perihippocampal region as well, resulting in sensory specificity in many areas of the MTL (see Figure 1 and Table 1). Feedback, feedforward, auto- and reciprocal connections result in a conversion of unimodal information to polymodal, supermodal, or amodal information, and allow abstractions in the HC complex before being returned to isocortex.

MTL afferents to unimodal sensory cortex can interact with lower level information processed or stored in unimodal cortex. Efferent projections from entorhinal and perirhinal cortex are necessary for maintenance and consolidation of pair codings in auditory area TE and may be responsible for short-term memory maintenance (since these areas activate during the delay phase of a delayed nonmatch to sample, or DNMS, task). Perirhinal neurons are multimodal and probably encode more than sensory attributes. The entorhinal cortex is less involved in object/sensory analysis and coding than is the perirhinal cortex. These neurons may respond only to simultaneous activation from multiple (multimodal) areas; the ERC, for example, is thought to respond to “compound” stimuli. ERC and PRC θ patterns are coherent during REM sleep, which is thought to participate in memory consolidation. The θ origin is probably driven by the ERC and/or subiculum. The PRC does not get input from the medial septum, the HC/ERC pacemaker, but it does receive inputs from the neurons in the deep ERC, which have intrinsic θ firing patterns (Lavenex and Amaral 2000). The hippocampus, in

contrast, responds only to supermodal or amodal information and returns abstracted representations to the originating areas of isocortex.

Role of other memory systems in episodic retrieval

Three non-declarative memory systems — the perceptual representation system, procedural memory, and working memory — may also interact with the declarative memory system, depending on task demands (see Table 2).

The *perceptual representation system* (PRS), memory for word and object identification, can be subdivided into three subsystems: the *visual word form subsystem* (extrastriate visual cortex and temporal and frontal cortex), which appears to process orthography, the *auditory word form subsystem* (superior temporal and frontal cortex), which processes auditory information, and the *structural description subsystem* (occipitotemporal regions, *e.g.* inferior temporal and fusiform gyri), which processes parts of objects and matches them to global structure. Although the PRS has been functionally and anatomically dissociated from declarative memory through PET and lesion studies, it is possible, if not likely, that a declarative memory task involving word or visual recognition (such as the task proposed in the present dissertation) would also engage the PRS (Eichenbaum *et al.*, 1996; Gabrieli, 1998).

Procedural memory is memory for habits and skills. Procedural memory does not recruit the MTL and is almost therefore anatomically independent of declarative (semantic and episodic) memory. Neuropsychological and pathological studies of amnesic patients have revealed that procedural memory is dependent upon a

corticostriatal system, as well as the motor cortex and basal ganglia (Eichenbaum *et al.*, 1996; Gabrieli, 1998).

Working memory enables short-term retention of information over several seconds (Eichenbaum *et al.*, 1996; Gabrieli, 1998). Like the PRS, working memory can be anatomically and functionally categorized into two *slave subsystems*: the *phonological loop* (auditory and parietal cortex), which contains auditory information for working memory, and the *visuospatial sketch pad*, which is anatomically composed of the visual association cortex, inferior parietal lobule, and inferior prefrontal cortex (Eichenbaum *et al.*, 1996).

Table 2 Regions typically involved in episodic retrieval tasks. *LH*, left hemisphere; *RH*, right hemisphere; *BL*, bilateral. Several of these regions will be used as target ROIs in the present study (see next chapter).

Working memory	Maintenance	Precentral sulcus (BL) ¹ VISUOSPATIAL SKETCH PAD ² : Visual association cortex Inferior parietal lobule Inferior prefrontal cortex (area 45) Inferior frontal gyrus (BL) ¹ Anterior frontal gyrus (LH) ¹ Medial frontal gyrus (RH) ¹ Phonological loop ² : Parietal cortex Auditory cortex
	Recognition	Precentral sulcus (BL) ¹ Inferior frontal gyrus (BL) ¹ Posterior middle frontal gyrus (BL) ¹ Middle frontal gyrus (BL) ¹ Anterior prefrontal cortex (LH) ¹
Long-term memory	Retrieval	Entorhinal cortex (θ source) ³ Medial septum (θ source) ⁴ Perihippocampal cortex ³ Perirhinal cortex ³ Dorsal hippocampus ⁵ Right frontal cortex ⁶
	Recognition	AUDITORY WORD FORM SUBSYSTEM ² : Superior temporal gyrus Right frontal cortex STRUCTURAL DESCRIPTION SYSTEM ⁷ : Inferior temporal gyrus Fusiform gyrus

¹ (Ranganath, Johnson *et al.* 2003)

² (Eichenbaum, Schoenbaum *et al.* 1996)

³ (Lavenex and Amaral 2000)

⁴ (Chrobak and Buzsaki 1998b)

⁵ (Bannerman, Rawlins, McHugh, Deacon, Yee, Bast, Zhang, Pothuizen and Feldon 2004)

⁶ (Buckner, Koutstaal *et al.* 1998b)

⁷ (Haxby, Horwitz, Ungerleider, Maisog, Pietrini and Grady 1994)

REGIONS OF INTEREST

Regions of interest (ROIs) for the present study were delineated according to the AFNI implementation of the Talairach-Tourneaux human brain atlas (Talairach and Tournoux 1988) by warping the individual datasets to Talairach space. In this section, the significance of the various ROIs, according to recently published literature, will be discussed in order to place them into the context of the previously-stated hypotheses.

Ten ROIs were selected for the present study based on their functional significance as long-term memory, visual, or motor regions. Four, including hippocampus and entorhinal, ectorhinal, and perirhinal cortex, constitute the majority of the MTL with the exception of the periamygdaloid area (also known as the semilunar gyrus), posterior PHG, the prepyriform area (also called piriform cortex; laterally bounded by the retrosubicular area 48), and the presubiculum, which are not known to play a pivotal role in declarative memory storage or recall. An additional four ROIs, including visual areas V1, V2, and V3 and the fusiform gyrus, were included in order to facilitate sampling from lower (V1 and V2) and higher-order (V3 and fusiform) visual areas, particularly in the ventral visual stream. Primary motor (M1) cortex and premotor (PMC) cortex were also included as control and motor attention areas (see below), respectively.

MEDIAL TEMPORAL AREAS: LONG-TERM MEMORY ROIS

The hippocampus (HC), entorhinal cortex (ERC: Brodmann areas 28 and 34), ectorhinal cortex (EcRC: Brodmann area 36), and perirhinal cortex (PRC: Brodmann area 35) were

identified as regions of interest for the present study based largely on the neuroanatomical and neuropsychological studies of Lavenex and Amaral (2000), Eichenbaum and colleagues (1996), Gabrieli (1998), and Nadel and colleagues (2000). The functional neuroanatomy of these long-term memory regions is further described in the introductory chapters. To review: information is conveyed from isocortex to the perirhinal and parahippocampal regions, depending on the modality of the stimulus; PRC appears to be specialized for visual object information, whereas PHG seems to be related to the storage and conveyance of visuospatial information. It has been suggested that PRC and PHG are necessary for the maintenance and consolidation of pair codings, and as such are of particular interest in the present study. Furthermore, current anatomical models suggest that information exchange takes place between the PRC/PHG and HC, parietal cortex, anterior cingulate, and the insula (Lavenex and Amaral 2000). The PRC is located along the banks of the rhinal sulcus and is bounded medially by entorhinal area 28 and laterally by entorhinal area 36; the PHG is defined for the purposes of this dissertation as consisting of the periamygdaloid area (also known as the semilunar gyrus), posterior PHG, the prepyriform area (also called piriform cortex; laterally bounded by the retrosubicular area 48), and the presubiculum, and is not included as an ROI in the present dissertation.

Output from the PHG/PRC region is sent to the ERC (Lavenex and Amaral, 2000), which also interacts with parietal association cortex (PAC) for spatial perception and cognition. The ERC in turn sends its output to the dentate gyrus (in the hippocampus). The function of the ERC is not well understood, however, except that it plays a role in all phases of long-term memory acquisition, consolidation, and recall, and

seems to function in the pairing of stimuli that are temporally dispersed (Egorov, Hamam, Fransen, Hasselmo and Alonso 2002; Frank and Brown 2003). The ERC is divided into Brodmann areas 28 and 34; both areas are located on the medial-caudal aspect of the temporal lobe.

Information is sent from the hippocampal dentate gyrus to the CA3 field and finally to the subiculum (also in the HC), which returns abstracted information to isocortex. The nature of abstraction in the hippocampal complex is not well understood; however, it is believed that the HC responds only to supramodal or amodal information, such as salient unified features of a memory, and it is this supramodal and amodal information that is returned to cortex. As discussed previously, the HC itself has been shown to activate during acquisition, consolidation, and recall, although the time course of its influence upon these phenomena is a matter of controversy (Eichenbaum, Schoenbaum *et al.* 1996; Nadel and Land 2000; Nadel, Samsonovich, Ryan and Moscovitch 2000).

The ectorrhinal cortex (EcRC: area 36) has been shown to have backprojections onto V1 and is heavily interconnected with area TE in simians (Naya, Yoshida and Miyashita 2003a; Naya, Yoshida, Takeda, Fujimichi and Miyashita 2003b; Clavagnier, Falchier and Kennedy 2004). It appears to be part of a visual long-term memory system (along with other visual areas) in these higher primates, but its role in humans has not been decisively determined. Extrapolation from animal data, however, suggests that area 36 may also participate in long-term visual memory in humans. EcRC is located primarily in the fusiform gyrus (this area is excluded from the fusiform gyrus ROI in the

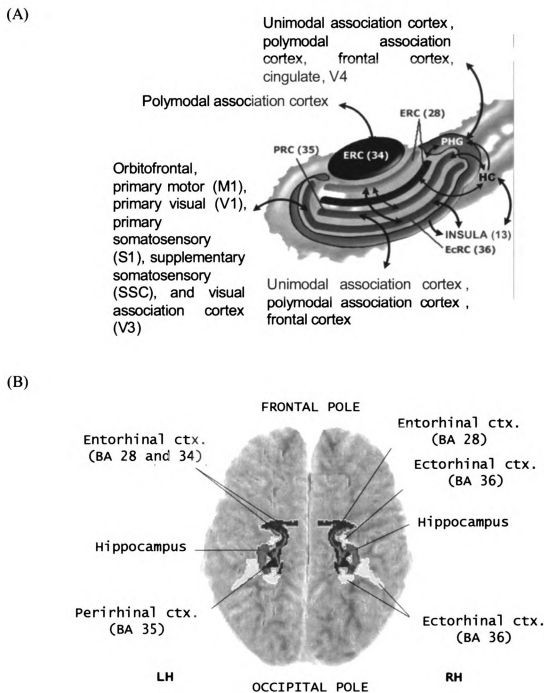


Figure 2 (A) Interconnections among constituent regions of the MTL and other areas of interest in the present study. Blue arrows indicate neuronal projections between areas as determined by anatomical studies of the cortex and temporal lobe. Arrow locations do not accurately reflect the anatomical location of interregional projections (Sources: Deacon, Eichenbaum, Rosenberg and Eckmann 1983; Schacter, Buckner, Koutstaal, Dale and Rosen; Burwell and Amaral; Burwell and Amaral; Lavenex and Amaral; Save and Poucet 2000a; Save and Poucet 2000b). (B) The anatomical locations of MTL areas in the Talairach-Tourneaux template brain, obtained from the AFNI suite's Talairach Daemon. Abbreviations: LH, left hemisphere; RH, right hemisphere; ctx., cortex; BA, Brodmann area.

present study) and is bounded laterally and caudally by inferotemporal area 20, medially by PRC area 35, and rostrally by temporopolar area 38.

MTL areas, which, again, serve to associate salient features of encoded declarative stimuli, also appear to be affected by consolidation processes. Intuitively, this would mean that changes in plasticity would drive the amalgamation of pre-consolidation medial temporal interneurons serving to link memory traces stored in isocortex, such that fewer interneurons are required for the linkage at post-consolidation (see Figure 2).

PREMOTOR CORTEX AS A VISUOSPATIAL ATTENTION AREA

Brodman area 6 has been cited as an attentional area since its activation is strongly correlated with tasks involving covert shifts of attention, and particularly in tasks that demand shifts in visuospatial attention (Nobre, Sebestyen, Gitelman, Mesulam, Frackowiak and Frith 1997). Furthermore, area 6 has been subdivided into medial and lateral regions, which are differentially activated by verbal and spatial memory sequencing tasks, respectively. This finding was also supported by a repetitive transcranial magnetic stimulation (TMS) inference study, in which TM stimulation to the medial Brodman area 6 selectively disrupted verbal but not spatial cognitive processing, whereas TM stimulation to the lateral Brodman area 6 disrupted spatial but not verbal cognitive processing (Tanaka, Honda and Sadato 2005). Area 6 comprises parts of the superior and middle frontal gyri as well as the rostral precentral gyrus and is bounded medially by the cingulate sulcus and laterally by the lateral sulcus.

VISUAL AREAS

It is beyond the scope of this dissertation to discuss in depth the function and history of research into visual cortex. Here, the functional architecture of the visual streams from V1 to V5 will be highlighted (with the exception of V4/IPL, discussed above). For a more thorough review of human visual neuroanatomy, the reader is referred to the recent review by Wichmann and Muller-Forell (Wichmann and Muller-Forell 2004); the seminal paper on the dorsal and ventral streams by Ungerleider and Mishkin (Ungerleider and Mishkin 1982) is also a good reference.

Visual area V1, located in Brodmann area 17, gets input from the thalamic lateral geniculate nucleus (LGN) and responds selectively to (*i.e.*, its cells are tuned to) orientation-specific contours and (in some cases) respond to color (Hubel and Wiesel 1959; Hubel and Wiesel 1962). V1 exhibits complex within-region circuitry, as well as interactions with the LGN, in addition to visual areas V2 and MT/V5, through unidirectional and reciprocal projections, which may serve simple attentional functions in visual selection (Livingstone and Hubel 1984b; Livingstone and Hubel 1984a; Albright 1993). V1 is bounded by Brodmann area 18 and surrounds the calcarine fissure. It is anatomically identifiable by the presence of the bands of Gennari.

Visual areas V2 and V3, located in Brodmann areas 18 and 19, respectively, are the first of many so-called extrastriate visual areas. V2 shares both feedback connections with area V1 and feedforward connections with V3, V4/IPL, and V5/MT. Neurons comprising area V2 are, like area V1, tuned to feature orientation and color, but

additionally have figure-ground tuning (Qiu and von der Heydt 2005). V2 is also interconnected with areas V4 and MT, and exhibits some attentional modulation (Albright 1993; Rao 2005). Visual information is relayed from V2 to V3 as part of a ventral visual stream (vVS), which has a role in object recognition, and from V2 to V5/MT as part of a dorsal visual stream (dVS), which functions in spatiotemporal tasks (Ungerleider and Mishkin 1982). V3 (Brodmann area 19), part of the vVS, is tuned to aspects of visual motion (Braddick, O'Brien, Wattam-Bell, Atkinson, Hartley and Turner 2001). Area V3 has strong interconnections with both area V2 and area V4/IPL (Albright 1993). Brodmann area 18/V2 is bounded by area 17/V1 and area 19/V3; area 19/V3 is further bounded by areas 37 and 39.

The fusiform gyrus is a functionally heterogeneous area most recently shown to be involved in face processing (Kanwisher, McDermott and Chun 1997; Haxby, Gobbini, Furey, Ishai, Schouten and Pietrini 2001; Haxby, Hoffman and Gobbini 2002; Rossion, Schiltz and Crommelinck 2003; Yovel and Kanwisher 2005). However, it also seems to be involved in other aspects of visual processing and computation, including visual working memory, lexical tasks, and mental manipulation of orientation of visual stimuli (Orban and Vogels 1998; Pammer, Lavis and Cornelissen 2004; Uncapher and Rugg 2005a; Uncapher and Rugg 2005b). The fusiform gyrus consists of entorhinal area 36 (which was included as the EcRC ROI but excluded from the fusiform ROI in the present study) as well as area 37. Area 37 is bounded caudally by area 19/V3, rostrally by area 20/V5 and area 21, and dorsally by area 39.

PRIMARY MOTOR CORTEX: A CONTROL AREA

Finally, primary motor cortex (M1, Brodmann area 4) was included in the analyses in order to assess its connectivity with cortical and subcortical areas during our episodic retrieval task. It has been shown that increased within-M1 neural firing rate coherence is related to corticospinal (descending voluntary) control of muscle movement, and, furthermore, that this coherence is further correlated with coherence between M1 and motor neurons in the beta frequency range (Gerloff, Braun, Staudt, Hegner, Dichgans and Krageloh-Mann 2006). Area 4/M1 is bounded rostrally by premotor area 6 and caudally by area 3.

FMRI SPATIAL AND TEMPORAL SPECIFICITY

The present study endeavors to assess changes in cortical recruitment, metabolic demands, and FMRI signal entropy and rate of change as correlates of memory consolidation. In order to formulate a proper methodology to perform this assessment, however, the arguments must be made that (a) the BOLD signal is substantially coupled to, and co-registered with, neural activity; (b) that BOLD-FMRI is satisfactorily colocalized to neural activity, so one may infer details about the underlying neural activity; and (c) that one may extrapolate, based on certain features of the FMRI dataset, where in the brain the T_2^* -weighted signal change originates (*i.e.*, at which locations the BOLD signal arises from increased metabolic activity as opposed to passive diffusion of deoxyhemoglobin). This chapter, then, will turn to the principal methodology of the present dissertation, functional magnetic resonance imaging (FMRI). The underlying physiology of the FMRI signal will be examined and the implications of this physiology for investigations of functional neural architecture, as well as the spatial and temporal resolution of the FMRI method and its colocalization with aspects of neural electrophysiological phenomena, will be highlighted.

BOLD SIGNAL PHYSIOLOGY

FMRI is an extension of anatomical MRI that relies on a T_2^* -weighted, blood oxygenation-level dependent (BOLD) signal (Ogawa, Lee, Kay and Tank 1990) that

arises indirectly from the metabolic sequelae of postsynaptic potentials, particularly local field potentials (LFPs), which correspond to cooperative population activity (synchronized somatodendritic potentials: see Logothetis, Pauls, Augath, Trinath and Oeltermann 2001; Logothetis 2002; Logothetis 2003; Logothetis and Pfeuffer 2004; Logothetis and Wandell 2004). LFPs fluctuate relatively slowly; the magnitude of this fluctuation is not related to cell size but with the geometry and extent of dendritic arborization. Thus, the parallel arrangement of apical dendrites heavily influences LFP measurements due to their “open field” arrangement. LFPs reflect a net effect of cellular events – synaptic events, voltage responsive membrane oscillations, afterhyperpolarizations, and afterdepolarizations due to K_{Ca} channels (Logothetis, Pauls *et al.* 2001). Anatomically, the density of brain vasculature seems to be related to the location of perisynaptic elements, rather than the location of neural somata, which suggests that cerebral blood flow (CBF) is related to neurotransmitter release rather than perikaryal metabolic demands. This is further verified by increases in CBF only with *orthodromic*, not *antidromic*, microstimulation. Logothetis (2001) has noted that glucose uptake, the postsynaptic effects of glutamate, and the restoration of ion gradients after an action potential – all of which can be categorized under the heading “synaptic events” – are the most energy-consuming processes in the brain and drive CBF changes. Of these, presynaptic and postsynaptic currents drive the energy demand and are the dominant elements in LFPs (Logothetis *et al.*, 2001).

Just as cortical areas are delineated anatomically by differences in cyto- and myeloarchitecture, they can be delineated functionally by differential physiological properties (electrophysiology) and connectivity (neuroimaging, tract tracing).

Neuroimaging methods like fMRI have the advantage over invasive methods in that they permit longitudinal studies (e.g. on learning, plasticity, reorganization). The BOLD contrast signal used in fMRI is derived from magnetic field inhomogeneities caused by differential deoxyhaemoglobin (dHb) concentrations. dHb is confined to the intracellular space of erythrocytes, which are in turn confined to the vasculature. Thus, the field gradient responsible for the BOLD signal is a result of the susceptibility differences between the dHb-containing compartments and the surrounding space. fMRI pulse sequences are sensitive to these differences and alter the signal when dHb concentration changes. Upon neural activation the increase in dHb concentration would be expected to enhance the difference in magnetic susceptibility, thereby decreasing the BOLD signal; however, the exact opposite occurs. This is due to an increase in CBF that overcompensates for the increase in oxygen uptake: an oversupply of oxygenated blood is delivered to the site (Raichle 1998). Thus, changes in CBF corresponding to neural processes are reflected by an increase in the BOLD signal.

SPATIOTEMPORAL RESOLUTION OF fMRI

The development in the late 1980s of high-field (1.5T) MR imaging techniques (echo-planar imaging and spiral imaging) and discovery of two endogenous “contrast” mechanisms – BOLD (Ogawa, Lee *et al.* 1990) and differential net longitudinal magnetization with changes in tissue perfusion – initiated a revolution in functional neuroimaging, largely replacing paramagnetic tracer technology for in-depth studies of cognition. The temporal relationship of neural and vascular events (neurovascular

coupling) was actually first described by Angelo Mosso in 1881, but the nature of this relationship has only recently been defined (Logothetis *et al.*, 2001). Whisker barrel stimulation in murine models demonstrated that CBF increases within approximately 2 sec of stimulation onset and peaks within 5-7 sec. However, paramagnetic tracer studies have revealed that gross cerebral volume changes actually lag behind changes in CBF, likely due to a “capacitance system” in the capillaries and post-capillary beds, and Hb/HbO₂ changes even precede CBF changes. Thus, changes in hemoglobin concentrations, local CBF, and gross CBF are related temporally but perhaps not causally. The implication of the BOLD signal technique is that the block design, which was necessary for single-photon and positron emission tomography (since they require a quasi-equilibrium state of > 60 sec), became superfluous for fMRI, and event-related designs, such as the one proposed in the present dissertation, were made possible. Consequently, the short history of fast (event-related or ER)-fMRI has been characterized by investigations of ever-smaller sampling windows. Blamire *et al.* demonstrated detectable signal changes after stimulus durations as short as 2 seconds; Bandettini *et al.* decreased this window to as little as 500 msec (Bandettini, Wong, Hinks, Tikofsky and Hyde 1992; Blamire, Ogawa, Ugurbil, Rothman, McCarthy, Ellermann, Hyder, Rattner and Shulman 1992). More recently, Savoy *et al.* established that the BOLD signal could be detected after a 34 msec-duration visual stimulus and Boynton *et al.* showed that responses can be summated linearly over time (with some limitations) (Savoy 2005). The computability of a hemodynamic response function (HRF) is directly related to the strength of the field; as field strength increases (e.g. 1.5T to 3T) the signal-to-noise ratio (SNR) increases. In the lower magnetic fields, time series can be reconstructed with (a)

overlap correction methods similar to those used in ERP research and (b) averaging across trials, which brings out the modal tendencies in the HRF. Rosen *et al.* note that temporal sensitivity is a function of the SNR (and by implication, field strength) as well as the haemodynamic response (HRF) variance and the methods used to characterize it (Rosen, Buckner and Dale 1998). They also report that variance in HRF latency within and between brain regions is not merely a matter of vasculature diameter. Although larger vessels do exhibit longer latencies (a significant factor within regions such as V1) the longest delays are seen in anterior PFC, an area with a minimum of large vessels. Savoy *et al.* (1995) have reported latencies of 500 msec in V1; Buckner *et al.* report latencies of 500 to 1000 msec between visual and prefrontal areas; and at the other extreme, Schacter *et al.* note delays of 2 to 4 sec between various prefrontal regions (Buckner, Bandettini, O'Craven, Savoy, Petersen, Raichle and Rosen 1996; Schacter, Buckner *et al.* 1997; Savoy 2005).

The *spatial* resolution of fMRI has been examined most closely with manganese contrast, which is paramagnetic and emphasizes the calcium-dependent sites of neural activity. Manganese enters voltage-operated calcium channels and mimic calcium's role in neurotransmitter release. In a recent study with manganese MRI contrast in rats, Duong *et al.* demonstrated a co-registration of $< 200\ \mu\text{m}$ between synaptic activity and BOLD contrast, suggesting that the BOLD signal (at high fields [9.4T]) resolves synaptic activity to a satisfactory degree (Duong, Silva, Lee and Kim 2000). It is therefore reasonable to conclude that the BOLD signal satisfactorily exemplifies the localization of [post]synaptic activity.

Aguirre *et al* have investigated the variability in HRF shape and timing within subjects (different brain regions), across subjects, and at different times of the same day or on different days (Aguirre, Zarahn and D'Esposito 1998). Formerly the best estimates for the HRF were (1) a Poisson distribution (Friston *et al*, 1994) or (2) a gamma distribution with two free parameters and a phase delay (Boynton *et al*, 1996). It was determined that the mean time-to-peak in subjects was 4.7 ± 1.1 sec and ranged from 2.7 to 6.2 sec; HRFs across subjects were significantly more variable than those within a subject, even across several days. Additionally, the Poisson function accounted for only 25% of the HRF variances; the gamma function accounted for 70%, which was a significant difference ($p < 0.001$). When a single subject-specific HRF estimate was used (generated empirically from the single-subject data) approximately 96% of variance was accounted for. Therefore, the authors conclude that an empirical estimate of the HRF is much more desirable than an *a priori* estimate. For blocked fMRI paradigms, in which the HRF is oversampled, an *a priori* estimate will not decrease statistical sensitivity significantly; however, the authors note that an empirical HRF lends to the analysis a measurable increase in sensitivity – as it will for event-related designs (which are much more sensitive to the statistical decrement imposed by the *a priori* function). Therefore, the HRF varies within and between subjects and a deconvolution analysis (discussed in the *Methodology* chapter) will be utilized to overcome this variance in the present dissertation.

AIMS AND THEORETICAL TREATMENT OF CONSOLIDATION NEURODYNAMICS

A paired-associate task (described in the *Methodology* chapter) was utilized to examine changes in task performance and BOLD physiology with episodic memory consolidation. This task required subjects to learn, via a computer-based training session, to associate visually presented words with abstract pictures, then identify correctly matched, incorrectly-matched, and control condition pairings during a testing session, which took place within an MRI magnet. Two fMRI time points were established by dividing the subject pool into a pre-consolidation time point group (TP₁), whose constituents were tested in the MRI magnet immediately after the training session, and a post-consolidation time point group (TP₂), who were tested in the MRI magnet seven days after the initial training session.

This paradigm, coupled with a non-invasive, systems-level approach, functional MRI (fMRI), enabled the assessment of changes in subject memory performance and physiology with consolidation. Although many fMRI investigations of mnemonic functions have been performed, a majority has dealt with modular cortical activity correlated with a given memory function; fewer are the studies of such memory functions as a system (e.g., a recent analysis of cortical connectivity during episodic encoding by Summerfield, Greene, Wager, Egner, Hirsch and Mangels 2006), and none, to the knowledge of the author, have attempted to analyze differences in the fMRI signal entropy or signal response rate in episodic memory areas with consolidation.

This scarcity of neuroimaging-based mnemonic neurodynamics research is likely due to the indirect relationship between neural activity and the fMRI signal: the BOLD signal, upon which most fMRI studies are founded, is an epiphenomenon of glycolytic activity concomitant to synaptodendritic metabolic demands (Ogawa, Lee *et al.* 1990). As such, neural activity and the BOLD signal are said to be related through a black box or “transfer function” of unknown parameters, and these parameters vary both across brain areas within a given subject as well as across subjects and task demands. Nevertheless, the correlation between the BOLD signal and neural activity (more specifically, the local field potential phenomenon) has been shown to exhibit a rough linearity across low to moderate metabolic magnitudes, such that neuroimaging research may generate probative, albeit admittedly indirect, neurodynamics data (Logothetis, Pauls *et al.* 2001).

CONSOLIDATION AS AN OPTIMIZING PROCESS

A discussion of the theoretical basis of the hypotheses of the present dissertation is best approached through a conceptualization of the episodic memory system as a self-tuning network that aims to minimize its energy expenditure relative to the storage and recall of a given memory trace.

For the purposes of the present dissertation, *retrieval efficiency* was defined as the speed, recruitment, and retrieval success or *efficacy* of the mnemonic (long-term memory) and supporting (working memory, attentional and executive, and visual and motor) networks recruited during trace recall. Retrieval “speed” and “success” were characterized *behaviorally* by subject response time and accuracy, respectively, on the

paired associates task, whereas retrieval-concomitant “recruitment” was characterized *physiologically* by the degree of cortical recruitment and metabolic demand relative to subject retrieval speed and success. It should be noted that this definition of “efficiency” is closely related to the use of the term in thermodynamics in that it is conceptually a ratio of useful output (behavioral trace retrieval performance) versus energy expenditure (metabolic intensity per unit recruited volume):

$$\frac{\text{performance}}{\text{recruitment}} \text{ or } \frac{\text{performance}}{PC / AV} .$$

where *PC* represents the percent BOLD signal change from baseline and *AV* represents the degree of cortical recruitment (activation volume). Although it is beyond the scope of the present work to attempt to typify this ratio as a quantitative index of neural systems efficiency (although such attempts have been made: see Chance 2007), this *conceptualization* of retrieval efficiency was used exhaustively in the origination of the theory and hypotheses in the current study.

It is imperative to note that, by this definition, increased efficiency over a consolidation interval could be argued to have occurred in any of several cases. Namely, the output-to-energy expenditure ratio would increase if

- (a) subject performance on a recall task improved without a corresponding decrease in metabolic demand or cortical recruitment;
- (b) metabolic demand *and* cortical recruitment decreased without a corresponding improvement in subject performance;
- (c) metabolic demand decreased without corresponding improvements in cortical recruitment or subject performance; or

- (d) cortical recruitment decreased without corresponding improvements in metabolic demand or subject performance.

EVIDENCE FOR INTERIM PHYSIOLOGICAL CHANGES IN RETRIEVAL SUBSTRATES

Prior behavioral, electrophysiological, and neuroimaging studies of memory performance in well-trained versus poorly-trained subjects have in fact provided some evidence that performance on episodic memory tasks are dependent upon the “attunement” of perceptual and trace retrieval circuits toward task specificity, *i.e.*, the identification of previously learned stimuli, and, therefore, do exhibit some hallmarks of optimization (Tulving 1983; Weldon, Roediger *et al.* 1989; Rugg and Wilding 2000; Robb and Rugg 2002; Wheeler and Buckner 2003). In particular, well-trained subjects appear to exhibit an enhanced capacity for quickly identifying, through covert attentional mechanisms, *distinctive characteristics of presented stimuli in order to expedite retrieval* of those features from memory; and, furthermore, such subjects also exhibit an enhanced capacity for *reactivating, upon recall, the cortical networks recruited during encoding*. These phenomena have become known as *retrieval orientation* and *cortical reinstatement* (or “transfer-appropriate processing”) effects, respectively (Lockhart 2002; Vaidya, Zhao, Desmond and Gabrieli 2002; Herron and Rugg 2003b; Herron and Wilding 2004; Hornberger, Morcom and Rugg 2004; Herron and Wilding 2006a; Hornberger, Rugg and Henson 2006b; Mulligan and Lozito 2006; Stenberg, Johansson and Rosen 2006; Woodruff, Uncapher and Rugg 2006). Clearly, such changes in perceptual and retrieval circuits, if they exist, are relevant to an understanding of pre- and post-consolidation

retrieval efficiency; however, *these phenomena have not yet been examined in a time-dependent or consolidation context.*

It is logical to assume that the shifts in recall neurophysiology predicted by the retrieval orientation and cortical reinstatement phenomena, as well as the Hebbian changes in neuronal efficacy that would ostensibly cause them, would likely occur *both* within the trace network *and* the visual cortices recruited for future recognition of the stimuli the traces represent. To the knowledge of the author, the ideal test of this assumption – the presence or absence of retrieval orientation and/or cortical reinstatement effects in the context of a MTL lesion – has not been performed. Given the robust evidence for close connectivity between episodic and attentional brain regions, however, it is unlikely that these phenomena are asymmetric across the regions that mediate attention to remembered stimuli and the memory traces which drive them (Chun and Turk-Browne 2007); therefore, correlates of retrieval orientation and cortical reinstatement were expected in medial temporal, attentional, *and* visual areas, except where direct descending attentional input is lacking (e.g. V1: Rao 2005).

It was of particular interest in the current work to substantiate or refute retrieval orientation effects in the right hemisphere fusiform gyrus and ventral visual stream, where such effects have been reported (Vaidya, Zhao *et al.* 2002; Woodruff, Uncapher *et al.* 2006). The ventral, or object identification, visual stream and fusiform gyri, especially in the right cortical hemisphere, are believed to subserve more holistic or “global” feature processing (Brown and Kosslyn 1993; Johannes, Wieringa, Matzke and Munte 1996; Yamaguchi, Yamagata and Kobayashi 2000). Therefore, three predictions were made:

- 1) that increased synaptic weights within visuospatial networks concomitant to the cortical reinstatement phenomenon would increase the efficacy of neuronal firing, such that *the BOLD signal rates of all areas (except primary visual and primary motor cortices) would be accelerated* (H. 3);
- 2) that post-consolidation subjects would exhibit *shifts in the laterality of metabolic demands in extrastriate areas* relative to pre-consolidation subjects, thereby evincing changes in visual attention with consolidation (H. 4); and
- 3) that increased synaptic weights within visuospatial networks concomitant to the cortical reinstatement phenomenon, as well as the differential modulation of the activity of those networks by descending attentional neurons due to retrieval orientation effects, would moderate the requisite amount of information processing in all extrastriate visual areas, such that *both left- and right-hemisphere post-consolidation visual cortices would exhibit lower metabolic demands than at pre-consolidation* (H. 4).

COMPUTATIONAL EFFICIENCY AND CORTICAL DEMANDS: ACTIVATION VOLUME AND ENTROPY

A fundamental assumption in the present study is that the number of neurons required to accomplish an encoding or computational function decreases as the encoding or computational efficiency of a neuron or population of neurons increases, an assumption that is supported by molecular, electrophysiological, and neuroanatomical evidence that repeated neuronal activity drives changes in proximal and distal dendritic morphology, which in turn effect changes in synaptic integration and therefore the computational

functions of the neuron (Holmes and Levy 1990; Zador, Koch and Brown 1990; Bailey, Chen, Keller and Kandel 1992; Bailey, Montarolo *et al.* 1992; Yuste and Denk 1995; Mallot and Giannakopoulos 1996; Shepherd 1996; Zhang, Endo *et al.* 1997; Hausser, Spruston and Stuart 2000; Verzi 2004; Frith 2005; Segev 2006). Thus, if memory consolidation is a process of mnemonic network optimization, the number of recruited neurons (or voxels, in the present case) would be expected to decrease. Two important exceptions in the present study are the premotor cortex, which appears to subserve attentional functions, and primary motor cortex, which subserves the motor response. Neither ROI was expected to differ with respect to recruitment nor metabolic demands with consolidation, since no changes in their computational functions were expected.

In the present study, therefore, the spatial extent of BOLD signal activation is quantitatively assessed through statistical analysis of the *activation volume* (in mm³) per region of interest. However, activation volume measures are susceptible to noise in the MR magnet environment and intersubject variability (Saad, Ropella, DeYoe and Bandettini 2003), and furthermore, it is not informative with respect to the nature or degree of information processing in signals from the neural populations (*remnant voxels*) that remain correlated with the task after consolidation. Moreover, interpretation of observed decreases in activation volume is further complicated by the indirect relationship between neuronal activity and the BOLD signal which underlies the definition of “activated” voxels. A change in activation volume may, however, be due to any number of factors — internalization of salient stimulus features, circuit multiplexing, or increased neuronal computational efficiency — but in the absence of data indicating that these changes in recruitment are accompanied by increases in (or stability of) the

task-specificity and magnitude of neuronal activity, it is equally justifiable to conclude that such decreased recruitment is a consequence of, for example, subject inattentiveness or task habituation. *If, however, a region of interest was shown to exhibit a higher information load or entropy*, suggesting an increase in computational efficiency, and/or a higher covariance between the regional BOLD signal and stimulus presentation, suggesting task attunement, a stronger argument could be made that network optimization had occurred in the region. In the present study, therefore, computational efficiency and task attunement are quantitatively assessed through statistical analysis of the entropy (voxel Shannon time series entropy, or voxel TSE, a novel application to FMRI) and voxel/task cross-correlation (VTCC, or the BOLD signal response rate), respectively. The particulars of both metrics are discussed in the *Methodology* chapter.

An analysis of task-related signal change and voxel TSE will also serve to support or refute an inference that remnant voxels exhibiting a post-consolidation increase in entropy are as metabolically active as (or more metabolically active than) significantly task-correlated voxels at pre-consolidation. This issue is of interest because, again, the assessment of BOLD signal entropy is a novel application for an FMRI-based study of human neurodynamics, and it is as yet unclear how faithfully BOLD signal entropy corresponds to neuronal signal entropy; a statistical concurrence of task-correlated increases in metabolic intensity and voxel TSE would suggest that remnant voxels both carry more information and are more metabolically active after consolidation, thereby supporting the assumption that the metrics discussed above are in actuality assessing the degree of synaptic integration (and therefore the computational intensity) within the region of interest.

CORTICAL REINSTATEMENT AND RETRIEVAL ORIENTATION EFFECTS IN VISUAL AND MEDIAL-TEMPORAL AREAS

Cortical reinstatement and retrieval orientation effects should be evinced by a *decrease in cortical recruitment* in long-term memory (LTM) *and* visual substrates, consequent to Hebbian competition over the consolidation interval, as well as *an increase in BOLD response rates* subsequent to the onset of neural activity, as correlates of enhanced synaptic weights of neurons still participatory in the LTM network after consolidation (Kida, Josselyn, de Ortiz, Kogan, Chevere, Masushige and Silva 2002; Bozon, Davis and Laroche 2003; Bozon, Kelly, Josselyn, Silva, Davis and Laroche 2003). Furthermore, LTM and visual circuit attunement (reinstatement) and retrieval orientation effects should be at least correlated with behavioral performance improvement, consequent to the efficacy of the post-consolidation network. However, one would not expect consolidation to have the *same* effect magnitude on all retrieval-related networks: differential retrieval efficiency concomitant to memory consolidation was expected to manifest differently in attentional areas, which support the trace retrieval process, than in medial temporal and visual networks, which actually store and retrieve previously-stored memory traces.

Shifts in the orienting of attention from local features to global features with consolidation, corresponding to retrieval orientation effects, were predicted to be evinced by bilateral activation in pre-consolidation subjects and right-hemisphere dominance (fewer left-hemisphere and more right-hemisphere clusters: Brown and Kosslyn 1993; Johannes, Wieringa *et al.* 1996; Yamaguchi, Yamagata *et al.* 2000), particularly in extrastriate ventral visual stream (EVVS) components in post-consolidation subjects

(H.3-4: Knierim and Van Essen 1992b; Knierim and van Essen 1992a; Polat and Norcia 1998; Haxby, Gobbini *et al.* 2001; Lerner, Hendler, Ben-Bashat, Harel and Malach 2001). Internalization, a consolidation-driven shift in attention from external lexical and visual features to comparison of external features with stored representations of salient stimulus features (Tulving 1983) and a possible consequence of cortical reinstatement, was also predicted to be evinced by a decrease in activation volume *as well as* metabolic demand in striate visual cortex (V1) and EVVS components with consolidation.

In contrast, “mnemonic” areas of the MTL are believed to function as a “linkage” site between traces stored in isocortex, as discussed in the *Regions of Interest* chapter (see also Sakai and Miyashita 1991; Miyashita, Morita, Naya, Yoshida and Tomita 1998; Egorov, Hamam *et al.* 2002; Egorov, Heinemann and Muller 2002; Frank and Brown 2003; Naya, Yoshida *et al.* 2003a; Naya, Yoshida *et al.* 2003b; Clavagnier, Falchier *et al.* 2004). Thus, recruitment of the ectorhinal, perirhinal and entorhinal cortices was predicted to *decrease while metabolic demand remained constant* between pre- and post-consolidation time points. Intracellular competition among trace neurons over the consolidation interval should result in an amalgamation of, and diminution in, the number of these trace neurons (Alvarez and Squire 1994; Chrobak and Buzsaki 1998b; Chrobak and Buzsaki 1998a; Kida, Josselyn *et al.* 2002; Bozon, Davis *et al.* 2003; Bozon, Kelly *et al.* 2003). This diminution should be reflected in a decrease in recruitment of “mnemonic” medial temporal areas (ectorhinal, perirhinal, and perihippocampal cortices). Furthermore, retrieval orientation effects were assumed to depend on both visuospatial information (subserved by entorhinal cortex and anterior hippocampus) and visual recognition (subserved by the majority of the MTL and posterior hippocampus).

However, it is worthy of note that, as discussed in the introductory chapters of this dissertation, there exists as yet no clear consensus as to the computational operations of the individual MTL areas; instead, most research has focused on a “visuospatial” versus “mnemonic” functional categorization scheme (see, for example, Preston and Gabrieli 2002). Moreover, the simple DMTS task utilized in the present study was not designed to disambiguate these visuospatial and mnemonic functions.

HYPOTHESES

In the present dissertation, mnemonic neurodynamics are investigated with respect to differences in behavior, with respect to differential static, or *modular*, brain activity, and with respect to differences in metabolic demands, between pre-consolidation and post-consolidation subjects. In particular, these differences were evaluated in two phases. In the first phase, conventional fMRI statistics – percent signal change from baseline and activation volume (task-correlated cortical recruitment) were applied in order to calculate changes in regional recruitment and the correlation between these changes and improvements in subject performance on a forced-choice delayed match-to-sample variant (paired-associate) task. In the second phase, two novel statistical assessments, the cross-correlation or covariance (VTCC) between stimulus presentation timing and subsequent BOLD responses and the BOLD signal complexity (the Shannon entropy of a voxel time series, or voxel TSE) – were employed to aid in the interpretation of the data returned by the conventional metrics.

It should be noted that both behavioral and physiological results are interpreted in the present study in the absence of direct (*e.g.*, molecular or cellular) evidence that memory consolidation occurred over the 7-day interval. *In this context, a MATCH condition accuracy significantly greater than chance (i.e., a normalized accuracy of $\geq 66\%$) was taken as evidence that consolidation had indeed occurred*, since (ostensibly) neither successful retrieval nor recognition effects can occur after intervals longer than 6

hours in the absence of stage IA protein synthesis (Abel and Lattal 2001; Walker 2004; Walker and Stickgold 2004; Wang, Hu *et al.* 2006).

The present study attempted to quantitatively describe differences in neurophysiology between pre- and post- stage I consolidation subject groups and correlate such differences, if present, with subject performance on the recall of *previously learned (correctly-matched) paired associates*, in order to test the working hypothesis that episodic memory consolidation is a process of optimization of the memory trace network for recall. More precisely, it was hypothesized that, based on recent evidence of consolidation-interval competition among neurons for inclusion in the final memory trace (Alvarez and Squire 1994; Chrobak and Buzsaki 1998b; Chrobak and Buzsaki 1998a; Kida, Josselyn *et al.* 2002; Bozon, Davis *et al.* 2003; Bozon, Kelly *et al.* 2003), consolidation would effect decreased cortical recruitment in anatomical substrates of long-term memory storage and recall, but that neurons surviving competition would “compensate” computationally for their excluded counterparts. *Thus, metabolic demands were expected to remain constant in mnemonic substrates (i.e., the medial temporal lobe) across pre- and post-consolidation subjects.* Furthermore, consolidation was hypothesized to result in “attunement” of retrieval networks to recognition of previously-learned stimuli, such that post-consolidation subjects would exhibit faster visual, mnemonic, and motor attention (*i.e.*, premotor cortex) BOLD signal response rates relative to the presentation of previously-learned associates, increased BOLD signal entropy, and better overall subject memory performance.

Thus, consolidation-related optimization was hypothesized, first, (H.1) to correlate positively with recall performance (corresponding to plasticity changes among memory traces), resulting in decreased subject response time and increased subject accuracy in identifying previously learned associates. Second (H. 2), anatomical substrates of pre- and post-consolidation memory storage and recall were hypothesized to exhibit equivalent metabolic demands, evinced by the BOLD signal magnitude, with decreased cortical recruitment, evinced by the spatial extent of task-correlated activation (activation volume), relative to the presentation of previously learned associates, in medial temporal (hippocampus, entorhinal, ectorhinal, and perirhinal) and attentional (premotor) ROIs, corresponding to greater activity at the level of the individual neuron. Extrastriate visual (V1-V3 and fusiform) ROIs, in contrast, were predicted to exhibit decreased metabolic demand *and* decreased cortical recruitment, corresponding to diminished activity at the level of the individual neuron as a consequence of retrieval orientation effects (see below). Third (H. 3), all substrates, with the exception of primary motor cortex, were expected to exhibit faster rates of change, evinced by faster voxel BOLD signal rates, as a correlate of cortical reinstatement, as discussed previously.

And finally (H. 4), consolidation was hypothesized to drive changes in synaptic integration, thereby effecting *differential sensory processing (retrieval orientation)* of the learned associates, as evinced by right-hemisphere dominance in the ventral visual stream (Robb and Rugg 2002).

These hypotheses are summarized in Table 3; related predictions are summarized in Table 4.

Table 3 Summary of the *hypotheses* for the present study.

		See Table 4:
H. 1	Consolidation correlates positively with recall performance for previously learned associates due to plasticity changes among memory traces.	RT ACC
H. 2	Consolidation correlates negatively with task-oriented recruitment (<i>i.e.</i> , activation volume) of recall substrates. However, post-consolidation trace neurons are individually more active than pre-consolidation trace neurons, such that net metabolic demand remains constant over the consolidation interval, except in visual areas, which are less recruited overall at post-consolidation.	BOLD mag./ Recruitment
H. 3	Consolidation correlates positively with BOLD signal response rates (<i>cortical reinstatement</i>) in mnemonic, visual, and motor attention substrates.	VTCC
H. 4	Consolidation correlates positively with metabolic demands in right-hemisphere components of the ventral visual stream, including area V3 and the fusiform gyrus, corresponding to differential <i>retrieval orientation</i> .	(N/A)

Table 4 Summary of the *predictions* for the present study with respect to subject performance (reaction time and accuracy), as well as physiological descriptions of the shape and temporal characteristics of the BOLD signal on the delayed match-to-sample portions of the paired associates task. Both behavioral and physiological findings are represented as being greater (+), less (–), or equal (no change, N/C) in post-consolidation subjects relative to pre-consolidation subjects. Abbreviations: *HC*, hippocampus, *ERC*, entorhinal cortex, *EcRC*, ectorhinal cortex, *PRC*, perirhinal cortex, *V1*, *V2*, *V3*, visual areas 1-3, *FUSI*, fusiform gyrus, *M1*, primary motor cortex, *PMC*, premotor cortex; *RT*, subject reaction time, *Acc*, accuracy; *BOLD mag.*, percent BOLD signal change from baseline, *recruitment*, cortical recruitment (activation volume), *BOLD rate*, BOLD signal response rate (evaluated by the voxel-task cross-correlation, VTCC). Hypothesis 4 (H4), which predicts a predominance of right hemisphere activation in post-consolidation subjects, is not included in the table.

	RT/H 1	ACC/H 1	BOLD MAG./H ₂	RECRUITMENT/H 2	BOLD RATE/H ₃
HC			N/C	—	+
ERC			N/C	—	+
EcR			N/C	—	+
C			N/C	—	+
PRC			N/C	—	+
V1	--	+	—	N/C	+
V2			—	—	+
V3			—	—	+
FUSI			—	—	+
M1			N/C	N/C	N/C
PMC			N/C	N/C	+

All four of the above hypotheses (see Tables 3, 4) follow from the assumption that the phenomenon of consolidation is, in essence, a process of optimization of the mnemonic net. However, it should be noted that activation volume, regional signal change from baseline, voxel TSE, and VTCC will only be assessed and discussed for brain activity that was significantly correlated with the presentation of *correctly-matched stimulus pairs* (*matched associates*) in order to minimize the effect of BOLD signals corresponding to stable task-related sensory and lexical networks (*i.e.*, responses to control stimuli) and task-related but generalized attentional, executive, and search-and-retrieval mechanisms (*i.e.*, responses to mismatched stimulus pairs). Thus, the findings discussed in the present dissertation will be related exclusively to the recognition and processing of matched associates and the related memory traces putatively stored in the subject's cortex.

METHODOLOGY

Stage I episodic memory consolidation was assessed using a three-phase training and testing paradigm. In the training phase, subjects were given 20 pairs of abstract pictures and animal words (tiger, bear, jellyfish, etc.) to memorize. These 20 pairs were repeated 10 times in order to stabilize the pairings in memory; subjects were then immediately tested on their retention using a computer-based testing script. During testing, subjects were presented with 100 total stimulus pairs (33 correctly matched words and pictures, 33 incorrectly matched words and pictures, and 34 control stimuli: scrambled pictures and backwards words) in a slow event-related paradigm. Only metrics concerned with correctly-matched stimuli will be assessed in this dissertation. Subjects were then randomly assigned to one of two groups. Group A proceeded directly to the fMRI magnet and underwent the same testing paradigm encountered previously; Group B underwent the testing paradigm 7 days later. Thus, Group A represented a presumptive pre-consolidation cohort, whereas Group B represented a presumptive post-consolidation cohort (see Figure 4).

SUBJECT POOL AND PARTICIPANTS

Subjects for the present study were obtained from undergraduate and graduate students at Michigan State University and from the surrounding community. 93 subjects (43 female; mean age 19.45 yrs) were subjected to a computer-based (non-fMRI) version of the task, and 13 subjects (6 female, age = 26.08 ± 10.57 yrs) comprised the final testing (fMRI)

group. Of these, 6 (2 female) were assigned to the pre-consolidation group and 7 were assigned to the post-consolidation group (4 female). Informed consents were obtained in accordance with the Michigan State University Committee on Research Involving Human Subjects (UCRIHS). The study was also approved by UCRIHS (IRB #02-634). Demographically, the subject pool consisted of 1 Hispanic, 0 African-American, 1 Indo-European, 1 Asian, and 10 white subjects. Participants denied claustrophobia and significant neurological history, and were screened for handedness using the Edinburgh Handedness Inventory (Oldfield 1971). Only right-handed subjects were asked to participate in the study.

PARADIGM

Stimulus presentation scripts were designed, prepared, and tested using E-Studio software (Psychology Software Tools, Pittsburgh, Pennsylvania). Subjects were given a computer-

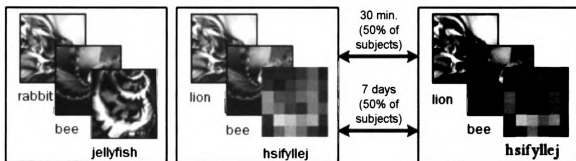


Figure 3 The training/testing paradigm for the present study. Stimuli consisted of 20 non-rehearsable, non-generalizable abstract pictures paired with animal nouns. Word stimuli were presented either audibly (computer-based training/testing) or visually (fMRI training/testing). Following a training session, during which the correct pairings of stimuli were learned, subjects were tested on their recall either immediately (pre-consolidation time point; 50% of subjects) or 7 days after training (post-consolidation time point; 50% of subjects). For the purposes of testing, subjects were presented with 33 correctly-matched, 33 incorrectly-matched, and 34 control (scrambled) stimulus pairs, and subjects were required to identify each type correctly by button press.

based training session, during which they learned 20 pairs of presumably non-rehearsable, non-generalizable abstract pictures and simultaneously-presented animal nouns, such as *rabbit*, *monkey*, *koala*, *jellyfish*, and *parrot*. The 20 pairs were each repeated ten times to ensure thorough learning, stipulatively defined as a 66% or better accuracy on the MATCH condition (DMTS) task. Following the training session, 50% of the participants were randomly selected to return after a 30-minute interval for the testing session; the other 50% were asked to return in seven days for testing (see Figure 3). In either case, subjects were instructed not to think about the task, nor attempt to remember or rehearse the presented stimuli.

The paradigm was tested with 93 subjects (43 female) using a computer-based version of the task. For these pilot subjects, the “animal words” were spoken by the computer simultaneously with the abstract picture presentation; thus, this version of the task was “dual modality.” However, technical difficulties in incorporating the audio system inside the MRI magnet necessitated the substitution of lexical stimuli for the auditory components for training as well as testing sessions for MRI subjects, such that the MRI version of the task was constituted wholly of visual stimuli (see Figure 4). Stimuli did not differ in any other respects. Differences in task performance between pilot and MRI groups were evaluated and are discussed in the “Changes in BOLD Physiology with Consolidation” section in the *Memory Consolidation and Retrieval Performance* chapter.

FMRI Paradigm. With the exception of stimulus modality, training and testing were consistent across computer-based and FMRI groups. During the testing phase,

(A)



jellyfish



Figure 4 (A) Example of a paired associate as presented for the FMRI version of the training/testing paradigm: note that the word component of FMRI training and testing associates was presented below the abstract visual component. The centroid of the presented paired associate was positioned in the center of the subjects' field of view. **(B)** A schematic of a single run from the FMRI testing paradigm: match, mismatch, and control-condition stimuli were presented with a constant interstimulus interval of 12.5 seconds. Presentation order was randomized across the three types of stimuli; x-axis represents TR (1 TR = 2.5 seconds).

subjects were asked to determine, based on their training session, whether presented stimulus pairs were correctly or incorrectly matched, and to respond accordingly by button press (thumb for match, index for mismatch). Additionally, control stimuli, consisting of heavily pixelated versions of the testing stimuli and either backwards audio (CBT subjects) or scrambled letters (for FMRI subjects), were presented at random

intervals. Subjects were asked to respond to these control stimuli by pressing both response buttons simultaneously.

MATCH, MISMATCH, and CONTROL condition stimuli were presented in random order³ with a constant interstimulus interval (ISI) of 12.5 seconds (Figure 4B). Subjects were given four runs of 25 stimuli and each stimulus was presented for one second, for a total run time of seven minutes in addition to 8 seconds of longitudinal magnetization equilibration time (total, 7 minutes 8 seconds).

DATA ACQUISITION

Behavioral measures acquisition. Correctly matched and mismatched paired associates and control stimulus pairs were presented to subjects within the MRI magnet, as described above, on an LCD display. Stimulus presentation was controlled, with millisecond accuracy, through an implementation of E-Prime and Integrated Functional Imaging Systems (IFIS) software (Psychology Software Tools, Pittsburgh, Pennsylvania). Subject response time and accuracy data were acquired through an electronic button response system tethered to the subject's right hand.

MR acquisition. Anatomical and functional data acquisition was carried out on a GE 3 Tesla MRI magnet (General Electric Medical Systems, Wisconsin, United States) with an 8-channel head coil. Passive control of sagittal and lateral subject head motion was established by using foam supports and medical tape secured to the subject's

³ *Random ordering* of stimuli was performed by assigned a given stimulus an integer between 1 and 100 using a random seed generation script in the Linux Bourne Again shell.

forehead, respectively. Single-shot gradient echo-planar image (EPI) functional slices (27.7 msec TE, 22 cm FOV, 3 mm slice thickness x 34 inferior-to-superior slices, 80° flip angle) were co-registered to high-resolution T₁-weighted sagittal anatomical volumes (5 msec TE, 24 cm FOV, 1.5 mm slice thickness x 120 slices, ±15.63 kHz bandwidth, 8° flip angle) for each subject. Anatomical and functional data was subjected to a 6-parameter (roll, pitch, yaw, and axial, sagittal, and coronal shift) iterated linear least squares motion correction algorithm using the programs 2dImReg and 3dvolreg, part of the AFNI FMRI analysis suite (NIMH), and also temporally realigned to correct for slice acquisition offset. A low-frequency bandstop was applied over the $(-\infty, 0.020]$ Hz interval to remove low-frequency artifacts in the data. A high-frequency bandstop was also applied on the $[0.080, +\infty)$ Hz interval in order to remove pulsatile cardiac (40-60 bpm) and respiratory-related (12-16 bpm) motion components. Although stimulus presentation order was randomized, stimuli of the *same* condition were *presented at an average* of 0.057 Hz, well within the data pass range of (0.020, 0.080) Hz. The bandstop filters were not expected to affect the entropy calculation (described below) since entropy is primarily influenced by moderate-probability events in a signal (e.g. random-walk-type phenomena), rather than pulsatile components, which are higher-probability (more predictable) signal components..

BEHAVIORAL ANALYSIS

Reaction time and behavioral data were analyzed with Minitab 14.0; performance statistics-related figures presented in the Results chapters were generated with SYSTAT 10.2 using the statistical results from Minitab. Inclusion criteria were established as

control stimulus response accuracy of at least 75%, in order to differentiate between high- and low-compliance subjects, and a paired-associates response accuracy (i.e., the mean of matched- and mismatched-associates accuracies) of at least 66%, in order to differentiate between relatively low-performers and moderately-high to high-performers. Low-performer data was not incorporated into the dataset for the present study; MRI data would also have been excluded for low-performers, however, none of the 13 MRI subjects exhibited data outside of the inclusion range.

For the purposes of analysis, both behavioral and MRI data were categorized as responses to correctly-matched stimuli (MATCH condition), incorrectly-matched stimuli (MISMATCH condition), or control stimuli (CONTROL condition). Reaction times and accuracies were then calculated for each condition and are reported for each condition separately, but only MATCH condition performance will be explored further in the present study.

MODULAR ANALYSIS

Deconvolution

In order to differentiate between BOLD/neural responses to MATCH, MISMATCH, and CONTROL stimuli, as well as responses to fixation crosses embedded in the paradigm, a deconvolution analysis was performed on the data using the AFNI program 3dDeconvolve. Deconvolution analysis de-overlaps contributors to the raw MR signal such that subject motion, arteriovenous signal, baseline trends, and task-related signal components can be isolated and analysed as statistical parametric maps (SPMs) (see Ward 1998).

Mathematically, given a raw voxel BOLD signal vector $y(t)$, the ``true'' haemodynamic response vector $x(t)$, an Dirac delta function denoted $\delta(t)$, an *a priori* polynomial vector γ , a Gaussian noise component ϵ , and k so-called *orthogonal* functions $\psi(t)$, representing subject motion and signal drift components (the error term for the linear regression of signal components) respectively, it is assumed that the raw voxel BOLD signal is a linear composition, or *convolution*, of the Dirac delta function, polynomial, and orthogonal vectors:

$$y(t) = x(t) \otimes \gamma(t) \otimes \psi(t) + \epsilon(t).$$

The objective of deconvolution analysis, then, is to remove the motion, noise, and drift components by linear least-squares estimation of $x(t)$. Thus, given

$$Z(t) = \sum y(t) \delta(t - \tau) = x(t) [1 \mid \gamma \mid \psi] + \epsilon(t),$$

where δ represents the Dirac delta function, the sum-square error, SSE, can be minimized,

$$\min SSE = \frac{d^2}{dt} \left(Z - \frac{x(x^T Z)}{x^T x} \right)^T \left(Z - \frac{x(x^T Z)}{x^T x} \right).$$

Using 3dDeconvolve, voxels that activated in response to matched associates, but not mismatched associates, control stimuli, or fixation crosses, were isolated by a subtraction method to create a MATCH condition SPM. Motion components were also deconvolved against the raw signal, and correlation coefficients between the voxel response vectors and an ideal hemodynamic response waveform (composed by convolving the binary stimulus onset vector with an empirically-determined hemodynamic response model waveform $r(t)$: R.W. Cox, *waver FAQ*, 2005):

$$r(t) = \begin{cases} 0 & \text{for all } \{x_i \mid -\infty < x_i < 0\}; \\ 0.502 \tanh[\tan(0.500\pi \cdot 1.600x - 0.800)] + 0.996 & \text{for all } \{x_i \mid 0 \leq x_i < 1\}; \\ 1 & \text{for all } \{x_i \mid 1 < x_i < \infty\} \end{cases}$$

where x_i represents the voxel response vector.

In order to control for type II errors, bias alpha correction, and prepare individual data for registration to the common Talairach-Tourneaux grid (see, for example, Salmond, Ashburner, Vargha-Khadem, Connelly, Gadian and Friston 2002; Breakspear, Brammer, Bullmore, Das and Williams 2004; Geissler, Lanzenberger, Barth, Tahamtan, Milakara, Gartus and Beisteiner 2005; Kriegeskorte, Goebel and Bandettini 2006; Scouten, Papademetris and Constable 2006), cluster analysis was performed on the deconvolved functional data using minimal-volume thresholds computed with the AFNI program AlphaSim. AlphaSim estimates the α level (and therefore the p -value) significance of random noise via Monte Carlo simulations within a virtual volume with the same dimensions as the dataset voxels, using the empirical filter width at half maximum (FWHM) of the data. Using this technique, it was found that a cluster size of 646 voxels (6379 μ L), corresponding to $\alpha \approx 0.955$, would yield a corrected p -value of 0.045 for the dataset (minimal connection radius = 5.7 mm).

Percent BOLD signal change from baseline, activation volume, voxel-task cross-correlation (VTCC) and entropy (TSE) statistics were obtained per region of interest (ROI) from these SPMs. ROIs (with the exception of the hippocampus) were defined by Brodmann area (Brodmann area assignments are described in the *Regions of Interest*

chapter) using the “Talairach” daemon in the AFNI analysis suite (see also Talairach and Tournoux 1988).

Percent BOLD signal change from baseline (see also Ward 1998)

Brain activation is often characterized in fMRI experiments by calculating the statistical significance of a regional BOLD signal, the percent BOLD signal change from baseline. In the present study, BOLD signal change was quantified for comparison with neurodynamic metrics, such as voxel entropy and voxel-task cross-correlation, and in the interest of assessing these latter statistics in the context of voxel recruitment (activation volume) and glycolytic intensity, from which the BOLD signal is largely derived (Raichle 1998; Logothetis, Pauls *et al.* 2001). Mathematically, given a reference vector $r(t)$, a voxel time series vector $x(t)$ having n data points x_i , an *a priori* polynomial vector γ_j and k so-called *orthogonal* functions ψ_j , representing subject motion and signal drift components (the error term for the linear regression of signal components) respectively, the percent BOLD signal change from baseline is calculated

$$\Delta P = 100 \times \frac{\hat{\alpha}(r_{\max} - r_{\min})}{B(x_i)},$$

where $\hat{\alpha}$ represents the voxel time series-to-reference waveform fit coefficient, r_{\max} and r_{\min} represent the maximum and minimum values of the reference vector defined above, and $B(x_i)$ represents the signal baseline, defined in turn as

$$B(x_i) = \sum_{i=1}^n \hat{B}_i n^{-1} \sum_{i=1}^n x_i + \sum_{j=1}^k \sum_{j=1}^n \hat{\gamma}_j n^{-1} \sum_{j=1}^n \varphi_j + \hat{\alpha} r_{\min}$$

meaning that ΔP is simply the echo-planar image intensity, weighted by the peak-to-peak variation of the reference time series, and divided by the linear combination of the “true” (neural activity-derived) voxel response and all “noise” contributors to the signal (B.D. Ward, *3dfim+ Reference Manual*, 2000).

Percent signal change was computed for individual subjects' MATCH condition SPMs using the AFNI program *3dfim+*. For the purposes of establishing a baseline, signal drift (γ) was assumed to be a first-order polynomial (*i.e.*, a linear trend) and motion components (ψ) were assumed to be negligible, since these components were removed from the raw EPI signal waveform during deconvolution. Only percent signal changes with an internal AFNI threshold of $R \geq 0.23$, corresponding to $p \leq 0.01$ (corrected), were considered to be statistically significant.

Activation volume (see also Ward 1998)

Activation volume (AV) is defined as the number of voxels significantly correlated with a reference waveform representing a task of interest. Specifically, given a constant rectangular prism voxel volume LWH over N voxels in a *deconvolved subject dataset* that exhibits an F -statistic (following the variable naming conventions in the “Percent Signal Change” section):

$$F = \frac{df_{B+x}[SSE(B) - SSE(B+x)]}{(df_B - df_{B+x})[SSE(B+x)]}$$

where SSE and df denote the residual sum of squares and degrees of freedom used in the deconvolution analysis, respectively, then

$$AV \equiv N(L \cdot W \cdot H)$$

Activation volume has been utilized in FMRI studies of auditory and motor cortex recruitment, as well as comparisons of neurological patients and control subjects following cortical recovery from stroke (Cramer, Weisskoff, Schaechter, Nelles, Foley, Finklestein and Rosen 2002; Lasota, Ulmer, Firszt, Biswal, Daniels and Prost 2003); however, it has been cautioned that activation volume should not be interpreted in the absence of other measures of brain function, since it is susceptible to intersubject variability (Saad, Ropella *et al.* 2003). Therefore, AV was utilized in the present study *only* in conjunction with voxel-task cross-correlation, percent signal change, and voxel entropy (see below).

Voxel-task cross-correlation (VTCC: see also Ward 1998)

The voxel-to-task cross-correlation (VTCC) is defined as the Pearson product-moment correlation coefficient between a voxel BOLD signal time series and a reference waveform (defined above). Following the variable naming conventions from the “Percent Signal Change” section,

$$\rho \equiv \frac{[\mathbf{x}(t) - \mu_{\mathbf{x}(t)}] \sum [\mathbf{r}(t) - \mu_{\mathbf{r}(t)}]}{\sqrt{\sum [\mathbf{x}(t) - \mu_{\mathbf{x}(t)}]^2 \sum [\mathbf{r}(t) - \mu_{\mathbf{r}(t)}]^2}},$$

such that, when signal drift (γ) is accounted for,

$$\rho = \frac{\left[\mathbf{x}(t) - \frac{\mathbf{x}(t) \cdot \gamma^T \gamma}{\gamma^T \gamma} \right] \sum \left[\mathbf{r}(t) - \frac{\mathbf{r}(t) \cdot \gamma^T \gamma}{\gamma^T \gamma} \right]}{\sqrt{\left[\mathbf{x}(t) - \frac{\mathbf{x}(t) \cdot \gamma^T \gamma}{\gamma^T \gamma} \right]^2 \sum \left[\mathbf{r}(t) - \frac{\mathbf{r}(t) \cdot \gamma^T \gamma}{\gamma^T \gamma} \right]^2}}$$

Note that motion components are not considered in the above equation since they were removed from the raw signal during deconvolution (B.D. Ward, *3dfim+ Reference Manual*, 2000).

VTCC was computed for individual subjects' MATCH condition SPMs using the AFNI program *3dfim+*. For the purposes of establishing a baseline, signal drift (γ) was assumed to be a first-order polynomial (*i.e.*, a linear trend). Only VTCCs with an internal AFNI threshold of $R \geq 0.23$, corresponding to $p \leq 0.01$ (corrected), were considered to be statistically significant.

Shannon entropy of the voxel time series (TSE)

In contrast to metrics based on BOLD signal intensity, many estimates of the amount of information in a time series based on information theory (also known as

“communications theory”) make no assumptions about the shape, origin, or stationarity of the signal under inspection, meaning that the conclusions based on such metrics are not biased due to underlying models of neurovascular coupling (Gonzalez Andino, Grave de Peralta Menendez, Thut, Spinelli, Blanke, Michel, Seeck and Landis 2000; de Araujo, Tedeschi, Santos, Elias, Neves and Baffa 2003). Of interest in the present study is an information theory-based metric known as the Shannon entropy of a time series (TSE), which was employed in order to quantify the “chaoticity” — that is, the disorder, or, more specifically, unstable aperiodicity (Shannon 1948) — of the BOLD response in discrete brain regions. This quantification of time series entropy is of interest in the present study because, by definition, the disorder of a time series is directly and positively related to the amount of information it carries, much as the instability in an audio signal is related to the complexity of the sound it represents (Shannon, 1948). Moreover, it has been suggested by electrophysiological studies that entropy is a direct aid to synchrony among cell populations since signal instability facilitates changes in neural firing rate oscillation (Fell, Fernandez and Elger 2003).

In the case of a voxel or group of voxels, such as fMRI regions of interest (ROIs), the Shannon entropy may be related to “chaotic” coupling between neural activity and the BOLD signal, or to chaos in the neural responses themselves, due to a surplus of neural connections prior to, for example, synaptic pruning. With respect to the former case, several instances exist in which neural activity and the BOLD signal become decoupled; for example, in patients with a history of stroke or vascular disorders, or subjects who have had caffeine or nicotine prior to their fMRI scan, or at very high and very low levels of neural activity (Logothetis, Pauls *et al.* 2001; Jacobsen, Gore, Skudlarski,

Lacadie, Jatlow and Krystal 2002; Laurienti, Field, Burdette, Maldjian, Yen and Moody 2002; Hamzei, Knab, Weiller and Rother 2003; Liu, Behzadi, Restom, Uludag, Lu, Buracas, Dubowitz and Buxton 2004; Krainik, Hund-Georgiadis, Zysset and von Cramon 2005). There is also some evidence that infants and toddlers have immature neurovascular coupling that may complicate interpretation of fMRI results as compared to adult fMRI data (Martin, Joeri, Loenneker, Ekatodramis, Vitacco, Hennig and Marcar 1999; Poldrack 2000). By age 8, however, the hemodynamic responses of children and adults are comparable (Kang, Burgund, Lugar, Petersen and Schlaggar 2003). In healthy, compliant adults and in children over three years of age, therefore, neural activity and the BOLD signal are believed to be tightly coupled (Martin, Joeri *et al.* 1999; Logothetis 2002). For this reason, it was inferred that, in the majority of subjects, voxel Shannon time series entropy (voxel TSE) arises from disorder in the underlying neural activity, and, given that the BOLD signal arises primarily from metabolic events at the synapse (Logothetis, 2002), this disorder likely occurs at synaptic connections. The precise relationship between BOLD signal chaos and neural activity, however, is as yet unknown. It was surmized that voxel TSE is directly correlated with the stability of synaptic integration, which is operationalized here as the ease with which multiple inputs undergo spatial or temporal summation at the synapse to create “coherent” output. Intuitively, spatial and temporal summation could be complicated by (a) an overabundance of inputs into a single output (*morphological* complexity), or (b) inefficiency of the connection at the synaptic junction (*connectivistic* complexity — due to, for example, a lack of Hebbian entrainment). This metric is therefore being applied in

the present study in order to determine whether TSE differs significantly in particular ROIs between pre- and post-consolidation groups.

The Shannon time series entropy (TSE) was calculated using the `wentropy` function in the MATLAB Wavelet Toolbox (The MathWorks, Inc., Natick, Massachusetts). As implemented in the `wentropy` program, the Shannon entropy $H(t)_{ROI}$, in Shannon bits (Sh), of the average time series across all voxels n meeting the threshold criterion (see above) in a region of interest was calculated as

$$H(t)_{ROI} \equiv -\frac{1}{n} \sum_{x=1}^n \sum_i x_i^2 \log(x_i^2),$$

where x_i represents a data point in the time series of a voxel x ($x \in ROI$). The Shannon entropy of the voxel time series is calculated directly from the bandpass-filtered voxel response vector as described in de Araujo *et al.* (de Araujo, Tedeschi *et al.* 2003). The contribution of response rates to the entropy therefore has a Poisson distribution, such that very low- and high-probability responses contribute little to the overall TSE, and the entropy calculation is biased toward x_i values that appear with moderate frequency. What this means conceptually, then, is that the voxel TSE is a quantification of how disordered a voxel response is, and consequently, it is also a measure of the amount of time- or frequency-encoded information that is potentially contained within the time series. With regard to the hypotheses outlined in the previous chapter, this means that the amount of disorder in voxel response can be used as an indirect measure of the amount of information carried in the BOLD response.

MEMORY CONSOLIDATION AND RETRIEVAL PERFORMANCE: EFFECTS OF STIMULUS MODALITY AND PAIR CONCORDANCE

Experience and intuition suggest that episodic memory recall declines with the passage of time. Yet episodic memory networks undergo a period of consolidation, during which neuronal connections are assumed to be optimized - meaning that the mnemonic circuits involved in the memory are indexed, transferred to isocortex, and made permanent. *In vivo* as well as *in vitro* studies in humans and higher primates have confirmed that decreased memory and memory trace lability, increased interneuronal firing coherence, decreased recruitment of memory-irrelevant (peripheral) brain areas, and heightened long-term depression (LTD) of firing coherence between these peripheral areas and mnemonic networks are hallmarks of episodic consolidation (Alvarez and Squire 1994; Eichenbaum 1996; Eichenbaum, Dusek *et al.* 1996; Eichenbaum, Schoenbaum *et al.* 1996; Chrobak and Buzsaki 1998b; Buchel, Coull *et al.* 1999; Abel and Lattal 2001; Eichenbaum 2001; Haist, Bowden Gore *et al.* 2001; Bodizs, Bokesy *et al.* 2002; Cantero, Atienza and Salas 2002a; Cantero, Atienza *et al.* 2002b). The “consolidation as optimization” hypothesis is further supported by the striking changes in proximal and distal dendritic morphology that have been observed in a consolidation-concomitant long-term potentiation (LTP) context (Bailey, Chen *et al.* 1992; Bailey, Montarolo *et al.* 1992; Zhang, Endo *et al.* 1997; Verzi 2004; Verzi, Rheuben and Baer 2005). Such changes in morphology have been shown to modulate synaptic integration, thereby modifying the computational functions of the neuron (Shepherd and Brayton 1987; Holmes and Levy 1990; Zador, Koch *et al.* 1990; Yuste and Denk 1995; Shepherd 1996; Hausser, Spruston

et al. 2000; London and Hausser 2005; Segev 2006). It would therefore be reasonable to expect that, as a consequence of this modified neuronal computation, post-consolidation networks would be comprised of fewer neurons that nevertheless individually exhibit more complex firing rate patterns. This expectation could be substantiated or falsified by evaluating pre- and post-consolidation glycolytic magnitude, firing rate entropy and magnitude, and the number of neural populations recruited for recall.

Conventional wisdom holds that, in spite of this putative consolidation-related mnemonic network optimization, recall performance declines with time, except when the items to be encoded are repeatedly presented; yet research into the neurodynamic consequences of the consolidation phenomenon at the whole-brain level have only recently been undertaken, and many of the published studies on the subject have focused on the hippocampal, rather than cortical and medial-temporal, contributions to recall.

The primary aim of the present fMRI study was to test the hypothesis that optimization does indeed enhance retrieval efficiency, where an “enhanced retrieval efficiency” is defined, for the purposes of this study, as (a) improvements in behavioral performance — subject response time and accuracy — and (b) decreased overall metabolic demand. The working hypothesis was tested in 93 subjects on a computer-based bimodal paired associates (delayed match-to-sample or DMTS) task, and in 13 other subjects on an fMRI-based unimodal version of the same task.

It should be noted that both behavioral and physiological results are interpreted in the present study in the absence of direct (*e.g.*, molecular or cellular) evidence that memory consolidation occurred over the 7-day interval. *In this context, a MATCH*

condition accuracy significantly greater than chance (i.e., a normalized accuracy of \geq 66%) was taken as evidence that consolidation had indeed occurred, since (ostensibly) neither successful retrieval nor recognition effects can occur after intervals longer than 6 hours in the absence of stage IA protein synthesis (Abel and Lattal 2001; Walker 2004; Walker and Stickgold 2004; Wang, Hu et al. 2006)

Please refer to the *Methodology* chapter for details of the data acquisition and analysis procedures.

BEHAVIORAL RESULTS

Subject performance, operationalized as reaction time and accuracy, were assessed with two ANOVAs. Whereas fMRI and CBT training sessions differed only in the modality of stimulus presentation, testing sessions differed with respect to both environment and presentation modality. Therefore, the first MANOVA tested the effect of paradigm type (fMRI versus computer-based testing, CBT) and time point (pre- versus post-consolidation) on reaction time and accuracy for previously learned (MATCH or delayed match to sample, DMTS) stimuli, mismatched stimuli, and control stimuli. Whereas MATCH and MISMATCH reaction times and accuracy were expected to differ between the two paradigm types due to attentional demands, CONTROL performance was predicted to remain constant across paradigm types and time points, and serve instead as a measure of subject compliance. Furthermore, it was predicted that accuracy would increase whereas reaction time would decrease as a function of time point but not paradigm type, consistent with the stated hypothesis that task performance would improve with memory consolidation.

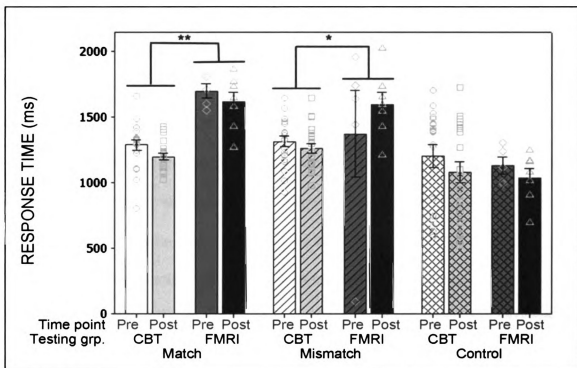


Figure 5 Mean reaction times for the paired-associate task by testing group (computer-based, CBT, versus FMRI subjects), pair concordance (matched, mismatched, or control), and time point (pre- versus post-consolidation). FMRI subjects, who were given unimodal (visual) training and testing stimulus pairs, were slower at identifying both correctly-matched and mismatched stimulus pairs than CBT subjects, who were given dual-modal (visual and auditory) training and testing stimulus pairs. This effect was seen at both pre- and post-consolidation time points. However, neither FMRI nor CBT subjects were significantly faster at identifying correctly-matched stimulus pairs after one week. Neither group improved with respect to reaction time with consolidation for control stimuli, nor did CBT and FMRI subjects differ significantly with respect to reaction time for control stimuli at either time point. Error bars represent standard errors of the means. * $p < .05$.

Reaction time (H. 1)

Reaction time was defined as the response time, in msec, between the presentation of stimulus pairs and button press response to matched (MATCH reaction time), mismatched (MISMATCH reaction time), and control (CONTROL reaction time) stimulus presentations separately. A two-way (2x2) ANOVA using paradigm type (FMRI versus computer-

based training/testing, CBT) and time point (pre- versus post-consolidation) as independent factors indicated that neither FMRI nor CBT subjects were faster at identifying previously-learned (correctly-matched) stimulus pairs at post-consolidation than at pre-consolidation (FMRI pre-consolidation matched associate reaction time $\mu \pm \sigma = 1701.8 \pm 120.4$ msec, post-consolidation reaction time $\mu \pm \sigma = 1615.7 \pm 207.3$ msec; CBT pre-consolidation matched-associate reaction time $\mu \pm \sigma = 1288.9 \pm 174.8$ msec, post-consolidation reaction time $\mu \pm \sigma = 1201.4 \pm 112.6$ msec; $F(1, 54) = 2.22$, $MSE = 23399$, $p = 0.119$), although pre- and post-consolidation FMRI subjects were slower at identifying correctly-matched associates than their CBT counterparts ($F(1, 54) = 67.07$, $MSE = 23399$, $p < .001$). Moreover, FMRI subjects were slower at identifying mismatched stimuli than were CBT subjects at both pre- and post-consolidation time points (FMRI pre-consolidation mismatched associate reaction time $\mu \pm \sigma = 1376.0 \pm 739.0$ msec, post-consolidation reaction time $\mu \pm \sigma = 1599.6 \pm 253.2$ msec; CBT pre-consolidation mismatched-associate reaction time $\mu \pm \sigma = 1315.6 \pm 182.3$ msec, post-consolidation reaction time $\mu \pm \sigma = 1262.3 \pm 164.2$ msec; $F(1, 54) = 4.87$, $MSE = 74470$, $p = 0.032$), although there was no significant difference in reaction time for mismatched stimuli as a function of time (consolidation: $F(1, 54) = 1.18$, $MSE = 74470$, $p = 0.314$). The reaction time findings thus contradicted the predictions following from H. 1. (See Figure 5 and Appendix A.)

Accuracy (H. 1)

Accuracy was defined as the number of correct identifications of matched (MATCH accuracy), mismatched (MISMATCH accuracy), and control (CONTROL accuracy) stimulus

presentations separately. Using a two-way 2x2 ANOVA, FMRI and computer-based training/testing (CBT) subjects were found to exhibit comparable accuracy on correctly-matched stimulus pairs (FMRI pre-consolidation accuracy $\mu \pm \sigma = 76.79 \pm 9.13\%$, post-consolidation accuracy $\mu \pm \sigma = 71.29 \pm 15.35\%$; CBT pre-consolidation accuracy $\mu \pm \sigma = 73.74 \pm 11.79\%$, post-consolidation accuracy $\mu \pm \sigma = 79.06 \pm 11.56\%$), indicating that neither FMRI nor CBT subjects differed with respect to the number of false negatives ($F(1, 54) = 0.350$, $MSE = 143.80$, $p = 0.554$), nor did the number of false negatives increase or decrease in either group as a function of time ($F(2, 54) = 1.370$, $MSE = 143.8$, $p = 0.264$). FMRI subjects were found to exhibit lower accuracies, however, for mismatched stimulus pairs (pre-consolidation accuracy $\mu \pm \sigma = 72.39 \pm 10.74\%$, post-consolidation accuracy $\mu \pm \sigma = 66.54 \pm 15.06\%$) than their CBT counterparts (pre-consolidation accuracy $\mu \pm \sigma = 79.22 \pm 13.60\%$, post-consolidation accuracy $\mu \pm \sigma = 82.78 \pm 13.30\%$), indicating that the number of false positives were higher in FMRI subjects than in CBT subjects ($F(1, 54) = 6.74$, $MSE = 181.1$, $p = 0.012$), although neither group exhibited a significant change in accuracy for mismatched stimulus pairs as a function of time ($F(2, 54) = 0.65$, $MSE = 181.1$, $p = 0.526$). These findings suggest that both FMRI and CBT subjects identified the correctly matched associates learned during training with statistically equal accuracy, but FMRI subjects were more likely to incorrectly identify mismatched stimuli as a previously learned paired associate (See Figure 6).

Moreover, the putatively post-consolidation subjects in both CBT and FMRI groups identified the previously-learned paired associates as accurately as pre-consolidation subjects, but, conversely, subjects neither improved at correct rejections of

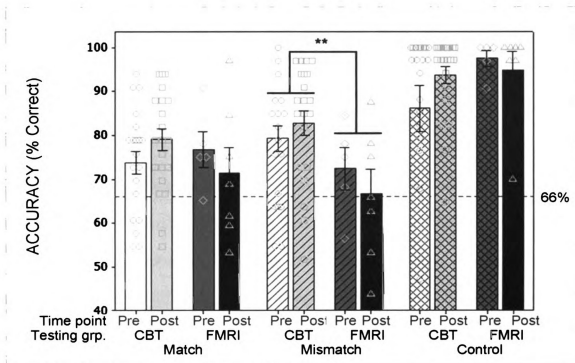


Figure 6 Mean subject accuracy for the paired-associate task by testing group (computer-based, CBT, versus FMRI subjects), pair concordance (matched, mismatched, or control), and time point (pre- versus post-consolidation). FMRI subjects, who were given unimodal (visual) training and testing stimulus pairs, were more likely to identify mismatched associates as matched associates (exhibited more false positives) than CBT subjects, who were given dual-modal (visual and auditory) training and testing stimulus pairs. However, neither FMRI nor CBT subjects improved with respect to the number of false positives over the putative memory consolidation period, nor did either group improve with respect to accuracy with consolidation for matched associates (false negatives) or control stimuli. CBT and FMRI subjects did not differ significantly with respect to accuracy for correctly-matched associates or control stimuli at either time point. Symbols (light grey) indicate individual data points; error bars represent standard errors of the means. * $p < .05$; ** $p < 0.01$.

mismatched stimuli nor improved at accurately identifying learned associates (correctly-matched stimulus pairs) as a function of memory consolidation. An absence of statistically significant effects of time (consolidation: $F(1, 54) = 1.43$, $MSE = 277.6$, $p = 0.238$) or testing group (CBT versus FMRI: $F(1, 54) = 1.03$, $MSE = 277.6$, $p = 0.316$) on accuracy for control stimuli indicated equivalent subject task compliance in all four

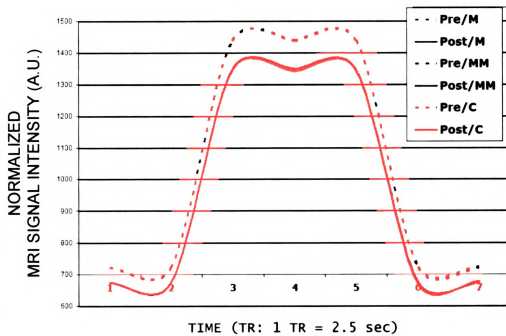
conditions (FMRI pre-consolidation accuracy $\mu \pm \sigma = 97.50 \pm 4.07\%$, post-consolidation accuracy $\mu \pm \sigma = 94.79 \pm 11.13\%$; CBT pre-consolidation accuracy $\mu \pm \sigma = 86.13 \pm 24.01\%$, post-consolidation accuracy $\mu \pm \sigma = 93.72 \pm 9.40\%$). Thus, accuracy did not appear to reflect memory consolidation effects, contradicting H. 1 (see Figure 6).

Thus, the multivariate ANOVA performed on CBT and FMRI subject response time and accuracy failed to confirm the stated hypothesis (H. 1) that the putative period of memory consolidation was positively correlated with subject recall performance, although the observed differences in recall performance between the CBT (bimodal) and FMRI (unimodal) paradigms may also indicate that such changes are sensitive to the number and type of modalities used to present the stimulus pairs to be learned. Interestingly, however, the conservation of subject response time and accuracy across pre- and post-consolidation subject groups suggests the possibility that access to memory traces was not reduced over the consolidation period, over and above a reduction in trace neurons as a consequence of the intraneuronal Hebbian competition that is believed to occur within hours of episodic memory encoding (Kida, Josselyn *et al.* 2002; Bozon, Davis *et al.* 2003; Bozon, Kelly *et al.* 2003).

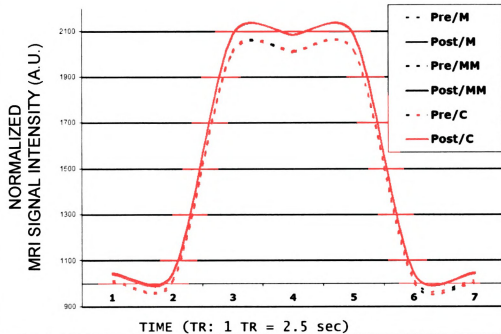
Figure 7 Group statistical parametric maps (SPMs) of voxel BOLD signal correlation with presentation of match, mismatch, and control-condition stimuli by region of interest. Voxel BOLD signal changes shown are significant at a full-model $F = 3.786$ ($p = 0.001$, corrected); colors represent whether changes are positive (yellow) or negative (blue) relative to the baseline. Group SPMs were obtained by studentizing individual BOLD datasets and registering them to a common Talairach-Tourneaux coordinate system (Talairach and Tourneaux, 1988). Datasets were then subjected to cluster analysis using a minimal 5mm, 10 μ l Gaussian kernel (to correct for type II error: see Salmond, Ashburner, et al. 2002; Geissler, Lanzenberger, et al. 2005) and averaged by condition. The location of the calcarine fissure (visual area V1) is shown on an axial slice in each case for reference (yellow boxes). Hemodynamic response functions for representative subjects were also obtained for ectorhinal area 36 (red box) and visual area V3/19 (green box) and are shown in Figure 9. *Abbreviations:* *Fus*, fusiform gyrus; *Ins*, *AIC*, anterior insular complex; *STG*, superior temporal gyrus; *IPL*, inferior parietal lobule; *SPL*, superior parietal lobule; *DG*, dentate gyrus; *pul*, pulvinar nucleus of the thalamus, *Ver*, cerebellar vermis, *Cal*, calcarine fissure. *Numbers* represent Brodmann areas: *3a*, digit somatosensory area; *4*, digit motor area; *31*, posterior cingulate cortex.

Figure 8 Estimated event-related average hemodynamic response functions (HRFs) for pre- (dotted line) and post- (solid line) consolidation right hemisphere ectorhinal cortex (EcRC, Brodmann area 36) and visual area V3 (Brodmann area 19) seed locations indicated in Figure 7. HRFs were obtained from the same studentized representative subject data as in Figure 7. Talairach-Tourneaux coordinates for each region are also given (see Talairach and Tourneaux, 1988).

Ectorhinal Cortex: (41,-33,-6)



Visual Area v3: (36,-83,7)



CHANGES IN BOLD PHYSIOLOGY WITH CONSOLIDATION

Initial three-way 2x11(2) ANOVAs were performed only on fMRI subject data to test the effects of the training-testing interval (“time point”: day 0 versus day 7), region of interest (ROI), and ROI hemisphere (left versus right) on various physiological measures – metabolic demand (percent BOLD signal change from baseline, PC), cortical recruitment (activation volume, AV), BOLD signal rate (voxel-task cross-correlation, VTCC), and BOLD signal entropy (time series Shannon entropy, TSE) – collapsed across all ROIs, using hemisphere as a nested variable within ROI. Inspection of the three-way ANOVA results indicated that only the “time point” factor had had significant effects; therefore, the effect of the putative consolidation period on regional metabolic demand, cortical recruitment, and BOLD response rates were subsequently assessed with a main-effect ANOVA, using time point as the independent factor. Physiological measures were collapsed across cerebral hemispheres and subjected to *t*-tests using “time point” as the grouping variable. (See also *Appendix B*.)

Group and representative subject percent BOLD signal change SPMs obtained from studentized data are shown for the *x*, *y*, and *z* planes crossing through entorhinal area 36 in Figure 7, and estimated studentized hemodynamic response functions from selected voxels from entorhinal cortex and area V3 are shown in Figure 8. The reader may refer to these figures to supplement the discussion of results in the following sections.

ROI analysis of metabolic demand (H. 2)

The main-effect ANOVA indicated a significant effect of time point on regional metabolic demand over all ROIs ($F(2,286) = 81.068$, $MSE = 2.003$, $p < 0.001$). However, post-hoc analysis by Tamhane's T2, applied due to heteroscedasticity between pre- and post-consolidation subjects (Levene's test), failed to return any significant differences at

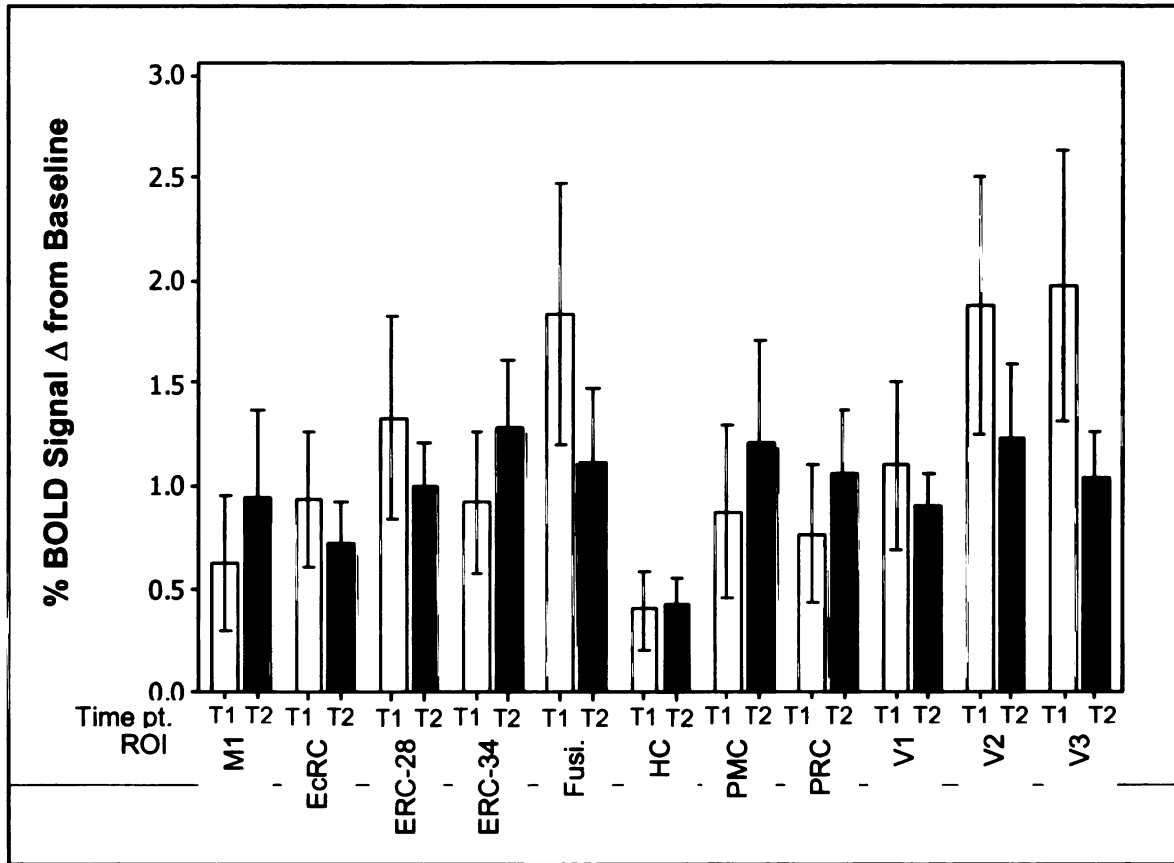


Figure 9 Percent BOLD signal change from baseline (BOLD signal magnitude) in significantly task-correlated voxels constituting regions of interest at pre- and post-consolidation for matched associates. Analysis by main effect ANOVA indicated a significant difference in BOLD magnitude between pre- (T1) and post- (T2) consolidation subjects ($p < 0.001$) overall, however, post-hoc analysis by Tamhane T2 failed to indicate any differences in per-region signal change with consolidation. These findings suggest that the BOLD response magnitude is not affected by consolidation in significantly task-correlated voxels in these regions. Error bars indicate standard errors.

the level of the individual ROIs. These findings may therefore suggest that decreases in metabolic demand (pre-consolidation BOLD change = $1.145 \pm 0.123\%$, post-consolidation BOLD change = $0.993 \pm 0.114\%$) were only apparent when all regions were pooled, possibly due to the large per-ROI variance in the BOLD signal change data. The present data thus failed to indicate any changes in metabolic demand with consolidation despite the observed decrease in per-region recruitment, contradicting some of the predictions following from H. 2 (Figure 9).

Interestingly, the fusiform gyrus was found to exhibit significant differences between pre- ($6532.292 \pm 538.623 \mu\text{L}$) and post- ($5340.595 \pm 498.668 \mu\text{L}$) consolidation activation volumes (a difference of 18.24%, $p \leq 0.05$) in the right hemisphere. The left-hemisphere fusiform gyrus did not differ significantly with respect to activation volume with respect to time point.

ROI analysis of cortical recruitment (H. 2)

The ANOVA also indicated a significant effect of time point on cortical recruitment in response to the presentation of previously-learned (matched) stimulus pairs ($3885.042 \pm 114.835 \mu\text{L}$, post = $3148.126 \pm 106.316 \mu\text{L}$, an average decrease of 18.97%; $F(2,286) = 1010.692$, $MSE = 1.76 \times 10^9$, $p < 0.001$). Post-hoc analysis by Tamhane's T2, applied due to heteroscedasticity between pre- and post-consolidation subjects (Levene's test), further indicated that post-consolidation subjects used a smaller cortical volume concomitant to recall than pre-consolidation subjects in the fusiform gyrus (pre = $6314.938 \pm 380.864 \mu\text{L}$, post = $5408.875 \pm 352.611 \mu\text{L}$, a 14.35% reduction in recruitment;

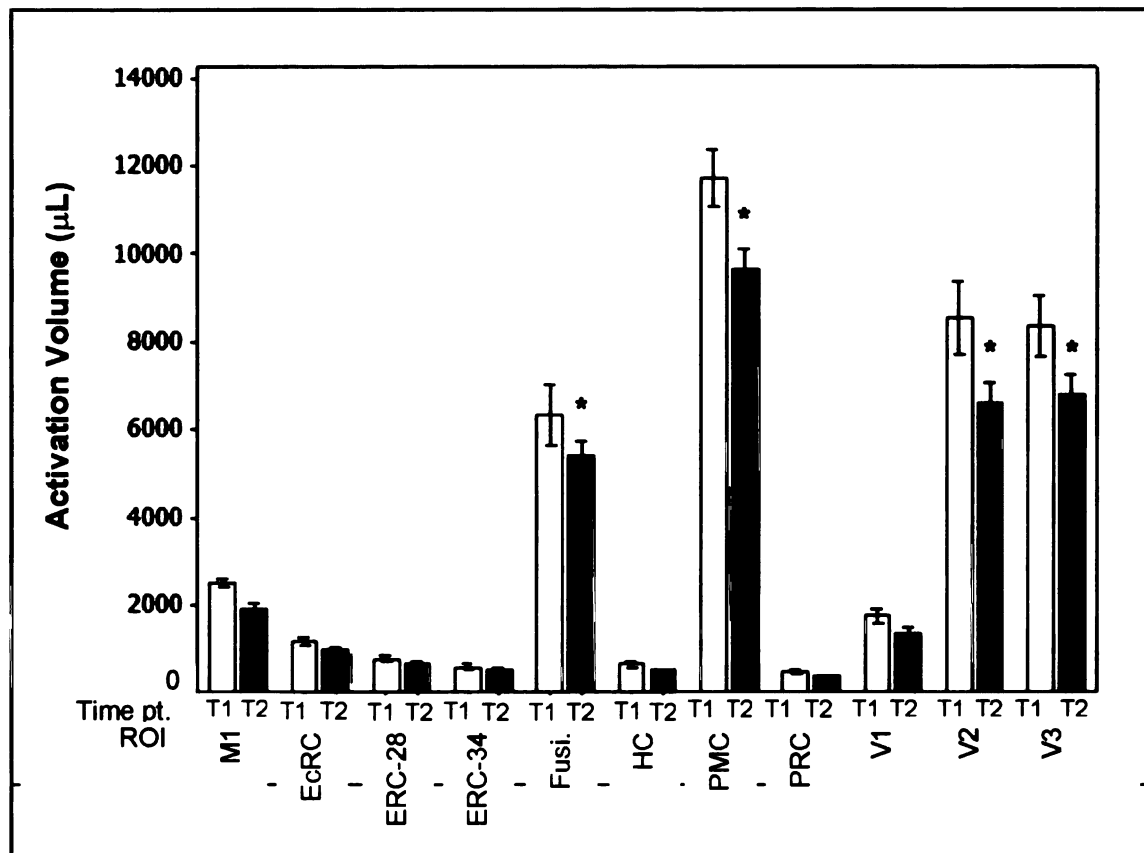


Figure 10 Activation volume of significantly task-correlated voxels at pre- and post-consolidation for matched associates. Analysis by main effect ANOVA indicated a significant difference in activation volume between pre- and post-consolidation subjects overall ($p < 0.001$). Post-hoc analysis by Tamhane T2 further indicated significant reductions in cortical recruitment in the fusiform gyrus, premotor cortex, and visual areas V2 and V3. These findings suggest that the number of significantly task-correlated voxels is affected by consolidation in premotor areas, area V2, and ventral visual areas, but not in medial temporal, primary motor, or primary visual areas. Error bars indicate standard errors; *indicates a significant difference in activation volume, $p < 0.05$. ROI significances computed by post-hoc Tamhane T2.

$p \leq 0.05$), premotor cortex (pre = 11717.083 ± 380.864 μL , post = 9617.042 ± 352.611 μL , a 17.92% reduction; $p \leq 0.05$), and visual areas V2 (pre = 8528.167 ± 380.864 μL , post = 6586.702 ± 352.611 μL , 22.77% reduction; $p \leq 0.05$) and V3 (pre = 8356.250 ± 380.864 μL , post = 6791.256 ± 352.611 μL , 18.73% reduction; $p \leq 0.05$). (See Figure 10.)

ROI analysis of BOLD response rate (VTCC; H. 3)

A main-effects ANOVA was also applied to the cross-correlation, or covariance, between the voxel BOLD response and a binary reference waveform representing the presentation of previously-learned (correctly-matched) stimulus pairs. This cross-correlation is denoted the VTCC for the present study, and represents the “goodness-of-fit” of the voxel response vector to the binary waveform, such that larger VTCC values correspond to a better fit between the two vectors, while smaller VTCC values correspond to a poorer fit. The VTCC therefore approximates the rate of the BOLD response relative to the presentation of correctly-matched stimuli, both in terms of time-to-peak (BOLD signal rising phase) and peak-to-baseline (falling phase).

The main-effect ANOVA indicated a significant difference in overall VTCC between pre- and post-consolidation subjects, such that post-consolidation VTCC (mean $R = 0.330 \pm 0.012$) was greater than pre-consolidation VTCC (mean $R = 0.475 \pm 0.011$) when all ROIs were pooled ($F(2,286) = 1365.942$, $MSE = 0.018$, $p < 0.001$). VTCC data was homoscedastic (Levene’s test), and post-hoc analysis by the Tukey HSD test for unequal sample sizes confirmed that regional VTCCs were indeed greater in post-consolidation subjects than in pre-consolidation subjects by an average of 30% ($p \leq 0.05$) in all ROIs studied, including primary motor cortex. These findings confirmed the prediction (H. 3) that mean regional BOLD signal response rates would increase significantly over the putative consolidation interval (Figure 11).

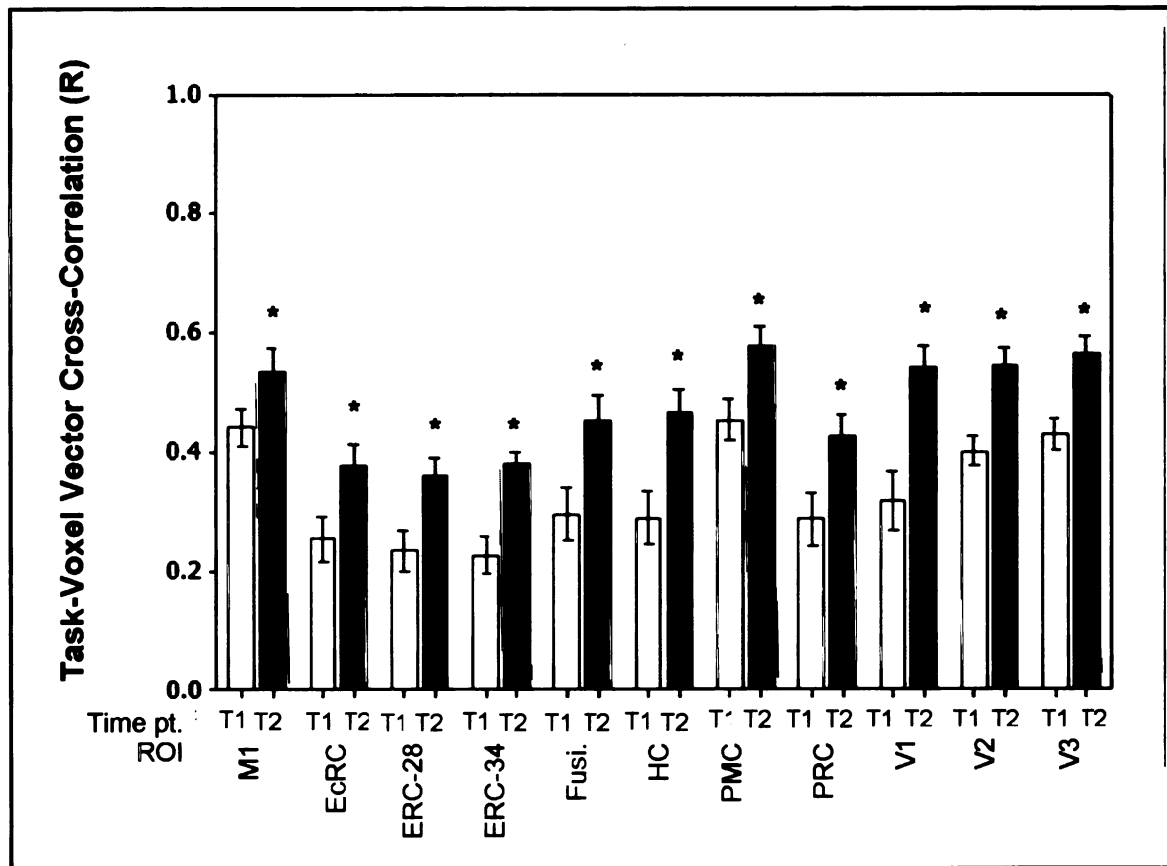


Figure 11 Mean voxel BOLD response-stimulus presentation covariance (voxel-task cross-correlation, VTCC) in significantly task-correlated voxels constituting regions of interest at pre- (T1) and post- (T2) consolidation for matched associates. Analysis by main effect ANOVA indicated a significant difference in VTCC between pre- and post-consolidation subjects overall ($p < 0.001$), and post-hoc analysis by Tukey HSD revealed significant differences in VTCC in all areas ($p < 0.05$). These findings suggest that the BOLD-task covariance is affected by consolidation in significantly task-correlated voxels in medial temporal, motor, premotor, and visual regions. Error bars indicate standard errors; *indicates a significant difference in VTCC, $p < 0.05$. ROI significances computed by post-hoc Tukey HSD unequal-N test.

Interestingly, primary motor cortex was observed to exhibit significant differences between pre- and post-consolidation VTCC in the right, but not left, hemisphere (right-hemisphere pre-consolidation M1 VTCC = 0.437 ± 0.055 , right-hemisphere post-consolidation M1 VTCC = 0.556 ± 0.051 , $p \leq 0.05$). As this was the only unilateral effect in an otherwise globally-affected VTCC dataset, and subjects responded only with their right hand, this surprising finding may suggest that left hemisphere primary motor cortex

may be exempt from the purported effects of the consolidation interval, thereby acting as a “negative control” area as previously proposed. The involvement of right hemisphere M1 in right-handed tasks has been reported anecdotally in the fMRI literature, but there is as yet no clear consensus on its anatomical basis or its function.

RETRIEVAL ORIENTATION AND CORTICAL REINSTATEMENT: INTERPRETATION OF PHYSIOLOGICAL FINDINGS IN THE CONTEXT OF SIGNAL ENTROPY

The above results suggest that episodic consolidation correlates with a generalized decrease in voxel recruitment in response to matched associates in premotor areas, area V2, and ventral visual areas, but not in medial temporal, primary motor, or primary visual areas, although the BOLD signal in all ROIs (with the exception of left-hemisphere M1) exhibited a faster response rate with respect to matched stimulus presentation in post-consolidation subjects relative to pre-consolidation subjects. Furthermore, per-ROI BOLD signal magnitudes in response to matched associates, corresponding to metabolic demand, did not appear to change significantly with consolidation *in spite of this decreased recruitment*.

One interpretation of these findings (see H. 4) is that the instantiation of differential visual processing strategies with consolidation — particularly, covert shifts in attention from local visual stimulus features to more global features (“retrieval orientation”) — and facilitation of network reinstatement through consolidation-related increases in the synaptic strength among trace neurons (“cortical reinstatement”) enhance the ability of trace neurons and ancillary retrieval networks to exchange and process information through synaptic integration, such that fewer neurons are required for trace encoding and/or retrieval (Rugg and Wilding 2000; Lockhart 2002; Robb and Rugg 2002; Vaidya, Zhao *et al.* 2002; Mulligan and Lozito 2006). This hypothesis is testable in that (a) it predicts the engagement and disengagement of particular brain regions upon recall, which may be revealed through parametric manipulation of memory task parameters, and (b) it predicts that the neural networks involved in the sensory processing of learned

mnemonic stimuli will differ with respect to the volume of information carried by the neurons constituting those networks. The former prediction has been tested successfully with functional MRI, but, surprisingly, the latter prediction has not (e.g., Rugg and Wilding 2000; Mulligan and Lozito 2006).

In the present study, the regions involved in sensory processing of matched associates were the fusiform gyrus and visual areas V1, V2, and V3. However, BOLD signal entropy in area V1 was *not* expected to differ significantly between time point groups due to the absence of corticocortical or corticothalamic afferents from attentional areas onto V1, which would ostensibly control differential sensory processing of presented associates (Rao 2005). Interestingly, the present data indicated that recruitment of the fusiform gyrus and visual areas V2 and V3, as well as premotor cortex — but not area V1 — differed substantially between pre- and post-consolidation subjects. Given that neither metabolic demand nor VTCC were observed to differ from region to region, it was of interest in the present study to attempt to quantify the entropy of BOLD signals in ROIs that exhibited significantly reduced cortical recruitment as a function of the time point factor.

A main-effect ANOVA on the Shannon entropy of the mean regional BOLD signals (time series entropy, TSE; see the *Methodology* chapter), a complexity metric, using time point as the independent factor, indicated a significant effect of time point on TSE overall ($F(1,242) = 10.355$, $MSE < 0.001$, $p \leq 0.001$), such that regional post-consolidation BOLD signal entropy (see the *Methodology* chapter) was greater than pre-consolidation signal entropy overall (pre-consolidation TSE = 0.032 ± 0.001 Sh, post-

consolidation TSE = 0.034 ± 0.001 Sh, a 5.88% increase). Post-hoc analysis by Tamhane T2, employed to compensate for heteroscedasticity in the TSE data, further indicated significant effects of time point on TSE at the ROI level in the fusiform gyrus (pre-consolidation TSE = 0.048 ± 0.002 Sh, post-consolidation TSE = 0.055 ± 0.002 Sh, a 12.73% increase) and visual areas V2 (pre-consolidation TSE = 0.066 ± 0.002 Sh, post-consolidation TSE = 0.073 ± 0.002 Sh, a 9.59% increase) and V3 (pre-consolidation TSE = 0.069 ± 0.002 Sh, post-consolidation TSE = 0.073 ± 0.002 Sh, a 5.48% increase), but not premotor cortex (pre-consolidation TSE = 0.103 ± 0.002 Sh, post-consolidation TSE = 0.104 ± 0.002 Sh), which had also exhibited differential cortical recruitment between the time point groups. Further post-hoc analysis by Tamhane T2 indicated a significant difference between pre- and post-consolidation TSE in the right (pre = 0.069 ± 0.002 Sh, post = 0.075 ± 0.002 Sh, +8.00%, $p \leq 0.05$), but not left (pre = 0.068 ± 0.002 , post = 0.072 ± 0.002 , +5.56%), hemisphere visual area V3. (See Figure 12.)

Thus, of the four ROIs — fusiform gyrus, premotor cortex, and visual areas V2 and V3 — that had previously been found to exhibit decreased cortical recruitment between pre- and post-consolidation subjects, three — fusiform gyrus, V2, and V3 — were also observed to exhibit increased signal entropy. However, these observations are likely to be mediated through a third explanatory variable, since premotor cortex, which exhibited differential activation volume as a function of time point, did not exhibit

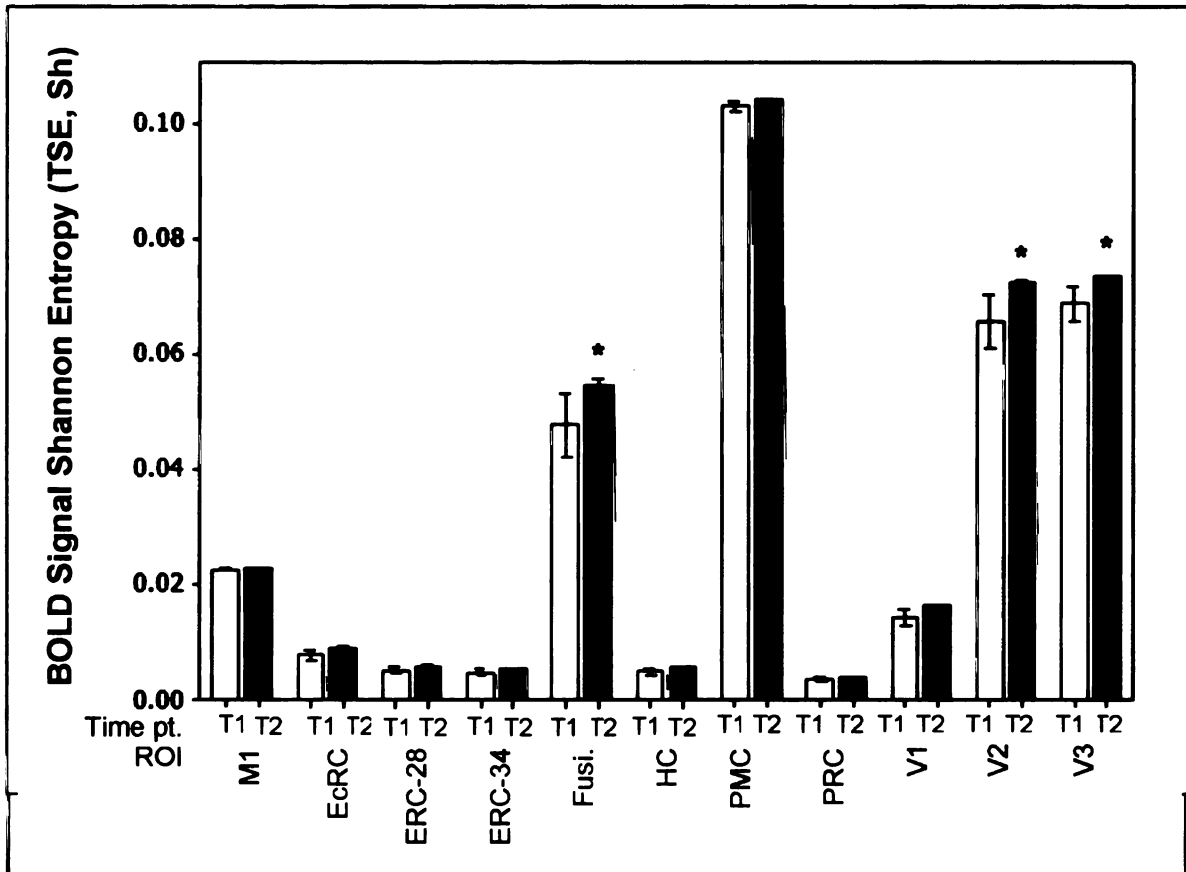


Figure 12 Mean BOLD signal Shannon entropy (TSE) in significantly task-correlated voxels constituting regions of interest at pre- and post-consolidation for matched associates. Analysis by main effect ANOVA indicated a significant difference in BOLD TSE between pre- and post-consolidation subjects overall ($p \leq 0.001$). Post-hoc analysis by Tamhane T2 further indicated significantly greater signal entropy in the fusiform gyrus and visual areas V2 and V3 ($p < 0.01$). These findings suggest that the BOLD signal entropy is affected by consolidation in significantly task-correlated voxels in extrastriate ventral visual areas, but not in medial temporal, premotor, or primary motor or visual cortex. Error bars indicate standard errors; * indicates a significant difference in TSE, $p < 0.01$. ROI significances computed by Tamhane T2.

differential signal entropy, whereas the converse was true for perirhinal cortex. It should be noted, however, that ROIs that are comparatively more active at the per-neuron level need not exhibit comparatively greater signal entropy. For example, the BOLD signal may increase in amplitude while maintaining its spectral characteristics; in this case, since no additional frequency components are introduced into the vector spectrum, its Shannon entropy will be equivalent. This could be the case with an attentional area such as the premotor cortex, which might exhibit an increased post-consolidation spectral power concomitant to “driving” descending (attentional) input to, for example, visual cortex, but would not necessarily exhibit an increase in its time series entropy.

It is also possible that one or both of these variables are modulated by different physiological effects. For example, premotor cortex, which appears to function as an attentional as well as motor planning area (Nobre, Sebestyen *et al.* 1997), and therefore a possible source of modulation of sensory processing, would only exhibit appreciable differences in firing rate entropy in the synaptodendritic compartments of visual cortices. As another example, perirhinal cortex, which functions in the maintenance and consolidation of pair codings (Eichenbaum, Schoenbaum *et al.* 1996; Nadel, Samsonovich *et al.* 2000), may not be subject to the putatively consolidation-related cortical recruitment effects reported for premotor, visual, and ventral visual areas, since it likely serves as a “linkage site” between trace networks for paired stimuli. Moreover, the present data are not sufficient to make a conclusive case for the hypothesis that increases in BOLD signal entropy and decreases in cortical recruitment are directly related, or even that the entropy of an indirect measure of neural activity such as the BOLD signal corresponds to the entropy of neural spike train vectors. Therefore, although the present

findings are probative, more studies are needed both to reproduce a correlation between BOLD signal entropy and cortical recruitment with consolidation, and to directly test the correspondence between BOLD and electrophysiological entropy. If this link is established by future research, however, BOLD signal entropy might be utilized to draw inferences about changes in the nature and degree of neural activity by noninvasive means.

Thus effects of both retrieval orientation and cortical reinstatement — two means by which episodic systems could become optimized with consolidation — may have been substantiated in the present dissertation. Retrieval orientation effects may be argued to have been evinced in that extrastriate visual areas were significantly less recruited, and their BOLD signals more complex, in post-consolidation subjects, phenomena that may be related to more “efficient” (*e.g.*, holistic) stimulus processing and differential neuronal firing rate responses in post-consolidation subjects. However, the more robust finding predicted in the context of H. 4 – that right-hemisphere (global) ventral visual stream regions would exhibit higher metabolic demands in post-consolidation subjects, was not borne out. Potential novel correlates of cortical reinstatement were also observed, in that BOLD signal response rates (VTCC) increased globally; again, however, future studies are required to demonstrate that this effect is not due to, for example, angiogenesis over the consolidation interval.

These findings are summarized in Table 5.

Table 5 A qualitative review of the results presented in the present chapter and the conclusions drawn from them. “Per-neuron activity” was determined by dividing the metabolic demand (PC) of an ROI by the extent of its recruitment (AV) to obtain a rudimentary $\Delta P/\text{mm}^3$ estimate. Abbreviations: *N/C*, no change; *fusi.*, fusiform gyrus; *Vx*, visual area x.

	Demand	Recruitment	Entropy	Resp. Rate	Conclusion
Medial-temporal	N/C	N/C	N/C	increased	Consolidation increases speed of recruitment only
Primary visual	N/C	N/C	N/C	increased	
Primary motor	N/C	N/C	N/C	increased	
Premotor*	N/C	decreased	N/C	increased	Consolidation correlates with higher per-neuron activity but <i>not</i> greater signal entropy
V2, V3, fusi.	N/C	decreased	increased	increased	Consolidation correlates with higher per-neuron activity <i>and</i> greater signal entropy

*It should be noted that, although Brodmann area 6 is referred to in this table and the rest of the dissertation as *premotor cortex* or *PMC* to follow convention, it does in fact appear to be an attentional (specifically, “motor-attentional”) region. See the *Regions of Interest* chapter for the relevant discussion.

NEURODYNAMICS OF EPISODIC MEMORY CONSOLIDATION: CONCLUSIONS AND DISCUSSION

In the introduction to the present dissertation, it was proposed that an interval of episodic memory consolidation may function as a temporal window during which memory traces are optimized and the memory retrieval process made more efficient. This “efficiency” was operationalized schematically, but not quantitatively, as an increase in, or conservation of, subject retrieval performance (useful output) — reaction time and accuracy — on a delayed-match-to-sample (DMTS) task and a decrease in regional metabolic intensity (energy expenditure), characterized by both regional BOLD magnitude and the degree of cortical recruitment, or the number of voxels significantly correlated with the DMTS task. By this stipulative definition, increased efficiency over a consolidation interval could be argued to have occurred in any of several cases. Namely, the useful output-to-energy expenditure ratio used to illustrate the present work’s approach to retrieval efficiency would increase had (a) subject performance on the DMTS task improved without a corresponding decrease in metabolic demand or cortical recruitment; (b) metabolic demand *and* cortical recruitment decreased without a corresponding improvement in subject performance; (c) metabolic demand decreased without corresponding improvements in cortical recruitment or subject performance; or (d) cortical recruitment decreased while subject performance and cerebral metabolic demand was conserved. The results provided in the present work indicate that, over a seven day interval putatively corresponding to a Stage I consolidation period, retrieval efficiency did in fact improve as in case (d). That is, neither subject response

Table 6 Summary of the predictions (“Predicted”) and findings (“Actual”) for the present study with respect to subject performance (reaction time and accuracy), as well as physiological descriptions of the shape and temporal characteristics of the BOLD signal on the delayed match-to-sample portions of the paired associates task. Both behavioral and physiological findings are represented as being greater (+), less (–), or equal (no change, N/C) in post-consolidation subjects relative to pre-consolidation subjects. *Abbreviations:* HC, hippocampus, ERC, entorhinal cortex, EcRC, ectorhinal cortex, PRC, perirhinal cortex, V1, V2, V3, visual areas 1-3, FUSI, fusiform gyrus, M1, primary motor cortex, PMC, premotor cortex; RT, subject reaction time, Acc, accuracy; *BOLD mag.*, percent BOLD signal change from baseline, *recruitment*, cortical recruitment (activation volume), *BOLD rate*, BOLD signal response rate (voxel-task cross-correlation).

	RT		ACC		BOLD MAG.		RECRUITMENT		BOLD RATE		TSE
	Predicted	Actual	Predicted	Actual	Predicted	Actual	Predicted	Actual	Predicted	Actual	
HC											
ERC					N/C	N/C	—	N/C	+	+	N/C
EcRC					N/C	N/C	—	N/C	+	+	N/C
PRC					N/C	N/C	—	N/C	+	+	N/C
					N/C	N/C	—	N/C	+	+	N/C
V1					—	N/C	—	N/C	+	+	N/C
V2	—	N/C	+	N/C	—	N/C	—	—	+	+	+
V3					—	N/C	—	—	+	+	+(3)
FUSI					—	N/C	—	— ⁽¹⁾	+	+	+
M1					N/C	N/C	N/C	N/C	N/C	+(2)	N/C
PMC					N/C	N/C	N/C	—	+	+	N/C

¹ Recruitment of the left hemisphere fusiform gyrus appeared to be unaffected by consolidation. The “—” here indicates an observation that right hemisphere fusiform gyrus was significantly (18%) less recruited in post- relative to pre-consolidation subjects.

² BOLD signal response rates in left hemisphere primary motor cortex appeared to be unaffected by consolidation. The “+” here indicates an observation that right hemisphere M1 BOLD response rates were significantly (78%) faster in post- relative to pre-consolidation subjects.

³ Left hemisphere area V3 signal entropy appeared to be unaffected by consolidation. The “+” here indicates an observation that right hemisphere area V3 BOLD signals were significantly (8%) more complex in post- relative to pre-consolidation subjects.

time nor subject accuracy, the numerator portion of the illustrative efficiency ratio, nor metabolic demand (BOLD signal magnitude), a measure of energy expenditure, differed significantly between putatively pre- and post-consolidation subjects, whereas cortical recruitment (activation volume), did decrease significantly at the ROI level, particularly in premotor, lower visual, and ventral visual areas. It is therefore argued that retrieval efficiency did in fact increase, at least in these particular ROIs, between pre- and post-consolidation testing groups.

Here, the results (Tables 5 and 6) and discussion portions of previous chapters will be elaborated, and their potential contributions to existing mnemonic theory will be discussed.

EFFECTS OF STIMULUS MODALITY AND TESTING INTERVAL ON TASK PERFORMANCE

Disparity between behavioral predictions and findings

Upon analysis, the computer-based testing (CBT) group was found to differ significantly from the FMRI group in that FMRI subjects were slower at identifying correctly-matched and mismatched associates than their CBT counterparts, and exhibited more false positives than CBT subjects overall, but neither CBT nor FMRI subjects differed with respect to accuracy for previously learned associates at either time point. Neither group was faster or more accurate at identifying learned associates after consolidation, and neither group improved with respect to the number of false positives or false negatives with time. These differences were not likely due to differences in training or testing

environments or subject compliance, as both fMRI and CBT subjects were trained in the same environment and exhibited the same reaction times and accuracy for control stimuli at both time points. Instead, the performance differences could be ascribed to the requisite differences in attentional demands between testing groups: fMRI subjects, who were given lexical rather than auditory stimuli, were required to divide their visual attention between two simultaneously-presented stimuli that were wholly within the visual modality, in contrast to CBT subjects, who were required to divide their attention between two simultaneously-presented stimuli in two modalities. Such divided-attention effects have been well documented in both behavioral and neuroimaging literature, and it is generally agreed that bimodal attentional demands consistently have an effect on reaction time during encoding but not retrieval, unless the task stimuli being retrieved, such as simultaneous retrieval of different (“discordant”) lexical and auditory words, require access to the same representational areas of cortex (e.g., Grunwald, Boutros, Pezer, von Oertzen, Fernandez, Schaller and Elger 2003; Naveh-Benjamin, Kilb and Fisher 2006). In addition to these attentional effects, saccade times were likely to have a greater influence on fMRI subject reaction time than in CBT subjects, for whom saccade times were relatively minimized.

Neither factor appeared to contribute to decreased accuracy for matched associates, however, as evinced by the absence of significant differences between the two groups. This is likely due to the indexing facility of the hippocampal formation, which appears to be independent of memory trace modality (Eichenbaum 2001; Ross and Eichenbaum 2006). More puzzling, however, was the observed consistency in reaction time accuracy across time points, contradicting the well-known Ebbinghaus retention

curve and Wickelgren power law, which predicts a power law relationship between memory performance and the delay between encoding and retrieval, such that retention declines with time (see, for example, Ebbinghaus 1913; Wickelgren 1974; Anderson and Schooler 1991; Rubin, Hinton and Wenzel 1999; Wixted 2004). Here, a possible explanation of this “non-Kamin” Ebbinghaus exception is presented based on the current literature in episodic reconsolidation.

Theoretical reconsolidative basis for the non-Kamin Ebbinghaus exception

Although improvements in memory performance — the so-called Kamin effect, an exception to the monotonicity of the Ebbinghaus curve — have been demonstrated in rodents, the mollusk *Sepia officinalis* and honeybees, these studies have been done, without exception, in the context of affective stimuli, such as avoidance responses, olfactory memory, and appetitive responses, and it is generally agreed that the Kamin effect is neuroendocrinologically mediated through the amygdalar body (Kamin 1957; Kamin 1963; Messenger 1971; Sanders and Barlow 1971; Woodruff and Kantor 1983; Rudy and Morledge 1994; Belcadi-Abbassi and Destrade 1995; Gerber and Menzel 2000; Rudy and Matus-Amat 2005). The present study, however, utilized stimuli that, being abstract, should have had neither affective influences nor rehearsability, eliminating the possibility of deep encoding.

Thus a larger question remains: how could subjects maintain retrieval accuracy and comparable response or retrieval times on a paired-associates task with no emotional content? A possible answer may lie in the physiology of episodic consolidation. As discussed in the introductory chapters of this dissertation, episodic memory consolidation

appears to occur in two major stages (Chrobak and Buzsaki 1998b; McGaugh 2000; Abel and Lattal 2001; Wang, Hu *et al.* 2006). In the first stage, memory traces are encoded in hippocampal area CA3 and interlinked through Hebbian processes over a period of hours to months to form metastable mnemonic networks that, in the second stage of consolidation, are gradually re-encoded into cortical, hippocampus-independent networks over a period of months to years (McClelland, McNaughton *et al.* 1995; Squire and Alvarez 1995; Ross and Eichenbaum 2006).

Stage I consolidation, with which the present study is concerned, has been further subdivided into three phases. In Stage I phase 0, a *short-term facilitation* phase, recently-encoded memory traces are associated through a protein synthesis inhibitor-insensitive AMPAR-NMDAR-PKC pathway, which appears to last up to six hours (Abel and Lattal 2001; Walker and Stickgold 2004; Wang, Hu *et al.* 2006). In Stage I phase IA, a *stabilization* phase, the memory traces undergo protein synthesis-dependent long-term potentiation through a PKA-tPA-BDNF pathway (Abel and Lattal 2001; Walker and Stickgold 2004; Wang, Hu *et al.* 2006). Memory traces can remain in this state for 6-12 hours before proceeding to Stage IB, an enhancement phase which appears to be primarily if not solely dependent on sleep (Stickgold, Scott *et al.* 1999; Datta 2000; Gais and Born 2004; Walker and Stickgold 2004). The profile of protein synthesis shifts in Stage IB to include several plasticity-related proteins, such as TrkB and the glutamate-aspartate transporter GLAST, probably in preparation for increases in dendritic arborization and other structural changes that are the hallmarks of this phase (Cirelli and Tononi 2000b; Cirelli and Tononi 2000a; Abel and Lattal 2001).

Stages IA and IB are also characterized by competition among neurons constituting a memory trace through a calcium-dependent calmodulin/CREB pathway, such that neurons exhibiting a higher influx of calcium will upregulate transcription, thereby outcompeting neighboring cells for inclusion in the final memory trace (Kida, Josselyn *et al.* 2002; Bozon, Davis *et al.* 2003).

Thus it is likely that trace networks are destabilized prior to the onset of cytostructural changes in consolidation phase IB due to factors modulating short-term facilitation, such as AMPA and NMDA receptor turnover and differential activity-dependent calcium influx at encoding, as well as cellular competition within the network in stage IA (Abel and Lattal 2001; Bozon, Davis *et al.* 2003). Consequently, the number of cells constituting a trace would be smaller at the onset of phase IB than immediately after encoding. The consistency of retrieval accuracy and retrieval time across time points in the present study therefore indicates persistence in trace network accessibility over and above this loss of trace neurons: that is, the trace is retrieved as easily after consolidation than after encoding despite a decrease in the number of neurons in the memory trace.

One possible explanation for this persistence in trace accessibility is that the sum of synaptic weights remains approximately equal across pre- and post-consolidation time points, both within the trace network and between the trace network and other retrieval-associated brain areas, while the activation thresholds of the neurons constituting the trace network decrease. This conjecture would necessitate an increase in the synaptic weight, and decrease in the activation threshold, per trace neuron across the consolidation interval. These two parameters are not entirely independent, since the effective firing

rate, and therefore the probability of activation, of a trace neuron is a function of both the presynaptic neuron's firing rate and synaptic weight and the activation threshold of the trace neuron. Extending this logic to a population of neurons, then, the sum synaptic weight of a trace network could be kept constant by an increase in the postsynaptic cell's firing rate through a decrease in the postsynaptic cell activation threshold, or by an increase in the presynaptic cell's firing rate through a decrease in the presynaptic cell activation threshold.

Although this model is, at present, speculative, it would indicate that the trace retrieval time and accuracy could *theoretically* be maintained while also maintaining a relatively constant level of accessibility. Consequently, the neural populations involved in long-term memory storage and retrieval should both activate more quickly and produce a more complex signal after consolidation. These predictions were tested in the present study through measurements of the voxel BOLD signal/task cross-correlation (VTCC) and Shannon entropy of the voxel BOLD signal time series vector (TSE), respectively. Furthermore, the number of recruited voxels (activation volume) and degree of metabolic activity (percent BOLD signal change from baseline) were assessed in order to support or refute the assumption that the number of neural structures required for trace retrieval decreased with consolidation.

Disparity between physiological predictions and findings

As discussed in the previous chapter, the present results suggest that metabolic demand was conserved across *all* observed ROIs and was not accompanied by a decrease in recruitment of the MTL, as was predicted. In fact, excluding increased BOLD signal response rates, hippocampal and perihippocampal areas, as well as primary visual and motor cortices, appeared to be *unaffected* across the conservation interval, even when signal entropy was taken into account. Moreover, components of the extrastriate ventral visual stream (EVVS), which were predicted to demonstrate both decreased metabolic demand and decreased recruitment over the consolidation interval —thereby reflecting a diminution of per-neuron activity — instead exhibited no change in metabolic demand but significant reductions in recruitment (except the left hemisphere fusiform area, which was unaffected), indicating that EVVS neurons participating in trace retrieval after the consolidation interval were *individually more active* than their pre-consolidation counterparts. BOLD signal entropy data further revealed that, of all ROIs inspected in the present study, only EVVS areas exhibited an increase in entropy with consolidation. It must therefore be concluded that the consolidation-concomitant *Hebbian* changes in episodic retrieval networks (and particularly in the MTL) described in the literature are not necessarily reflected in changes in cortical recruitment, metabolic demand, or BOLD signal entropy, which may derive from cellular and/or network phenomena that are unrelated, or secondarily or more distantly related, to Hebbian effects.

In the introductory chapters of the present dissertation, it was hypothesized that areas comprising the MTL, which serve to associate salient features of encoded episodic stimuli, would also be affected by the proposed optimizing processes of consolidation. Intuitively, this would mean that changes in plasticity would drive the amalgamation of pre-consolidation medial temporal interneurons serving to link memory traces stored in isocortex, such that fewer interneurons are required for the linkage at post-consolidation. That the entorhinal, perirhinal, perihippocampal, and ectorhinal cortices and the hippocampus are both involved in and affected by stage I visual episodic memory consolidation has been reasonably well established: short-term glutamate receptor blockades, trauma, or neurotoxic lesions in the MTL disrupt visual long-term memory (Zola-Morgan, Squire, Amaral and Suzuki 1989; Meunier, Bachevalier, Mishkin and Murray 1993; Burwell, Bucci, Sanborn and Jutras 2004; Winters, Forwood, Cowell, Saksida and Bussey 2004; Winters and Bussey 2005c). Because day 7 subject accuracy was significantly greater than chance — which would not be the case if stage IA protein synthesis had not taken place — it must also be assumed that at least stage IA consolidation, and therefore plasticity effects, had also occurred (Abel and Lattal 2001; Walker and Stickgold 2004; Wang, Hu *et al.* 2006). Therefore, if these physiological changes do in fact occur as hypothesized, it is possible that they may do so on a spatial scale much smaller than an EPI voxel, or may not be correlated with changes in BOLD signal features. In such cases, confirmation of the present hypotheses in the medial temporal lobe will require direct electrophysiological observation *in vivo*.

Resolution issues, however, do not account for the absence of entropy effects in MTL areas. Therefore, if the theoretical reasoning underlying the entropy metric (see the

Methodology chapter, the “Retrieval Orientation and Cortical Reinstatement” section in the *Memory Consolidation and Retrieval Performance* chapter, and “Caveats” below) is correct, and BOLD signal entropy does in fact primarily reflect neuronal spike train information load, it must be concluded that these firing rates are no more complex after the consolidation interval than before, and, by deductive reasoning, the same (or very similar) computational operations must be taking place in the pre- and post-consolidation MTL. This conclusion contradicts the prediction that recruitment of, and demand from, the MTL areas would suggest increased (compensatory) per-neuron activity, as well as the underlying hypothesis that trace retrieval efficiency increases *in the MTL* over the consolidation interval. Thus the question arises: are current models of MTL function consistent with a position that the pre- and post-consolidation computational operations of the MTL are identical, in spite of well-documented changes in plasticity in the MTL with consolidation?

As discussed previously, neither the processing functions nor the temporal course of involvement of particular medial temporal areas relative to memory consolidation or storage are well understood; however, tetanic stimulation of hippocampus and frontal (primary motor), entorhinal, and perirhinal cortices *in vivo* indicates that these areas are not only plastic but also capable of effecting, and being affected by, long-term potentiation (LTP) via neuronal afferents and efferents (Ivanco and Racine 2000). Moreover, it has been proposed that the characteristic latency between direct stimulation and steady-state LTP in each of these areas may reflect their hierarchical (yet symmetrical) or time-sensitive functions. For example, the hippocampus, which potentiates quickly and sensitively to novel stimuli, may serve to stabilize memory traces

for the duration of stage I, and most of stage II, consolidation; isocortex, which potentiates slowly but exhibits enduring LTP once it is effected, likely serves as the long-term storage site for memory traces. In this view, components of the parahippocampal region, which exhibit plasticity latencies and stabilities intermediate between those of the hippocampus and isocortex, may perform their computational functions on a temporal interval between the effective periods of the hippocampus (stage I consolidation) and isocortex (stage II consolidation) (McClelland, McNaughton *et al.* 1995; Ivanko and Racine 2000; Eichenbaum 2001). However, parahippocampal activation is frequently reported during all phases of memory tasks (Eichenbaum, Schoenbaum *et al.* 1996; Gabrieli, Brewer and Poldrack 1998; Lavenex and Amaral 2000; Nadel and Land 2000; Egorov, Hamam *et al.* 2002; Frank and Brown 2003; Naya, Yoshida *et al.* 2003a; Naya, Yoshida *et al.* 2003b; Clavagner, Falchier *et al.* 2004). Furthermore, lidocaine inactivation of rodent perirhinal cortex, localized to Brodmann areas 35 and 36, has been shown to preclude performance on DNMS tasks when administered over intervals corresponding to episodic memory encoding, consolidation, and retrieval, which suggests that parahippocampal areas are vital to the functions of the episodic system in all three phases of the memory trace lifetime (Tassoni, Lorenzini, Baldi, Sacchetti and Bucherelli 1999; Winters and Bussey 2005b; Winters and Bussey 2005a; Winters and Bussey 2005c). Theories that address the problem of computational dissociations among parahippocampal areas by positing phasic or temporally hierarchical functions must therefore do so in light of the seemingly constant involvement of these areas in the trace network.

Despite the current controversy regarding the temporal upper bound of medial temporal involvement in trace *retrieval*, most theories of MTL function in declarative memory concur with respect to its involvement in trace *storage* and conclude, with some degree of consensus,⁴ that both the physiological characteristics of the medial temporal structures and the protracted nature of consolidation itself subserve the merging of the memory trace into the myriad of other isocortical memory traces, while simultaneously precluding, upon trace retrieval, a debilitating cascade of memory recall precipitated by the overlapping representations of similar, but non-identical, experiences known as *catastrophic hypermnesia* (McNaughton and Wickens 2003; Tse, Langston, Kakeyama, Bethus, Spooner, Wood, Witter and Morris 2007). In this context, then, the ostensible role of the parahippocampal region is to modulate information transfer to the hippocampus based on the novelty of the information, such that novel and salient stimulus features, but not features similar to those found in previously-encoded traces, will elicit hippocampal activation (see, for example, Fernandez and Tendolkar 2006). This theoretical function of the parahippocampal region is in line with behavioral, electrophysiological and neuroimaging data on correlates of repetition suppression, recognition, and recency effects in the MTL (Henson and Rugg 2003; Weis, Klaver, Reul, Elger and Fernandez 2004; Gonsalves, Kahn, Curran, Norman and Wagner 2005;

⁴ The most conspicuous exception to this consensus is the *multiple memory trace* theory propounded by Lynn Nadel. Nadel's theory maintains that trace retrieval *never* becomes completely independent of the hippocampal formation and, therefore, the MTL is *always* required for trace recall. It could be argued, however, that the hippocampal synaptic weight upon trace retrieval approaches, but would never physiologically attain, zero; by this argument, the upper bound of MTL involvement proposed by Nadel (infinity) and that proposed by other theorists (possibly, the lifetime of the organism) may differ mathematically, but in practical terms, the upper bound will always be the lifetime of the organism. Cf., for example, Moscovitch Moscovitch, M., L. Nadel, G. Winocur, A. Gilboa and R. S. Rosenbaum (2006). The cognitive neuroscience of remote episodic, semantic and spatial memory. *Current opinion in neurobiology* 16(2): 179-90. and Nadel Nadel, L., A. Samsonovich, L. Ryan and M. Moscovitch (2000). Multiple trace theory of human memory: computational, neuroimaging, and neuropsychological results. *Hippocampus* 10(4): 352-68..

Montaldi, Spencer, Roberts and Mayes 2006). Moreover, it is of particular relevance to the present discussion because it minimizes the distinction between encoding- and retrieval-concomitant roles for the parahippocampal areas and emphasizes instead a so-called *gatekeeper* function, by which neurons engaged in encoding are potentiated toward novel stimuli (Fernandez and Tendolkar 2006). The gatekeeper theory thus renders computational distinctions among the various MTL components (where such distinctions cannot be ascribed to the sensory specificity or aspecificity of their projections: cf. Kerr, Agster *et al.* 2007) less impedimentary and sustains the contention that the parahippocampal areas might retain uniform computational functions over and above changes in plasticity.

EVVS areas, with the exceptions of left hemisphere visual area V3, which exhibited greater putative per-neuron activity but not greater signal entropy, and left hemisphere fusiform gyrus, which exhibited greater signal entropy but no change in metabolic demand or recruitment, were observed to exhibit *greater* per-neuron activity and BOLD signal entropy at the post-consolidation time point. Based on the theory proposed in this dissertation (*cf.* “Caveats” below), this finding would indicate that — in contrast to predicted decreases in per-neuron activity in the extrastriate ventral visual stream (EVVS) consequent to differential retrieval orientation with consolidation — post-consolidation EVVS neurons exhibit more complex firing rates, a possible reflection of greater information load, than their pre-consolidation counterparts. Interestingly, primary visual cortex (visual area V1) appeared to be unaffected by consolidation (except for possible correlates of cortical reinstatement, described below), a finding which may indicate that the consolidation-correlated effects observed in the other visual ROIs may

be attentionally modulated (see the *Regions of Interest* chapter). Although this hypothesis remains speculative pending direct measurement of neuronal firing rate entropy during a DMTS paradigm, it is interesting to note that premotor cortex — an attentional area — exhibited greater per-neuron activity but, like parahippocampal areas, conserved entropy (and, per the discussion above, conserved computational functions) at post-consolidation. These characteristics are consistent with a hypothetical attentional region that modulates retrieval orientation in post-, but not pre-consolidation subjects.

Thus, the first component of the hypothesis stated above — that the neural populations involved in long-term memory storage and retrieval should *activate more quickly* following consolidation — may hold true for gatekeeper, ecphoric, and trace networks, whereas the second component — that neural populations involved in storage and retrieval should *produce a more complex signal* after consolidation — may hold true only for the trace networks themselves, that is, the EVVS. Although this model has not yet, to the knowledge of the author, been proposed in the literature, it is highly testable by future DMTS studies that directly examine firing rate entropy. The present model predicts that previously-learned visual DMTS stimuli will elicit greater post-consolidation than pre-consolidation firing rate entropy in visual cortices, where the traces are stored, but not in attentional or executive cortices, which subserve ecphory, or medial temporal structures, which appear only to *link* trace nodes and encode stimulus novelty. Furthermore, entropy effects should not occur in primary visual cortex. In contrast, *DNMS* stimuli should elicit greater firing rate entropy in medial temporal, and perhaps visual, but not attentional or executive, cortices. It would also be informative to

perform these future experiments in an FMRI context in order to attempt the replication of metabolic demand findings.

Caveats of the entropy metric

It should be noted that the BOLD signal has been shown to be primarily determined by the magnitude of perivascular oxidative glycolysis as a result of cooperative, or synchronized, somatodendritic potentials (Boynton, Engel, Glover and Heeger 1996; Logothetis 2002; Buxton, Uludag, Dubowitz and Liu 2004; Behzadi and Liu 2005), and appears to be more closely associated with energy demand concomitant to neurotransmitter release than with perikaryal metabolic demands (Logothetis 2002; Logothetis 2003; Logothetis and Pfeuffer 2004; Logothetis and Wandell 2004). The persistence with consolidation of BOLD signal magnitude within the observed ROIs would therefore suggest that the degree of perisynaptic activity, including pre- and post-synaptic currents, neurotransmitter release, and, consequently, neural firing rates, remained approximately constant across pre- and post-consolidation subjects. It could therefore plausibly be proposed that firing rates increased, relative to the post-encoding state, in the recall-associated neural populations of the post-consolidation EVVS, and, consequently, BOLD signal entropy would be expected to increase with consolidation within these areas.

Again, the hypothesis that firing rates increased in recall areas with consolidation was tested by computation of the Shannon, or information-theoretic, entropy of the BOLD response from each Brodmann area. This voxel BOLD signal time series Shannon entropy (TSE) was found to increase in three of the four regions that exhibited decreased

cortical recruitment between the two subject groups, indicating that the BOLD signal per Brodmann area was more complex in still-participatory neural populations after the consolidation interval than in the neural populations recruited for recall immediately after encoding in those Brodmann areas. Although this entropy arguably arises from increased neural firing rates, the TSE results could also be the result of nonlinearities in neurovascular coupling or due to other physiological variables, such as cytogeometry, as discussed in the *Methodology* chapter. However, as was argued previously, in healthy, compliant adults and in children over three years of age, neural activity and the BOLD signal are believed to be somewhat linearly coupled (Martin, Joeri *et al.* 1999; Logothetis 2002) and it was inferred that, in the majority of subjects, voxel TSE arises from entropy in neurotransmitter release in the perisynaptic compartment (Logothetis 2002). The precise relationship between BOLD signal chaos and neural activity, however, is as yet unknown. Thus, while the findings of the present study are probative, they must be interpreted with caution, since more investigation is indicated as to the nature and origin of the entropy in the BOLD signal that the voxel TSE represents.

THEORY: CORTICAL REINSTATEMENT AND RETRIEVAL ORIENTATION

An implicit assumption underlying the generation of the hypotheses of the present dissertation was that subjects would exhibit non-conscious (covert) shifts in attention from local to global presented visual stimulus features after the consolidation interval, a phenomenon called *retrieval orientation* (Rugg and Wilding 2000; Robb and Rugg 2002). In the *Aims and Hypotheses* chapter, it was proposed that changes in retrieval orientation would be evinced by a shift from bilateral visual cortex activation in both

dorsal and ventral visual streams at pre-consolidation to right-hemisphere dominance in the ventral visual stream at post-consolidation (H. 4). This prediction follows from divergent activation profiles observed in functional MRI studies in which mnemonic demands were parametrically manipulated (Herron and Rugg 2003a; Hornberger, Morcom *et al.* 2004; Herron and Wilding 2006a; Herron and Wilding 2006b; Hornberger, Rugg *et al.* 2006b; Hornberger, Rugg and Henson 2006a; Stenberg, Johansson *et al.* 2006; Woodruff, Uncapher *et al.* 2006). However, in contrast to those studies, which utilized the conventional BOLD magnitude metric, *no differences in signal intensity were observed in the ventral visual stream* in the present study, contradicting the predictions following from H. 4.

Interestingly, however, increases in BOLD signal *entropy*, which may correspond to the complexity of neural firing rates, *were* observed in visual area V2, as well as area V3 and the fusiform gyrus (V4), two components of the ventral visual stream. This observation was particularly surprising in area V3, in that right, but not left, hemisphere V3 differed significantly with respect to signal entropy as a function of time point: area V3 is considered the first region that comprises the ventral visual stream (Ungerleider and Mishkin 1982), and, furthermore, the right hemisphere ventral visual stream is believed to function in the processing of global visual stimulus features (Knierim and Van Essen 1992b; Knierim and van Essen 1992a; Brown and Kosslyn 1993; Johannes, Wieringa *et al.* 1996; Polat and Norcia 1998; Yamaguchi, Yamagata *et al.* 2000; Haxby, Gobbini *et al.* 2001; Lerner, Hendler *et al.* 2001). Area V2 and the fusiform gyrus, visual area V4, are also known to be heavily interconnected (Albright 1993), and, although V2 is not considered to be a ventral visual component, the finding that both V2 and V4

exhibited greater entropy in post-consolidation subjects may indicate that increases in BOLD signal entropy may indeed correspond to a ventral visual network effect. Notable, too, is the absence of a significant effect of time point on either recruitment or signal entropy in area V1, since, as discussed previously, V1 activity has *not* been shown to be attentionally modulated, and it is the attentional network that would likely modulate differential retrieval effects with consolidation, if they exist. Admittedly, however, the present data are insufficient to substantiate the previously stated hypothesis that retrieval orientation effects occurred in the DMTS task; yet these findings may nevertheless be seen as seminal in that differential sensory cortex effects were observed in domains other than the conventional BOLD magnitude statistic.

Possible cortical reinstatement effects

A second assumption in the dissertation was that post-consolidation subjects would exhibit faster reactivation of retrieval networks, and therefore BOLD response rates relative to the presentation of previously-learned stimuli, as a consequence of increased synaptic weighting after the consolidation interval. This effect has been referred to as “transfer-appropriate processing” or *cortical reinstatement* (Lockhart 2002; Vaidya, Zhao *et al.* 2002; Mulligan and Lozito 2006). BOLD response rates (VTCC) were in fact greater in post-consolidation subjects in all observed ROIs with the exception of left hemisphere primary motor cortex, which did not differ with respect to VTCC as a function of time point. Thus, the present data did substantiate the hypothesized time point effect on network reinstatement.

Notably, regional BOLD signals in all Brodmann areas except left hemisphere primary motor cortex were *also* found to exhibit a significant increase in covariance (voxel-task cross-correlation, VTCC) with a reference vector representing the temporal presentation of previously learned (matched) stimuli with consolidation, meaning that both the rising and falling phases of the BOLD response occurred at a faster rate relative to the onset and offset of correctly-matched stimulus presentation in post-consolidation subjects. This result could feasibly be interpreted as a consolidation-related decrease in the activation threshold of the neurons constituting the voxels of interest, such that the roughly linear relationship between neural activity and the hemodynamic response remained unchanged with consolidation but increased presynaptic weighting or decreased postsynaptic neuron activation thresholds facilitated a faster response onset and offset in the neural activity underlying the BOLD signal. In this case, the altered BOLD signal trajectory could reflect heightened efficiency of synaptic integration, such that neural populations were activated more quickly (lower neuronal time constants facilitate higher presynaptic firing rates or vice versa) and maintained activity for shorter durations. Alternatively, however, a change in the metabolic components of neurovascular coupling, such as increased receptor or ion channel expression, neurogenesis, differential enzyme kinetics, and alterations to the pathways of signal transduction or time course of the relevant neurochemical cascades, could also explain the accelerated trajectory of the hemodynamic response. Additionally, although the positive VTCC-TSE relationship appears to be preserved in visual areas V2 and V3 and the fusiform gyrus, it should also be noted that this relationship was *not* preserved in perirhinal or premotor cortex. If, therefore, the TSE and VTCC metrics do in fact correspond to neuronal spike train

complexity and synaptic efficacy respectively, the conclusion must also be drawn that one does not necessarily predict the other, and may in fact be mediated through a third explanatory variable.

CLOSING REMARKS

The present study yielded probative, albeit preliminary, neurodynamics data that have not yet been reported in prior fMRI-based studies, particularly in the context of episodic memory consolidation. Notably, unique physiological profiles of recruitment, metabolic demand, BOLD signal rates, and BOLD signal entropy were reported that suggest that post-consolidation trace recall and retrieval support networks are characterized by increased trace retrieval efficiency at the regional (rather than behavioral) level, and differential sensory processing, which may reflect changes in synaptic integration both within the episodic memory system and supporting networks. The reader should be cautioned, however, that two of the methods used in the present dissertation – BOLD signal entropy and VTCC – have not been replicated or interpreted by other researchers, and their reliability must be established by repeated investigations in the future.

It is hoped that the present study will be utilized as groundwork for future neurodynamics research, especially with respect to neuroimaging investigations.

APPENDICES

APPENDIX A: ANOVA TABLES FOR BEHAVIORAL DATA

A two-way 2x2 ANOVA was utilized to test for the effect of computer-based (CBT) versus FMRI testing scenarios and time point (immediate versus day-7 testing), the independent factors, on task performance (reaction time and accuracy, the dependent variables). *Abbreviations: m, match; mm, mismatch; c, control; Acc, Accuracy; RT, reaction time; FMRI, FMRI/unimodal testing group; CBT, computer-based (pilot/bimodal) testing group.*

Analysis of Variance for match-condition accuracy

Adjusted SS for Tests

Source	DF	Seq SS	Adj SS	Adj MS	F	P
FMRI v CBT	1	77.8	51.0	51.0	0.35	0.554
TimePoint(FMRI v CBT)	2	393.0	393.0	196.5	1.37	0.264
Error	51	7334.3	7334.3	143.8		
Total	54	7805.1				

S = 11.9921 R-Sq = 6.03% R-Sq(adj) = 0.50%

Analysis of Variance for mismatch-condition accuracy

Adjusted SS for Tests

Source	DF	Seq SS	Adj SS	Adj MS	F	P
FMRI v CBT	1	1366.0	1221.5	1221.5	6.74	0.012
TimePoint(FMRI v CBT)	2	235.9	235.9	118.0	0.65	0.526
Error	51	9236.4	9236.4	181.1		
Total	54	10838.3				

S = 13.4576 R-Sq = 14.78% R-Sq(adj) = 9.77%

Analysis of Variance for control-condition accuracy

Adjusted SS for Tests

Source	DF	Seq SS	Adj SS	Adj MS	F	P
FMRI v CBT	1	327.1	354.8	354.8	1.28	0.264
TimePoint(FMRI v CBT)	2	639.2	639.2	319.6	1.15	0.325
Error	51	14190.8	14190.8	278.3		
Total	54	15157.0				

S = 16.6808 R-Sq = 6.37% R-Sq(adj) = 0.87%

Analysis of Variance for match-condition response time

Adjusted SS for Tests

Source	DF	Seq SS	Adj SS	Adj MS	F	P
FMRI v CBT	1	1557152	1569349	1569349	67.07	0.000
TimePoint(FMRI v CBT)	2	103726	103726	51863	2.22	0.119
Error	51	1193331	1193331	23399		
Total	54	2854209				

S = 152.966 R-Sq = 58.19% R-Sq(adj) = 55.73%

Analysis of Variance for mismatch-condition response time
Adjusted SS for Tests

Source	DF	Seq SS	Adj SS	Adj MS	F	P
FMRI v CBT	1	446193	362692	362692	4.87	0.032
TimePoint(FMRI v CBT)	2	176495	176495	88247	1.18	0.314
Error	51	3797985	3797985	74470		
Total	54	4420672				

S = 272.892 R-Sq = 14.09% R-Sq(adj) = 9.03%

Analysis of Variance for control-condition response time
Adjusted SS for Tests

Source	DF	Seq SS	Adj SS	Adj MS	F	P
FMRI v CBT	1	37284	29640	29640	0.23	0.631
TimePoint(FMRI v CBT)	2	190481	190481	95240	0.75	0.478
Error	51	6479807	6479807	127055		
Total	54	6707572				

S = 356.448 R-Sq = 3.40% R-Sq(adj) = 0.00%

APPENDIX B: MAIN-EFFECT ANOVA AND POST-HOC RESULTS FOR PHYSIOLOGICAL STATISTICS

Initial three-way 2x11x2 ANOVAs were performed *on FMRI subject data only* to test the effects of the training-testing interval (“testing group”: day 0 versus day 7), region of interest (ROI), and ROI hemisphere (left versus right) on various physiological measures – metabolic demand (percent BOLD signal change from baseline, PC), cortical recruitment (activation volume, AV), BOLD signal rate (voxel-task cross-correlation, VTCC), and BOLD signal entropy (time series Shannon entropy, TSE) – collapsed across all ROIs. Inspection of the three-way ANOVA results indicated that only the “testing group” factor had had significant effects; therefore, physiological measures were collapsed across cerebral hemispheres and subjected to *t*-tests using “testing group” as the grouping variable. Results of the initial 2x11x2 three-way ANOVA, the main-effect ANOVA on “testing group,” and the post-hoc *t*-tests are given below.

Between-Subjects Factors			
		Value Label	N
Testing group	1	Pre-Con.	132
	2	Post-Con.	154
ROI	1	M1	26
	2	EcRC	26
	3	ERC-28	26
	4	ERC-34	26
	5	Fusi.	26
	6	HC	26
	7	PMC	26
	8	PRC	26
	9	V1	26
	10	V2	26
	11	V3	26
Hemi.	1	LH	143
	2	RH	143

Descriptive Statistics						
	Testing group	ROI	Hemi.	Mean	Std. Deviation	N
TSE	Pre-Con.	M1	LH	.022511883	.0002462143	6
			RH	.022656133	.0009594639	6
			Total	.022584008	.0006720651	12

Post-Con.	EcRC	LH	.007849723	.0032996832	6
		RH	.007687307	.0032204328	6
		Total	.007768515	.0031097299	12
	ERC-28	LH	.005074413	.0021863221	6
		RH	.005078771	.0021307093	6
		Total	.005076592	.0020582360	12
	ERC-34	LH	.004856060	.0019542089	6
		RH	.004670026	.0018783718	6
		Total	.004763043	.0018300495	12
	Fusi.	LH	.047433535	.0199516547	6
		RH	.048122593	.0200966724	6
		Total	.047778064	.0190958069	12
	HC	LH	.005222804	.0021049161	6
		RH	.004643110	.0018678021	6
		Total	.004932957	.0019212903	12
	PMC	LH	.102977050	.0021604937	6
		RH	.103268100	.0044204021	6
		Total	.103122575	.0033206321	12
	PRC	LH	.003478535	.0013976280	6
		RH	.003536042	.0014128557	6
		Total	.003507288	.0013402017	12
	V1	LH	.014195012	.0050104708	6
		RH	.014452598	.0051148192	6
		Total	.014323805	.0048291729	12
	V2	LH	.065361417	.0169169178	6
		RH	.066070500	.0171777214	6
		Total	.065715958	.0162586746	12
	V3	LH	.068396833	.0110750137	6
		RH	.069438183	.0110375615	6
		Total	.068917508	.0105557898	12
	Total	LH	.031577933	.0338500076	66
		RH	.031783942	.0341854976	66
		Total	.031680938	.0338882348	132
	M1	LH	.022607029	.0001433439	7
		RH	.022986486	.0000733493	7
		Total	.022796757	.0002252388	14
	EcRC	LH	.009000927	.0012446179	7
		RH	.008701497	.0012300932	7

	ERC-28	Total	.008851212	.0011989426	14
		LH	.005848276	.0013244864	7
		RH	.005757686	.0012778602	7
	ERC-34	Total	.005802981	.0012512108	14
		LH	.005533653	.0003491237	7
		RH	.005318517	.0003253545	7
	Fusi.	Total	.005426085	.0003428892	14
		LH	.054608200	.0037027525	7
		RH	.054964086	.0038352458	7
	HC	Total	.054786143	.0036264012	14
		LH	.006068603	.0000473126	7
		RH	.005387920	.0000446476	7
	PMC	Total	.005728261	.0003559433	14
		LH	.103731714	.0006860585	7
		RH	.104786286	.0008732983	7
	PRC	Total	.104259000	.0009320111	14
		LH	.003964633	.0003591451	7
		RH	.003995126	.0003618858	7
	V1	Total	.003979879	.0003467357	14
		LH	.016223814	.0000610444	7
		RH	.016505586	.0000243196	7
	V2	Total	.016364700	.0001528675	14
		LH	.071977414	.0002680646	7
		RH	.073243100	.0002200723	7
	V3	Total	.072610257	.0006977218	14
		LH	.072436043	.0003597663	7
		RH	.074517029	.0002322144	7
Total	Total	Total	.073476536	.0011182709	14
		LH	.033818210	.0340363952	77
		RH	.034196665	.0346751205	77
	M1	Total	.034007437	.0342453058	154
		LH	.022563115	.0001948588	13
		RH	.022834015	.0006447040	13
	EcRC	Total	.022698565	.0004866363	26
		LH	.008469602	.0023807497	13
		RH	.008233409	.0023140481	13
	ERC-28	Total	.008351506	.0023033547	26
		LH	.005491108	.0017406991	13

AV	Pre-Con.	ERC-34	RH	.005444340	.0016829120	13
			Total	.005467724	.0016776284	26
			LH	.005220918	.0013325833	13
		Fusi.	RH	.005019214	.0012791666	13
			Total	.005120066	.0012838846	26
			LH	.051296816	.0136592807	13
		HC	RH	.051806474	.0137199833	13
			Total	.051551645	.0134155955	26
			LH	.005678234	.0014282274	13
		PMC	RH	.005044161	.0012664790	13
			Total	.005361198	.0013614544	26
			LH	.103383408	.0015275990	13
		PRC	RH	.104085585	.0030238253	13
			Total	.103734496	.0023742770	26
			LH	.003740280	.0009705726	13
		V1	RH	.003783241	.0009767072	13
			Total	.003761760	.0009542246	26
			LH	.015287444	.0034015245	13
		V2	RH	.015558053	.0034692378	13
			Total	.015422748	.0033689627	26
			LH	.068923877	.0114482789	13
		V3	RH	.069932669	.0116971219	13
			Total	.069428273	.0113512004	26
			LH	.070571792	.0074541203	13
		Total	RH	.072172946	.0075982398	13
			Total	.071372369	.0074195146	26
			LH	.032784236	.0338494023	143
		M1	RH	.033083101	.0343499673	143
			Total	.032933668	.0340410542	286
			LH	2396.79166666666700	343.764069409044900	6
		EcRC	RH	2627.70833333333300	270.795514026112800	6
			Total	2512.25000000000000	318.731470049632800	12
			LH	1152.37500000000000	368.942941049154600	6
		ERC-28	RH	1140.50000000000000	347.416356840031300	6
			Total	1146.43750000000000	341.721329930610900	12
			LH	780.58333333333300	216.623328999133100	6
		ERC-28	RH	736.66666666666600	239.919031480761600	6
			Total	758.62500000000000	219.134674759195000	12

Post-Con.	ERC-34	LH	566.79166666666600	237.881032065750600	6
		RH	555.50000000000000	226.227374559313600	6
		Total	561.14583333333300	221.403284300939000	12
	Fusi.	LH	6097.58333333333000	2661.727280670705000	6
		RH	6532.29166666666000	2492.086492362708000	6
		Total	6314.93750000000000	2468.775000161103000	12
	HC	LH	629.16666666666600	257.032763800000100	6
		RH	628.91666666666600	210.872749938598400	6
		Total	629.04166666666600	224.148079943648500	12
	PMC	LH	11183.16666666666000	2085.183167413996000	6
		RH	12251.00000000000000	2359.040207372481000	6
		Total	11717.08333333333000	2194.747900032477000	12
	PRC	LH	463.29166666666600	157.056949596847400	6
		RH	468.95833333333300	149.098576172499500	6
		Total	466.12500000000000	146.033211509013800	12
	V1	LH	1689.16666666666700	631.852230878918000	6
		RH	1801.62500000000000	568.038395489248000	6
		Total	1745.39583333333300	575.836540276339000	12
	V2	LH	8454.00000000000000	3109.152597573815000	6
		RH	8602.33333333333000	2939.190290992855000	6
		Total	8528.16666666666000	2885.612516381395000	12
	V3	LH	8185.70833333333000	2290.067299320408000	6
		RH	8526.79166666666000	2735.842500111559000	6
		Total	8356.25000000000000	2412.000784429994000	12
	Total	LH	3781.69318181818300	4048.169774201730000	66
		RH	3988.39015151515100	4309.866734091935000	66
		Total	3885.04166666666600	4166.369184832200000	132
	M1	LH	1771.88095238095200	583.713556355354000	7
		RH	2050.70238095238100	338.747214889271200	7
		Total	1911.29166666666700	480.778376130965000	14
	EcRC	LH	980.98809523809500	171.099632744774900	7
		RH	937.91666666666600	200.789535334887400	7
		Total	959.45238095238100	180.606275725684200	14
	ERC-28	LH	639.73809523809500	186.390311481808800	7
		RH	640.90476190476100	181.309954506570400	7
		Total	640.32142857142800	176.655390475714000	14
	ERC-34	LH	528.17857142857100	125.600450693003900	7
		RH	494.21428571428500	104.505325678828900	7

Total	Fusi.	Total	511.19642857142800	112.393033701939300	14
		LH	5477.15476190476000	1292.566117325813000	7
		RH	5340.59523809523000	1156.092512226161000	7
	HC	Total	5408.87499999999000	1180.251998818816000	14
		LH	507.66666666666600	97.855051535989200	7
		RH	465.26190476190400	112.896712346862200	7
	PMC	Total	486.46428571428500	103.856871196612100	14
		LH	9458.72619047619000	1896.560198702268000	7
		RH	9775.35714285714000	1829.605962001238000	7
	PRC	Total	9617.04166666666000	1797.803883395435000	14
		LH	375.25000000000000	80.405482814710200	7
		RH	346.73809523809520	82.943092223638700	7
	V1	Total	360.99404761904760	79.861822872020600	14
		LH	1331.48809523809500	480.400391043019000	7
		RH	1380.08333333333300	398.043444027575100	7
	V2	Total	1355.78571428571400	424.590658468662200	14
		LH	6487.77380952381000	2042.972063242783000	7
		RH	6685.63095238095000	1690.252806711244000	7
	V3	Total	6586.70238095238000	1804.293010532696000	14
		LH	6615.04761904761000	1486.316257016997000	7
		RH	6967.46428571428000	1867.076650076772000	7
	Total	Total	6791.25595238095000	1631.548548821854000	14
		LH	3106.71753246753200	3278.067296044561000	77
		RH	3189.53354978354900	3368.237671369055000	77
	M1	Total	3148.12554112554000	3312.840011204467000	154
		LH	2060.30128205128200	569.857910062022000	13
		RH	2317.01282051282000	421.385420103307600	13
	EcRC	Total	2188.65705128205100	508.173191347050000	26
		LH	1060.08974358974300	281.535060192369900	13
		RH	1031.41666666666600	285.479135499523900	13
	ERC-28	Total	1045.75320512820500	278.170298039777100	26
		LH	704.74358974358900	205.581780782596600	13
		RH	685.10256410256400	207.097554714688500	13
	ERC-34	Total	694.92307692307600	202.420027998819200	26
		LH	545.99999999999900	178.513946700717600	13
		RH	522.50000000000000	166.722542716934300	13
	Fusi.	Total	534.25000000000000	169.652969322673500	26
		LH	5763.50641025641000	1972.560704559704000	13

PC	Pre-Con.	HC	RH	5890.60897435897000	1907.439834005929000	13
			Total	5827.05769230769000	1902.176409737195000	26
			LH	563.74358974358900	190.498534131919800	13
		PMC	RH	540.79487179487100	179.197260357568300	13
			Total	552.26923076923000	181.575260349366300	26
			LH	10254.62179487179000	2100.176776238846000	13
		PRC	RH	10917.96153846153000	2375.409863419525000	13
			Total	10586.29166666666000	2222.610191900255000	26
			LH	415.88461538461530	124.889101447069400	13
		V1	RH	403.14743589743580	129.321887710571400	13
			Total	409.51602564102570	124.725585496121900	26
			LH	1496.57051282051200	562.303189691070000	13
		V2	RH	1574.64102564102500	511.376313727428000	13
			Total	1535.60576923076900	528.087298421646000	26
			LH	7395.26282051282000	2674.990017255117000	13
		V3	RH	7570.26282051282000	2452.973657833618000	13
			Total	7482.76282051282000	2516.115091177523000	26
			LH	7339.96794871794000	1988.447561372168000	13
		Total	RH	7687.15384615384000	2348.681255731743000	13
			Total	7513.56089743589000	2139.403893164543000	26
			LH	3418.24475524475600	3656.043869491610000	143
		M1	RH	3558.23659673659500	3838.530913552827000	143
			Total	3488.24067599067600	3742.473090933987000	286
			LH	.85089145	1.537649016	6
		EcRC	RH	.38727509	.555898274	6
			Total	.61908327	1.128625767	12
			LH	.68080263	.799111367	6
		ERC-28	RH	1.17851141	1.422076321	6
			Total	.92965702	1.130066059	12
			LH	1.74269839	2.259973998	6
		ERC-34	RH	.90825018	.891324727	6
			Total	1.32547428	1.694875235	12
			LH	.77425600	.574329137	6
		Fusi.	RH	1.06495108	1.686967330	6
			Total	.91960354	1.211012895	12
			LH	1.67876346	2.149966979	6
		Fusi.	RH	1.98403296	2.463441070	6
			Total	1.83139821	2.210184443	12

Post-Con.	HC	LH	.08606634	.098187227	6
		RH	.69826655	.868660526	6
		Total	.39216644	.670510421	12
	PMC	LH	.81440086	1.323246837	6
		RH	.93062219	1.683175102	6
		Total	.87251152	1.444765639	12
	PRC	LH	.88558190	1.395247788	6
		RH	.63907800	.945276099	6
		Total	.76232995	1.143503746	12
	V1	LH	1.24357595	1.648098816	6
		RH	.95398377	1.231949979	6
		Total	1.09877986	1.395487637	12
	V2	LH	2.07361138	2.592721737	6
		RH	1.67178188	1.872496062	6
		Total	1.87269663	2.166409648	12
	V3	LH	1.89407285	2.333836180	6
		RH	2.05014999	2.442076943	6
		Total	1.97211142	2.278870050	12
	Total	LH	1.15679284	1.669374766	66
		RH	1.13335483	1.546187388	66
		Total	1.14507383	1.602850797	132
	M1	LH	1.28997136	2.130608518	7
		RH	.59479899	.662871889	7
		Total	.94238517	1.558223273	14
	EcRC	LH	.85655908	.936790008	7
		RH	.58876108	.532664040	7
		Total	.72266008	.745181660	14
	ERC-28	LH	.74865004	.535930013	7
		RH	1.24345362	.961349252	7
		Total	.99605183	.790588253	14
	ERC-34	LH	1.10803735	.961041938	7
		RH	1.45942736	1.483619664	7
		Total	1.28373235	1.214671079	14
	Fusi.	LH	.92817579	.909673342	7
		RH	1.31251708	1.708918088	7
		Total	1.12034643	1.330253114	14
	HC	LH	.52380035	.601616115	7
		RH	.32784621	.307622419	7

Total	PMC	Total	.42582328	.470174608	14
		LH	1.12738879	1.605994737	7
		RH	1.29061159	2.249267636	7
	PRC	Total	1.20900019	1.879521008	14
		LH	.97495718	1.245592929	7
		RH	1.13793967	1.137182917	7
	V1	Total	1.05644842	1.148949082	14
		LH	.68161343	.315719693	7
		RH	1.10694226	.774550423	7
	V2	Total	.89427785	.609590648	14
		LH	1.18908140	1.448003766	7
		RH	1.26738360	1.389250536	7
	V3	Total	1.22823250	1.363870371	14
		LH	.98732820	.772842024	7
		RH	1.09030159	1.001293898	7
	Total	Total	1.03881490	.860963588	14
		LH	.94686936	1.101387011	77
		RH	1.03818028	1.202037265	77
	M1	Total	.99252482	1.149950178	154
		LH	1.08731910	1.818461854	13
		RH	.49901873	.600044870	13
	EcRC	Total	.79316891	1.360175297	26
		LH	.77544072	.844499236	13
		RH	.86095354	1.038330805	13
	ERC-28	Total	.81819713	.928294107	26
		LH	1.20744159	1.593036019	13
		RH	1.08874434	.907398605	13
	ERC-34	Total	1.14809296	1.271616461	26
		LH	.95398442	.793243310	13
		RH	1.27736138	1.525855024	13
	Fusi.	Total	1.11567290	1.202819095	26
		LH	1.27460087	1.578421689	13
		RH	1.62244748	2.027354147	13
	HC	Total	1.44852418	1.788915209	26
		LH	.32176927	.486390318	13
		RH	.49880944	.631396776	13
	PMC	Total	.41028936	.559520513	26
		LH	.98293282	1.430230644	13

VTCC	Pre-Con.	PRC	RH	1.12446264	1.935185274	13
			Total	1.05369773	1.668726705	26
			LH	.93370705	1.260568642	13
		V1	RH	.90769582	1.042067785	13
			Total	.92070144	1.133201847	26
			LH	.94098075	1.125444544	13
		V2	RH	1.03634603	.968833575	13
			Total	.98866339	1.029995758	26
			LH	1.59732601	2.014924555	13
		V3	RH	1.45402896	1.571614437	13
			Total	1.52567748	1.771916320	26
			LH	1.40582573	1.670178585	13
		Total	RH	1.53330854	1.798396796	13
			Total	1.46956714	1.701650583	26
			LH	1.04375712	1.391374196	143
		M1	RH	1.08210699	1.367451187	143
			Total	1.06293206	1.377176277	286
			LH	.44507004	.130550553	6
		EcRC	RH	.43743954	.091516895	6
			Total	.44125479	.107563351	12
			LH	.24730587	.133432042	6
		ERC-28	RH	.25832407	.134996747	6
			Total	.25281497	.128099876	12
			LH	.23754938	.136888303	6
		ERC-34	RH	.23012875	.116080521	6
			Total	.23383907	.121067476	12
			LH	.22761942	.119423977	6
		Fusi.	RH	.22325383	.115075707	6
			Total	.22543663	.111835796	12
			LH	.26886496	.135443432	6
		HC	RH	.32141688	.179959414	6
			Total	.29514092	.154312752	12
			LH	.26912671	.157984561	6
		PMC	RH	.30790513	.170930999	6
			Total	.28851592	.158227091	12
			LH	.43934162	.132224323	6
		PMC	RH	.46703875	.117315491	6
			Total	.45319019	.120050131	12

Post-Con.	PRC	LH	.27174938	.153988830	6
		RH	.30126992	.169674973	6
		Total	.28650965	.155249116	12
	V1	LH	.29852083	.157580325	6
		RH	.33727887	.195611962	6
		Total	.31789985	.170556456	12
	V2	LH	.39750771	.092134955	6
		RH	.40445642	.095899462	6
		Total	.40098206	.089733260	12
	V3	LH	.41866000	.102052433	6
		RH	.44236813	.087301008	6
		Total	.43051406	.091386816	12
	Total	LH	.32011963	.148107329	66
		RH	.33917093	.152711849	66
		Total	.32964528	.150156719	132
	M1	LH	.51595200	.145316575	7
		RH	.55604798	.160584513	7
		Total	.53599999	.148596682	14
	EcRC	LH	.37605029	.113948625	7
		RH	.37929010	.147133333	7
		Total	.37767019	.126439946	14
	ERC-28	LH	.34695571	.112547768	7
		RH	.37113461	.115290576	7
		Total	.35904516	.110174571	14
	ERC-34	LH	.38931757	.078620002	7
		RH	.37062995	.079476069	7
		Total	.37997376	.076564501	14
	Fusi.	LH	.44337374	.182738848	7
		RH	.46085218	.137815497	7
		Total	.45211296	.155758398	14
	HC	LH	.43954893	.120255395	7
		RH	.49183727	.165582236	7
		Total	.46569310	.141650238	14
	PMC	LH	.58688586	.136617170	7
		RH	.57030632	.119373759	7
		Total	.57859609	.123552591	14
	PRC	LH	.42188486	.131923089	7
		RH	.42773014	.155150921	7

Total	V1	Total	.42480750	.138389818	14
		LH	.53505787	.162012292	7
		RH	.54571619	.116600546	7
	V2	Total	.54038703	.135720193	14
		LH	.54352855	.135002651	7
		RH	.54444573	.105914992	7
	V3	Total	.54398714	.116574556	14
		LH	.55907493	.105822481	7
		RH	.57113193	.121570690	7
	Total	Total	.56510343	.109676370	14
		LH	.46887548	.146430781	77
		RH	.48082931	.146158549	77
	M1	Total	.47485240	.145939101	154
		LH	.48323725	.137886087	13
		RH	.50130562	.142024459	13
	EcRC	Total	.49227143	.137451703	26
		LH	.31662979	.135547251	13
		RH	.32345962	.149522867	13
	ERC-28	Total	.32004471	.139866357	26
		LH	.29646048	.131771746	13
		RH	.30605498	.132715610	13
	ERC-34	Total	.30125773	.129664963	26
		LH	.31468765	.126777265	13
		RH	.30261021	.120513543	13
	Fusi.	Total	.30864893	.121342489	26
		LH	.36283122	.180386890	13
		RH	.39649742	.168002702	13
	HC	Total	.37966432	.171643729	26
		LH	.36089252	.159529874	13
		RH	.40694551	.187058850	13
	PMC	Total	.38391902	.171938970	26
		LH	.51878852	.149925940	13
		RH	.52264437	.125422197	13
	PRC	Total	.52071644	.135439849	26
		LH	.35259156	.157005490	13
		RH	.36936389	.168336445	13
	V1	Total	.36097772	.159710126	26
		LH	.42588693	.196300471	13

		RH	.44951435	.185575388	13
		Total	.43770064	.187541340	26
	V2	LH	.47613431	.135611357	13
		RH	.47983528	.121313936	13
		Total	.47798479	.126076035	26
	V3	LH	.49426804	.123478360	13
		RH	.51170248	.122593657	13
		Total	.50298526	.120878296	26
	Total	LH	.40021893	.164484291	143
		RH	.41544852	.164713776	143
		Total	.40783373	.164487024	286

Box's Test of Equality of Covariance Matrices(a)

Box's M	2091.689
F	3.403
df1	430
df2	13583.779
Sig.	.000
Tests the null hypothesis that the observed covariance matrices of the dependent variables are equal across groups.	
a Design: COHORT+COHORT * ROI+COHORT * ROI * HEMI	

Multivariate Tests(d)

Effect		Value	F	Hypothesis df	Error df	Sig.	Partial Eta Squared	Noncent. Parameter	Observed Power(a)
COHORT	Pillai's Trace	1.332	119.678	8.000	480.000	.000	.666	957.427	1.000
	Wilks' Lambda	.006	708.227(b)	8.000	478.000	.000	.922	5665.814	1.000
	Hotelling's Trace	108.333	3222.910	8.000	476.000	.000	.982	25783.277	1.000
	Roy's Largest Root	107.815	6468.893(c)	4.000	240.000	.000	.991	25875.572	1.000
COHORT * ROI	Pillai's Trace	1.329	6.022	80.000	968.000	.000	.332	481.766	1.000
	Wilks' Lambda	.005	32.573	80.000	945.246	.000	.729	2541.679	1.000
	Hotelling's Trace	127.988	379.964	80.000	950.000	.000	.970	30397.132	1.000
	Roy's	127.592	1543.866(c)	20.000	242.000	.000	.992	30877.311	1.000

COHORT * ROI * HEMI	Largest Root								
	Pillai's Trace	.077	.217	88.000	968.000	1.000	.019	19.086	.363
	Wilks' Lambda	.924	.216	88.000	947.548	1.000	.019	18.789	.356
	Hotelling's Trace	.080	.215	88.000	950.000	1.000	.020	18.944	.359
	Roy's Largest Root	.041	.456(c)	22.000	242.000	.984	.040	10.037	.358

a Computed using alpha = .05

b Exact statistic

c The statistic is an upper bound on F that yields a lower bound on the significance level.

d Design: COHORT+COHORT * ROI+COHORT * ROI * HEMI

Levene's Test of Equality of Error Variances(a)

	F	df1	df2	Sig.
TSE	5.014	43	242	.000
AV	4.497	43	242	.000
PC	3.011	43	242	.000
VTCC	.491	43	242	.997

Tests the null hypothesis that the error variance of the dependent variable is equal across groups.

a Design: COHORT+COHORT * ROI+COHORT * ROI * HEMI

Tests of Between-Subjects Effects

Source	Dependent Variable	Type III Sum of Squares	df	Mean Square	F	Sig.	Partial Eta Squared	Noncent. Parameter	Observed Power(a)
Model	TSE	.631(b)	44	.014	386.273	.000	.986	16996.012	1.000
	AV	7050490984.130(c)	44	160238431.457	92.055	.000	.944	4050.407	1.000
	PC	378.903(d)	44	8.611	4.299	.000	.439	189.153	1.000
	VTCC	50.934(e)	44	1.158	64.449	.000	.921	2835.752	1.000
COHORT	TSE	.311	2	.155	4179.749	.000	.972	8359.498	1.000
	AV	3518595376.323	2	1759297688.161	1010.692	.000	.893	2021.383	1.000
	PC	324.784	2	162.392	81.068	.000	.401	162.137	1.000
	VTCC	49.069	2	24.534	1365.942	.000	.919	2731.884	1.000
COHORT * ROI	TSE	.321	20	.016	431.777	.000	.973	8635.548	1.000
	AV	3526000367.240	20	176300018.362	101.282	.000	.893	2025.637	1.000
	PC	43.192	20	2.160	1.078	.373	.082	21.562	.782

COHORT * ROI * HEMI	VTCC	1.819	20	.091	5.064	.000	.295	101.286	1.000
	TSE	3.59E-005	22	1.63E-006	.044	1.000	.004	.967	.068
	AV	5895240.567	22	267965.480	.154	1.000	.014	3.387	.126
	PC	10.927	22	.497	.248	1.000	.022	5.455	.189
Error	VTCC	.046	22	.002	.117	1.000	.011	2.582	.104
	TSE	.009	242	3.72E-005					
	AV	421246276.134	242	1740687.091					
	PC	484.762	242	2.003					
Total	VTCC	4.347	242	.018					
	TSE	.640	286						
	AV	7471737260.264	286						
	PC	863.665	286						
	VTCC	55.281	286						

a Computed using alpha = .05

b R Squared = .986 (Adjusted R Squared = .983)

c R Squared = .944 (Adjusted R Squared = .933)

d R Squared = .439 (Adjusted R Squared = .337)

e R Squared = .921 (Adjusted R Squared = .907)

CUSTOM HYPOTHESIS TESTS

Contrast Results (K Matrix)

Testing group Simple Contrast(a)		Dependent Variable				
		TSE	AV	PC	VTCC	
Level 2 vs. Level 1	Contrast Estimate	.002	-736.916	.153	.145	
	Hypothesized Value	0	0	0	0	
	Difference (Estimate - Hypothesized)	.002	-736.916	.153	.145	
	Std. Error	.001	156.493	.168	.016	
	Sig.	.001	.000	.364	.000	
	95% Confidence Interval for Difference	Lower Bound	.001	1045.179	.483	.114
		Upper Bound	.004	-428.653	.178	.177

a Reference category = 1

Multivariate Test Results								
	Value	F	Hypothesis df	Error df	Sig.	Partial Eta Squared	Noncent. Parameter	Observed Power(a)
Pillai's trace	.353	32.581(b)	4.000	239.000	.000	.353	130.323	1.000
Wilks' lambda	.647	32.581(b)	4.000	239.000	.000	.353	130.323	1.000
Hotelling's trace	.545	32.581(b)	4.000	239.000	.000	.353	130.323	1.000
Roy's largest root	.545	32.581(b)	4.000	239.000	.000	.353	130.323	1.000
a Computed using alpha = .05								
b Exact statistic								

Univariate Test Results									
Source	Dependent Variable	Sum of Squares	df	Mean Square	F	Sig.	Partial Eta Squared	Noncent. Parameter	Observed Power(a)
Contrast	TSE	.000	1	.000	10.355	.001	.041	10.355	.893
	AV	38597994.423	1	38597994.423	22.174	.000	.084	22.174	.997
	PC	1.654	1	1.654	.826	.364	.003	.826	.148
	VTCC	1.499	1	1.499	83.438	.000	.256	83.438	1.000
Error	TSE	.009	242	.000					
	AV	421246276.134	242	1740687.091					
	PC	484.762	242	2.003					
	VTCC	4.347	242	.018					
a Computed using alpha = .05									

ESTIMATED MARGINAL MEANS

1. Grand Mean

Dependent Variable	Mean	Std. Error	95% Confidence Interval	
	Lower Bound	Upper Bound	Lower Bound	Upper Bound
TSE	.033	.000	.032	.034
AV	3516.584	78.247	3362.452	3670.715
PC	1.069	.084	.903	1.234
VTCC	.402	.008	.387	.418

2. TESTING GROUP

		Estimates			
Dependent Variable	Testing group	Mean	Std. Error	95% Confidence Interval	
		Lower Bound	Upper Bound	Lower Bound	Upper Bound
TSE	Pre-Con.	.032	.001	.031	.033
	Post-Con.	.034	.000	.033	.035
AV	Pre-Con.	3885.042	114.835	3658.838	4111.245
	Post-Con.	3148.126	106.316	2938.702	3357.549
PC	Pre-Con.	1.145	.123	.902	1.388
	Post-Con.	.993	.114	.768	1.217
VTCC	Pre-Con.	.330	.012	.307	.353
	Post-Con.	.475	.011	.454	.496

			Pairwise Comparisons				
Dependent Variable	(I) Testing group	(J) Testing group	Mean Difference (I-J)	Std. Error	Sig.(a)	95% Confidence Interval for Difference(a)	
			Lower Bound	Upper Bound	Lower Bound	Upper Bound	Lower Bound
TSE	Pre-Con.	Post-Con.	-.002(*)	.001	.001	-.004	-.001
	Post-Con.	Pre-Con.	.002(*)	.001	.001	.001	.004
AV	Pre-Con.	Post-Con.	736.916(*)	156.493	.000	428.653	1045.179
	Post-Con.	Pre-Con.	-736.916(*)	156.493	.000	-1045.179	-428.653
PC	Pre-Con.	Post-Con.	.153	.168	.364	-.178	.483
	Post-Con.	Pre-Con.	-.153	.168	.364	-.483	.178
VTCC	Pre-Con.	Post-Con.	-.145(*)	.016	.000	-.177	-.114
	Post-Con.	Pre-Con.	.145(*)	.016	.000	.114	.177

Based on estimated marginal means

* The mean difference is significant at the .05 level.

a Adjustment for multiple comparisons: Bonferroni.

Multivariate Tests								
	Value	F	Hypothesis df	Error df	Sig.	Partial Eta Squared	Noncent. Parameter	Observed Power(a)
Pillai's trace	.353	32.581(b)	4.000	239.000	.000	.353	130.323	1.000
Wilks' lambda	.647	32.581(b)	4.000	239.000	.000	.353	130.323	1.000
Hotelling's trace	.545	32.581(b)	4.000	239.000	.000	.353	130.323	1.000
Roy's largest root	.545	32.581(b)	4.000	239.000	.000	.353	130.323	1.000

Each F tests the multivariate effect of Testing group. These tests are based on the linearly independent pairwise comparisons among the estimated marginal means.

a Computed using alpha = .05

b Exact statistic

		Univariate Tests							
Dependent Variable		Sum of Squares	df	Mean Square	F	Sig.	Partial Eta Squared	Noncent. Parameter	Observed Power(a)
TSE	Contrast	.000	1	.000	10.355	.001	.041	10.355	.893
	Error	.009	242	3.72E-005					
AV	Contrast	38597994.423	1	38597994.423	22.174	.000	.084	22.174	.997
	Error	421246276.134	242	1740687.091					
PC	Contrast	1.654	1	1.654	.826	.364	.003	.826	.148
	Error	484.762	242	2.003					
VTCC	Contrast	1.499	1	1.499	83.438	.000	.256	83.438	1.000
	Error	4.347	242	.018					

The F tests the effect of Testing group. This test is based on the linearly independent pairwise comparisons among the estimated marginal means.

a Computed using alpha = .05

3. Testing group * ROI

Dependent Variable	Testing group	ROI	Mean	Std. Error	95% Confidence Interval	
			Lower Bound	Upper Bound	Lower Bound	Upper Bound
TSE	Pre-Con.	M1	.023	.002	.019	.026
		EcRC	.008	.002	.004	.011
		ERC-28	.005	.002	.002	.009
		ERC-34	.005	.002	.001	.008
		Fusi.	.048	.002	.044	.051
		HC	.005	.002	.001	.008

AV

Post-Con.	PMC	.103	.002	.100	.107
	PRC	.004	.002	4.12E-005	.007
	V1	.014	.002	.011	.018
	V2	.066	.002	.062	.069
	V3	.069	.002	.065	.072
	M1	.023	.002	.020	.026
	EcRC	.009	.002	.006	.012
	ERC-28	.006	.002	.003	.009
	ERC-34	.005	.002	.002	.009
	Fusi.	.055	.002	.052	.058
	HC	.006	.002	.003	.009
	PMC	.104	.002	.101	.107
Pre-Con.	PRC	.004	.002	.001	.007
	V1	.016	.002	.013	.020
	V2	.073	.002	.069	.076
	V3	.073	.002	.070	.077
	M1	2512.250	380.864	1762.019	3262.481
	EcRC	1146.438	380.864	396.206	1896.669
	ERC-28	758.625	380.864	8.394	1508.856
	ERC-34	561.146	380.864	-189.086	1311.377
	Fusi.	6314.938	380.864	5564.706	7065.169
	HC	629.042	380.864	-121.190	1379.273
	PMC	11717.083	380.864	10966.852	12467.315
	PRC	466.125	380.864	-284.106	1216.356
Post-Con.	V1	1745.396	380.864	995.164	2495.627
	V2	8528.167	380.864	7777.935	9278.398
	V3	8356.250	380.864	7606.019	9106.481
	M1	1911.292	352.611	1216.712	2605.871
	EcRC	959.452	352.611	264.873	1654.032
	ERC-28	640.321	352.611	-54.258	1334.901
	ERC-34	511.196	352.611	-183.383	1205.776
	Fusi.	5408.875	352.611	4714.296	6103.454
	HC	486.464	352.611	-208.115	1181.044
	PMC	9617.042	352.611	8922.462	10311.621
	PRC	360.994	352.611	-333.585	1055.573
	V1	1355.786	352.611	661.206	2050.365
	V2	6586.702	352.611	5892.123	7281.282
	V3	6791.256	352.611	6096.677	7485.835

PC	Pre-Con.	M1	.619	.409	-.186	1.424
		EcRC	.930	.409	.125	1.734
		ERC-28	1.325	.409	.521	2.130
		ERC-34	.920	.409	.115	1.724
		Fusi.	1.831	.409	1.027	2.636
		HC	.392	.409	-.413	1.197
		PMC	.873	.409	.068	1.677
		PRC	.762	.409	-.042	1.567
		V1	1.099	.409	.294	1.904
		V2	1.873	.409	1.068	2.678
		V3	1.972	.409	1.167	2.777
	Post-Con.	M1	.942	.378	.197	1.687
		EcRC	.723	.378	-.022	1.468
		ERC-28	.996	.378	.251	1.741
		ERC-34	1.284	.378	.539	2.029
		Fusi.	1.120	.378	.375	1.865
		HC	.426	.378	-.319	1.171
		PMC	1.209	.378	.464	1.954
		PRC	1.056	.378	.311	1.802
		V1	.894	.378	.149	1.639
		V2	1.228	.378	.483	1.973
		V3	1.039	.378	.294	1.784
VTCC	Pre-Con.	M1	.441	.039	.365	.517
		EcRC	.253	.039	.177	.329
		ERC-28	.234	.039	.158	.310
		ERC-34	.225	.039	.149	.302
		Fusi.	.295	.039	.219	.371
		HC	.289	.039	.212	.365
		PMC	.453	.039	.377	.529
		PRC	.287	.039	.210	.363
		V1	.318	.039	.242	.394
		V2	.401	.039	.325	.477
		V3	.431	.039	.354	.507
	Post-Con.	M1	.536	.036	.465	.607
		EcRC	.378	.036	.307	.448
		ERC-28	.359	.036	.288	.430
		ERC-34	.380	.036	.309	.451
		Fusi.	.452	.036	.382	.523

HC	.466	.036	.395	.536
PMC	.579	.036	.508	.649
PRC	.425	.036	.354	.495
V1	.540	.036	.470	.611
V2	.544	.036	.473	.615
V3	.565	.036	.495	.636

4. Testing group * ROI * Hemi.							
Dependent Variable	Testing group	ROI	Hemi.	Mean	Std. Error	95% Confidence Interval	
				Lower Bound	Upper Bound	Lower Bound	Upper Bound
TSE	Pre-Con.	M1	LH	.023	.002	.018	.027
			RH	.023	.002	.018	.028
		EcRC	LH	.008	.002	.003	.013
			RH	.008	.002	.003	.013
		ERC-28	LH	.005	.002	.000	.010
			RH	.005	.002	.000	.010
		ERC-34	LH	.005	.002	-4.57E-005	.010
			RH	.005	.002	.000	.010
		Fusi.	LH	.047	.002	.043	.052
			RH	.048	.002	.043	.053
		HC	LH	.005	.002	.000	.010
			RH	.005	.002	.000	.010
		PMC	LH	.103	.002	.098	.108
			RH	.103	.002	.098	.108
		PRC	LH	.003	.002	-.001	.008
			RH	.004	.002	-.001	.008
		V1	LH	.014	.002	.009	.019
			RH	.014	.002	.010	.019
		V2	LH	.065	.002	.060	.070
			RH	.066	.002	.061	.071
		V3	LH	.068	.002	.063	.073
			RH	.069	.002	.065	.074
	Post-Con.	M1	LH	.023	.002	.018	.027
			RH	.023	.002	.018	.028
		EcRC	LH	.009	.002	.004	.014
			RH	.009	.002	.004	.013
		ERC-	LH	.006	.002	.001	.010
			RH	.006	.002	.001	.010

AV	Pre-Con.	28	RH	.006	.002	.001	.010
		ERC-34	LH	.006	.002	.001	.010
			RH	.005	.002	.001	.010
		Fusi.	LH	.055	.002	.050	.059
			RH	.055	.002	.050	.060
		HC	LH	.006	.002	.002	.011
			RH	.005	.002	.001	.010
		PMC	LH	.104	.002	.099	.108
			RH	.105	.002	.100	.109
		PRC	LH	.004	.002	-.001	.009
			RH	.004	.002	-.001	.009
		V1	LH	.016	.002	.012	.021
			RH	.017	.002	.012	.021
		V2	LH	.072	.002	.067	.077
			RH	.073	.002	.069	.078
		V3	LH	.072	.002	.068	.077
			RH	.075	.002	.070	.079
		M1	LH	2396.792	538.623	1335.804	3457.779
			RH	2627.708	538.623	1566.721	3688.696
		EcRC	LH	1152.375	538.623	91.388	2213.362
			RH	1140.500	538.623	79.513	2201.487
		ERC-28	LH	780.583	538.623	-280.404	1841.571
			RH	736.667	538.623	-324.321	1797.654
		ERC-34	LH	566.792	538.623	-494.196	1627.779
			RH	555.500	538.623	-505.487	1616.487
		Fusi.	LH	6097.583	538.623	5036.596	7158.571
			RH	6532.292	538.623	5471.304	7593.279
		HC	LH	629.167	538.623	-431.821	1690.154
			RH	628.917	538.623	-432.071	1689.904
		PMC	LH	11183.167	538.623	10122.179	12244.154
			RH	12251.000	538.623	11190.013	13311.987
		PRC	LH	463.292	538.623	-597.696	1524.279
			RH	468.958	538.623	-592.029	1529.946
		V1	LH	1689.167	538.623	628.179	2750.154
			RH	1801.625	538.623	740.638	2862.612
		V2	LH	8454.000	538.623	7393.013	9514.987
			RH	8602.333	538.623	7541.346	9663.321
		V3	LH	8185.708	538.623	7124.721	9246.696

PC	Post-Con.	M1	RH	8526.792	538.623	7465.804	9587.779
			LH	1771.881	498.668	789.598	2754.164
		EcRC	RH	2050.702	498.668	1068.419	3032.986
			LH	980.988	498.668	-1.295	1963.271
		ERC-28	RH	937.917	498.668	-44.367	1920.200
			LH	639.738	498.668	-342.545	1622.021
		ERC-34	RH	640.905	498.668	-341.379	1623.188
			LH	528.179	498.668	-454.105	1510.462
		Fusi.	RH	494.214	498.668	-488.069	1476.498
			LH	5477.155	498.668	4494.871	6459.438
		HC	RH	5340.595	498.668	4358.312	6322.879
			LH	507.667	498.668	-474.617	1489.950
		PMC	RH	465.262	498.668	-517.021	1447.545
			LH	9458.726	498.668	8476.443	10441.010
		PRC	RH	9775.357	498.668	8793.074	10757.641
			LH	375.250	498.668	-607.033	1357.533
		V1	RH	346.738	498.668	-635.545	1329.021
			LH	1331.488	498.668	349.205	2313.771
		V2	RH	1380.083	498.668	397.800	2362.367
			LH	6487.774	498.668	5505.490	7470.057
		V3	RH	6685.631	498.668	5703.348	7667.914
			LH	6615.048	498.668	5632.764	7597.331
	Pre-Con.	M1	RH	6967.464	498.668	5985.181	7949.748
			LH	.851	.578	-.287	1.989
		EcRC	RH	.387	.578	-.751	1.525
			LH	.681	.578	-.457	1.819
		ERC-28	RH	1.179	.578	.040	2.317
			LH	1.743	.578	.605	2.881
		ERC-34	RH	.908	.578	-.230	2.046
			LH	.774	.578	-.364	1.912
		Fusi.	RH	1.065	.578	-.073	2.203
			LH	1.679	.578	.541	2.817
		HC	RH	1.984	.578	.846	3.122
			LH	.086	.578	-1.052	1.224
		PMC	RH	.698	.578	-.440	1.836
			LH	.814	.578	-.324	1.953
		PRC	RH	.931	.578	-.208	2.069
			LH	.886	.578	-.253	2.024

VTCC	Post-Con.	V1	RH	.639	.578	-.499	1.777
			LH	1.244	.578	.105	2.382
		V2	RH	.954	.578	-.184	2.092
			LH	2.074	.578	.935	3.212
		V3	RH	1.672	.578	.534	2.810
			LH	1.894	.578	.756	3.032
		M1	RH	2.050	.578	.912	3.188
			LH	1.290	.535	.236	2.344
		EcRC	RH	.595	.535	-.459	1.649
			LH	.857	.535	-.197	1.910
		ERC-28	RH	.589	.535	-.465	1.643
			LH	.749	.535	-.305	1.802
		ERC-34	RH	1.243	.535	.190	2.297
			LH	1.108	.535	.054	2.162
		Fusi.	RH	1.459	.535	.406	2.513
			LH	.928	.535	-.126	1.982
		HC	RH	1.313	.535	.259	2.366
			LH	.524	.535	-.530	1.578
		PMC	RH	.328	.535	-.726	1.382
			LH	1.127	.535	.074	2.181
		PRC	RH	1.291	.535	.237	2.344
			LH	.975	.535	-.079	2.029
		V1	RH	1.138	.535	.084	2.192
			LH	.682	.535	-.372	1.735
		V2	RH	1.107	.535	.053	2.161
			LH	1.189	.535	.135	2.243
		V3	RH	1.267	.535	.214	2.321
			LH	.987	.535	-.066	2.041
		M1	RH	1.090	.535	.037	2.144
			LH	.445	.055	.337	.553
		EcRC	RH	.437	.055	.330	.545
			LH	.247	.055	.140	.355
		ERC-28	RH	.258	.055	.151	.366
			LH	.238	.055	.130	.345
		ERC-34	RH	.230	.055	.122	.338
			LH	.228	.055	.120	.335
		Fusi.	RH	.223	.055	.115	.331
			LH	.269	.055	.161	.377

Post-Con.	HC	RH	.321	.055	.214	.429
		LH	.269	.055	.161	.377
	PMC	RH	.308	.055	.200	.416
		LH	.439	.055	.332	.547
	PRC	RH	.467	.055	.359	.575
		LH	.272	.055	.164	.380
	V1	RH	.301	.055	.193	.409
		LH	.299	.055	.191	.406
	V2	RH	.337	.055	.230	.445
		LH	.398	.055	.290	.505
	V3	RH	.404	.055	.297	.512
		LH	.419	.055	.311	.526
	M1	RH	.442	.055	.335	.550
		LH	.516	.051	.416	.616
	EcRC	RH	.556	.051	.456	.656
		LH	.376	.051	.276	.476
	ERC-28	RH	.379	.051	.280	.479
		LH	.347	.051	.247	.447
	ERC-34	RH	.371	.051	.271	.471
		LH	.389	.051	.290	.489
	Fusi.	RH	.371	.051	.271	.470
		LH	.443	.051	.344	.543
	HC	RH	.461	.051	.361	.561
		LH	.440	.051	.340	.539
	PMC	RH	.492	.051	.392	.592
		LH	.587	.051	.487	.687
	PRC	RH	.570	.051	.471	.670
		LH	.422	.051	.322	.522
	V1	RH	.428	.051	.328	.528
		LH	.535	.051	.435	.635
	V2	RH	.546	.051	.446	.645
		LH	.544	.051	.444	.643
	V3	RH	.544	.051	.445	.644
		LH	.559	.051	.459	.659
		RH	.571	.051	.471	.671

APPENDIX C: DECONVOLUTION COMMAND LINE

The following command line templates were used to invoke the AFNI program 3dDeconvolve for Figure 7 of the present dissertation. 3dDeconvolve was run on individual, motion-corrected (“3dreg”) subject datasets which had been concatenated and detrended across the four runs (“allruns”). The baseline was specified to consist of six motion parameters – roll, pitch, yaw, and translations along the x , y , and z axes – as well as a linear trend. Computation of voxel impulse response functions (IRFs: see Figure 8) was found to be optimal at a maximum time lag of 4 TRs, or 10 seconds.

```
3dDeconvolve \
  -input 3dreg.$subj.allruns+orig \
  -automask -GOFORIT 2 -jobs 4 -num_stimts 9 \
  -stim_file 1 match.1D -stim_label 1 M \
  -stim_file 2 mismatch.1D -stim_label 2 MM \
  -stim_file 3 control.1D -stim_label 3 C \
  -stim_file 4 '$subj.allruns.1D[0]' -stim_label 4 ROLL \
  -stim_label 5 PITCH -stim_file 5 '$subj.allruns.1D[1]' \
  -stim_label 6 RAW -stim_file 6 '$subj.allruns.1D[2]' \
  -stim_label 7 dP -stim_file 7 '$subj.allruns.1D[3]' \
  -stim_label 8 dI -stim_file 8 '$subj.allruns.1D[4]' \
  -stim_label 9 dS -stim_file 9 '$subj.allruns.1D[5]' \
  -stim_base 4 -stim_base 5 -stim_base 6 -stim_base 7 \
  -stim_base 8 -stim_base 9 \
  -iresp 1 $subj.match_IRF_maxlag_4 \
  -iresp 2 $subj.mismatch_IRF_maxlag_4 \
  -iresp 3 $subj.control_IRF_maxlag_4 \
  -sresp 1 $subj.match_sdIRF_maxlag_4 \
  -sresp 2 $subj.mismatch_sdIRF_maxlag_4 \
  -sresp 3 $subj.control_sdIRF_maxlag_4 \
  -stim_maxlag 1 4 -stim_maxlag 2 4 -stim_maxlag 3 4 \
  -fout -rout -tout -vout -nobout -full_first \
  -bucket 3dd.$subj.allruns_maxlag_4
```

REFERENCES

- Abel, T. and K. M. Lattal (2001). Molecular mechanisms of memory acquisition, consolidation and retrieval. *Current opinion in neurobiology* **11**(2): 180-7.
- Aguirre, G. K., E. Zarahn and M. D'Esposito (1998). The variability of human, BOLD hemodynamic responses. *Neuroimage* **8**(4): 360-9.
- Albright, T. D. (1993). Cortical processing of visual motion. *Reviews of oculomotor research* **5**: 177-201.
- Alvarez, P. and L. R. Squire (1994). Memory consolidation and the medial temporal lobe: a simple network model. *Proceedings of the National Academy of Sciences of the United States of America* **91**(15): 7041-5.
- Anderson, J. R. and L. J. Schooler (1991). Reflections of the environment in memory. *Psychol Sci* **2**(6): 396-408.
- Bailey, C. H., M. Chen, F. Keller and E. R. Kandel (1992). Serotonin-mediated endocytosis of apCAM: an early step of learning-related synaptic growth in Aplysia. *Science (New York, N.Y)* **256**(5057): 645-9.
- Bailey, C. H., P. Montarolo, M. Chen, E. R. Kandel and S. Schacher (1992). Inhibitors of protein and RNA synthesis block structural changes that accompany long-term heterosynaptic plasticity in Aplysia. *Neuron* **9**(4): 749-58.
- Bandettini, P. A., E. C. Wong, R. S. Hinks, R. S. Tikofsky and J. S. Hyde (1992). Time course EPI of human brain function during task activation. *Magn Reson Med* **25**(2): 390-7.
- Bannerman, D. M., J. N. Rawlins, S. B. McHugh, R. M. Deacon, B. K. Yee, T. Bast, W. N. Zhang, H. H. Pothuizen and J. Feldon (2004). Regional dissociations within the hippocampus--memory and anxiety. *Neuroscience and biobehavioral reviews* **28**(3): 273-83.
- Behzadi, Y. and T. T. Liu (2005). An arteriolar compliance model of the cerebral blood flow response to neural stimulus. *Neuroimage* **25**(4): 1100-11.
- Belcadi-Abbassi, W. and C. Destradre (1995). Post-test apamin injection suppresses a Kamin-like effect following a learning session in mice. *Neuroreport* **6**(9): 1293-6.

- Blamire, A. M., S. Ogawa, K. Ugurbil, D. Rothman, G. McCarthy, J. M. Ellermann, F. Hyder, Z. Rattner and R. G. Shulman (1992). Dynamic mapping of the human visual cortex by high-speed magnetic resonance imaging. *Proceedings of the National Academy of Sciences of the United States of America* **89**(22): 11069-73.
- Bodizs, R., M. Bekesy, A. Szucs, P. Barsi and P. Halasz (2002). Sleep-dependent hippocampal slow activity correlates with waking memory performance in humans. *Neurobiology of learning and memory* **78**(2): 441-57.
- Boynton, G. M., S. A. Engel, G. H. Glover and D. J. Heeger (1996). Linear systems analysis of functional magnetic resonance imaging in human V1. *J Neurosci* **16**(13): 4207-21.
- Bozon, B., S. Davis and S. Laroche (2003). A requirement for the immediate early gene zif268 in reconsolidation of recognition memory after retrieval. *Neuron* **40**(4): 695-701.
- Bozon, B., A. Kelly, S. A. Josselyn, A. J. Silva, S. Davis and S. Laroche (2003). MAPK, CREB and zif268 are all required for the consolidation of recognition memory. *Philosophical transactions of the Royal Society of London* **358**(1432): 805-14.
- Braddick, O. J., J. M. O'Brien, J. Wattam-Bell, J. Atkinson, T. Hartley and R. Turner (2001). Brain areas sensitive to coherent visual motion. *Perception* **30**(1): 61-72.
- Breakspear, M., M. J. Brammer, E. T. Bullmore, P. Das and L. M. Williams (2004). Spatiotemporal wavelet resampling for functional neuroimaging data. *Hum Brain Mapp* **23**(1): 1-25.
- Brown, H. D. and S. M. Kosslyn (1993). Cerebral lateralization. *Current opinion in neurobiology* **3**(2): 183-6.
- Buchel, C., J. T. Coull and K. J. Friston (1999). The predictive value of changes in effective connectivity for human learning. *Science (New York, N.Y)* **283**(5407): 1538-41.
- Buckner, R. L., P. A. Bandettini, K. M. O'Craven, R. L. Savoy, S. E. Petersen, M. E. Raichle and B. R. Rosen (1996). Detection of cortical activation during averaged single trials of a cognitive task using functional magnetic resonance imaging. *Proceedings of the National Academy of Sciences of the United States of America* **93**(25): 14878-83.
- Buckner, R. L., W. Koutstaal, D. L. Schacter, A. M. Dale, M. Rotte and B. R. Rosen (1998a). Functional-anatomic study of episodic retrieval. II. Selective averaging

- of event-related fMRI trials to test the retrieval success hypothesis. *Neuroimage* **7**(3): 163-75.
- Buckner, R. L., W. Koutstaal, D. L. Schacter, A. D. Wagner and B. R. Rosen (1998b). Functional-anatomic study of episodic retrieval using fMRI. I. Retrieval effort versus retrieval success. *Neuroimage* **7**(3): 151-62.
- Burwell, R. D. and D. G. Amaral (1998a). Cortical afferents of the perirhinal, postrhinal, and entorhinal cortices of the rat. *The Journal of comparative neurology* **398**(2): 179-205.
- Burwell, R. D. and D. G. Amaral (1998b). Perirhinal and postrhinal cortices of the rat: interconnectivity and connections with the entorhinal cortex. *The Journal of comparative neurology* **391**(3): 293-321.
- Burwell, R. D., D. J. Bucci, M. R. Sanborn and M. J. Jutras (2004). Perirhinal and postrhinal contributions to remote memory for context. *J Neurosci* **24**(49): 11023-8.
- Buxton, R. B., K. Uludag, D. J. Dubowitz and T. T. Liu (2004). Modeling the hemodynamic response to brain activation. *Neuroimage* **23** Suppl 1: S220-33.
- Buzsaki, G. (1998). Memory consolidation during sleep: a neurophysiological perspective. *Journal of sleep research* **7** Suppl 1: 17-23.
- Cabeza, R., J. K. Locantore and N. D. Anderson (2003). Lateralization of prefrontal activity during episodic memory retrieval: evidence for the production-monitoring hypothesis. *Journal of cognitive neuroscience* **15**(2): 249-59.
- Cantero, J. L., M. Atienza and R. M. Salas (2002a). Effects of waking-auditory stimulation on human sleep architecture. *Behavioural brain research* **128**(1): 53-9.
- Cantero, J. L., M. Atienza, R. M. Salas and E. Dominguez-Marin (2002b). Effects of prolonged waking-auditory stimulation on electroencephalogram synchronization and cortical coherence during subsequent slow-wave sleep. *J Neurosci* **22**(11): 4702-8.
- Chance, F. S. (2007). Receiver operating characteristic (ROC) analysis for characterizing synaptic efficacy. *Journal of neurophysiology* **97**(2): 1799-808.
- Chrobak, J. J. and G. Buzsaki (1998a). Gamma oscillations in the entorhinal cortex of the freely behaving rat. *J Neurosci* **18**(1): 388-98.

- Chrobak, J. J. and G. Buzsaki (1998b). Operational dynamics in the hippocampal-entorhinal axis. *Neuroscience and biobehavioral reviews* **22**(2): 303-10.
- Chun, M. M. and N. B. Turk-Browne (2007). Interactions between attention and memory. *Current opinion in neurobiology* **17**(2): 177-84.
- Cirelli, C. and G. Tononi (2000a). Gene expression in the brain across the sleep-waking cycle. *Brain research* **885**(2): 303-21.
- Cirelli, C. and G. Tononi (2000b). On the functional significance of c-fos induction during the sleep-waking cycle. *Sleep* **23**(4): 453-69.
- Clavagnier, S., A. Falchier and H. Kennedy (2004). Long-distance feedback projections to area V1: implications for multisensory integration, spatial awareness, and visual consciousness. *Cognitive, affective & behavioral neuroscience* **4**(2): 117-26.
- Cramer, S. C., R. M. Weisskoff, J. D. Schaechter, G. Nelles, M. Foley, S. P. Finklestein and B. R. Rosen (2002). Motor cortex activation is related to force of squeezing. *Hum Brain Mapp* **16**(4): 197-205.
- Datta, S. (2000). Avoidance task training potentiates phasic pontine-wave density in the rat: A mechanism for sleep-dependent plasticity. *J Neurosci* **20**(22): 8607-13.
- de Araujo, D. B., W. Tedeschi, A. C. Santos, J. Elias, Jr., U. P. Neves and O. Baffa (2003). Shannon entropy applied to the analysis of event-related fMRI time series. *Neuroimage* **20**(1): 311-7.
- Deacon, T. W., H. Eichenbaum, P. Rosenberg and K. W. Eckmann (1983). Afferent connections of the perirhinal cortex in the rat. *The Journal of comparative neurology* **220**(2): 168-90.
- Dudukovic, N. M. and A. D. Wagner (2007). Goal-dependent modulation of declarative memory: Neural correlates of temporal recency decisions and novelty detection. *Neuropsychologia* **45**(11): 2608-20.
- Duong, T. Q., A. C. Silva, S. P. Lee and S. G. Kim (2000). Functional MRI of calcium-dependent synaptic activity: cross correlation with CBF and BOLD measurements. *Magn Reson Med* **43**(3): 383-92.
- Ebbinghaus, H. (1913). *Memory. A Contribution to Experimental Psychology*. New York, Teachers College, Columbia University.

- Egorov, A. V., B. N. Hamam, E. Fransen, M. E. Hasselmo and A. A. Alonso (2002). Graded persistent activity in entorhinal cortex neurons. *Nature* **420**(6912): 173-8.
- Egorov, A. V., U. Heinemann and W. Muller (2002). Differential excitability and voltage-dependent Ca²⁺ signalling in two types of medial entorhinal cortex layer V neurons. *The European journal of neuroscience* **16**(7): 1305-12.
- Eichenbaum, H. (1996). Learning from LTP: a comment on recent attempts to identify cellular and molecular mechanisms of memory. *Learning & memory (Cold Spring Harbor, N.Y)* **3**(2-3): 61-73.
- Eichenbaum, H. (2001). The long and winding road to memory consolidation. *Nature neuroscience* **4**(11): 1057-8.
- Eichenbaum, H., J. Dusek, B. Young and M. Bunsey (1996). Neural mechanisms of declarative memory. *Cold Spring Harbor symposia on quantitative biology* **61**: 197-206.
- Eichenbaum, H., G. Schoenbaum, B. Young and M. Bunsey (1996). Functional organization of the hippocampal memory system. *Proceedings of the National Academy of Sciences of the United States of America* **93**(24): 13500-7.
- Fell, J., G. Fernandez and C. E. Elger (2003). More than synchrony: EEG chaoticity may be necessary for conscious brain functioning. *Medical hypotheses* **61**(1): 158-60.
- Fernandez, G. and I. Tendolkar (2006). The rhinal cortex: 'gatekeeper' of the declarative memory system. *Trends Cogn Sci* **10**(8): 358-62.
- Frank, L. M. and E. N. Brown (2003). Persistent activity and memory in the entorhinal cortex. *Trends in neurosciences* **26**(8): 400-1.
- Frith, C. (2005). The neural basis of hallucinations and delusions. *Comptes rendus biologies* **328**(2): 169-75.
- Gabrieli, J. D. (1998). Cognitive neuroscience of human memory. *Annual review of psychology* **49**: 87-115.
- Gabrieli, J. D., J. B. Brewer and R. A. Poldrack (1998). Images of medial temporal lobe functions in human learning and memory. *Neurobiology of learning and memory* **70**(1-2): 275-83.

- Gais, S. and J. Born (2004). Declarative memory consolidation: mechanisms acting during human sleep. *Learning & memory (Cold Spring Harbor, N.Y)* **11**(6): 679-85.
- Geissler, A., R. Lanzenberger, M. Barth, A. R. Tahamtan, D. Milakara, A. Gartus and R. Beisteiner (2005). Influence of fMRI smoothing procedures on replicability of fine scale motor localization. *Neuroimage* **24**(2): 323-31.
- Gerber, B. and R. Menzel (2000). Contextual modulation of memory consolidation. *Learning & memory (Cold Spring Harbor, N.Y)* **7**: 151-158.
- Gerloff, C., C. Braun, M. Staudt, Y. L. Hegner, J. Dichgans and I. Krageloh-Mann (2006). Coherent corticomuscular oscillations originate from primary motor cortex: evidence from patients with early brain lesions. *Hum Brain Mapp* **27**(10): 789-98.
- Gonsalves, B. D., I. Kahn, T. Curran, K. A. Norman and A. D. Wagner (2005). Memory strength and repetition suppression: multimodal imaging of medial temporal cortical contributions to recognition. *Neuron* **47**(5): 751-61.
- Gonzalez Andino, S. L., R. Grave de Peralta Menendez, G. Thut, L. Spinelli, O. Blanke, C. M. Michel, M. Seeck and T. Landis (2000). Measuring the complexity of time series: an application to neurophysiological signals. *Hum Brain Mapp* **11**(1): 46-57.
- Grunwald, T., N. N. Boutros, N. Pezer, J. von Oertzen, G. Fernandez, C. Schaller and C. E. Elger (2003). Neuronal substrates of sensory gating within the human brain. *Biological psychiatry* **53**(6): 511-9.
- Haist, F., J. Bowden Gore and H. Mao (2001). Consolidation of human memory over decades revealed by functional magnetic resonance imaging. *Nature neuroscience* **4**(11): 1139-45.
- Hamzei, F., R. Knab, C. Weiller and J. Rother (2003). The influence of extra- and intracranial artery disease on the BOLD signal in FMRI. *Neuroimage* **20**(2): 1393-9.
- Hausser, M., N. Spruston and G. J. Stuart (2000). Diversity and dynamics of dendritic signaling. *Science (New York, N.Y)* **290**(5492): 739-44.
- Haxby, J. V., M. I. Gobbini, M. L. Furey, A. Ishai, J. L. Schouten and P. Pietrini (2001). Distributed and overlapping representations of faces and objects in ventral temporal cortex. *Science (New York, N.Y)* **293**(5539): 2425-30.

- Haxby, J. V., E. A. Hoffman and M. I. Gobbini (2002). Human neural systems for face recognition and social communication. *Biological psychiatry* **51**(1): 59-67.
- Haxby, J. V., B. Horwitz, L. G. Ungerleider, J. M. Maisog, P. Pietrini and C. L. Grady (1994). The functional organization of human extrastriate cortex: a PET-rCBF study of selective attention to faces and locations. *J Neurosci* **14**(11 Pt 1): 6336-53.
- Henson, R. N. and M. D. Rugg (2003). Neural response suppression, haemodynamic repetition effects, and behavioural priming. *Neuropsychologia* **41**(3): 263-70.
- Herron, J. E. and M. D. Rugg (2003a). Retrieval orientation and the control of recollection. *Journal of cognitive neuroscience* **15**(6): 843-54.
- Herron, J. E. and M. D. Rugg (2003b). Strategic influences on recollection in the exclusion task: electrophysiological evidence. *Psychonomic bulletin & review* **10**(3): 703-10.
- Herron, J. E. and E. L. Wilding (2004). An electrophysiological dissociation of retrieval mode and retrieval orientation. *Neuroimage* **22**(4): 1554-62.
- Herron, J. E. and E. L. Wilding (2006a). Brain and behavioral indices of retrieval mode. *Neuroimage* **32**(2): 863-70.
- Herron, J. E. and E. L. Wilding (2006b). Neural correlates of control processes engaged before and during recovery of information from episodic memory. *Neuroimage* **30**(2): 634-44.
- Holmes, W. R. and W. B. Levy (1990). Insights into associative long-term potentiation from computational models of NMDA receptor-mediated calcium influx and intracellular calcium concentration changes. *Journal of neurophysiology* **63**(5): 1148-68.
- Hornberger, M., A. M. Morcom and M. D. Rugg (2004). Neural correlates of retrieval orientation: effects of study-test similarity. *Journal of cognitive neuroscience* **16**(7): 1196-210.
- Hornberger, M., M. D. Rugg and R. N. Henson (2006a). ERP correlates of retrieval orientation: direct versus indirect memory tasks. *Brain research* **1071**(1): 124-36.
- Hornberger, M., M. D. Rugg and R. N. Henson (2006b). fMRI correlates of retrieval orientation. *Neuropsychologia* **44**(8): 1425-36.

- Hubel, D. H. and T. N. Wiesel (1959). Receptive fields of single neurones in the cat's striate cortex. *The Journal of physiology* **148**: 574-91.
- Hubel, D. H. and T. N. Wiesel (1962). Receptive fields, binocular interaction and functional architecture in the cat's visual cortex. *The Journal of physiology* **160**: 106-54.
- Ivanco, T. L. and R. J. Racine (2000). Long-term potentiation in the reciprocal corticohippocampal and corticocortical pathways in the chronically implanted, freely moving rat. *Hippocampus* **10**(2): 143-52.
- Jacobsen, L. K., J. C. Gore, P. Skudlarski, C. M. Lacadie, P. Jatlow and J. H. Krystal (2002). Impact of intravenous nicotine on BOLD signal response to photic stimulation. *Magnetic resonance imaging* **20**(2): 141-5.
- James, W. (1893). *The Stream of Consciousness*. Psychology. W. James. New York, Holt.
- Johannes, S., B. M. Wieringa, M. Matzke and T. F. Munte (1996). Hierarchical visual stimuli: electrophysiological evidence for separate left hemispheric global and local processing mechanisms in humans. *Neuroscience letters* **210**(2): 111-4.
- Kamin, L. J. (1957). The retention of an incompletely learned avoidance response. *J Comp Physiol Psychol* **50**: 457-460.
- Kamin, L. J. (1963). The retention of an incompletely learned avoidance response: some further analyses. *J Comp Physiol Psychol* **56**: 719-722.
- Kang, H. C., E. D. Burgund, H. M. Lugar, S. E. Petersen and B. L. Schlaggar (2003). Comparison of functional activation foci in children and adults using a common stereotactic space. *Neuroimage* **19**(1): 16-28.
- Kanwisher, N., J. McDermott and M. M. Chun (1997). The fusiform face area: a module in human extrastriate cortex specialized for face perception. *J Neurosci* **17**(11): 4302-11.
- Kerr, K. M., K. L. Agster, S. C. Furtak and R. D. Burwell (2007). Functional neuroanatomy of the parahippocampal region: The lateral and medial entorhinal areas. *Hippocampus*.
- Kida, S., S. A. Josselyn, S. P. de Ortiz, J. H. Kogan, I. Chevere, S. Masushige and A. J. Silva (2002). CREB required for the stability of new and reactivated fear memories. *Nature neuroscience* **5**(4): 348-55.

- Knierim, J. J. and D. C. van Essen (1992a). Neuronal responses to static texture patterns in area V1 of the alert macaque monkey. *Journal of neurophysiology* **67**(4): 961-80.
- Knierim, J. J. and D. C. Van Essen (1992b). Visual cortex: cartography, connectivity, and concurrent processing. *Current opinion in neurobiology* **2**(2): 150-5.
- Krainik, A., M. Hund-Georgiadis, S. Zysset and D. Y. von Cramon (2005). Regional impairment of cerebrovascular reactivity and BOLD signal in adults after stroke. *Stroke; a journal of cerebral circulation* **36**(6): 1146-52.
- Kriegeskorte, N., R. Goebel and P. Bandettini (2006). Information-based functional brain mapping. *Proceedings of the National Academy of Sciences of the United States of America* **103**(10): 3863-8.
- Kumaran, D. and E. A. Maguire (2007). Which computational mechanisms operate in the hippocampus during novelty detection? *Hippocampus*.
- Lasota, K. J., J. L. Ulmer, J. B. Firszt, B. B. Biswal, D. L. Daniels and R. W. Prost (2003). Intensity-dependent activation of the primary auditory cortex in functional magnetic resonance imaging. *Journal of computer assisted tomography* **27**(2): 213-8.
- Laurienti, P. J., A. S. Field, J. H. Burdette, J. A. Maldjian, Y. F. Yen and D. M. Moody (2002). Dietary caffeine consumption modulates fMRI measures. *Neuroimage* **17**(2): 751-7.
- Lavenex, P. and D. G. Amaral (2000). Hippocampal-neocortical interaction: a hierarchy of associativity. *Hippocampus* **10**(4): 420-30.
- Lerner, Y., T. Hendler, D. Ben-Bashat, M. Harel and R. Malach (2001). A hierarchical axis of object processing stages in the human visual cortex. *Cereb Cortex* **11**(4): 287-97.
- Liu, T. T., Y. Behzadi, K. Restom, K. Uludag, K. Lu, G. T. Buracas, D. J. Dubowitz and R. B. Buxton (2004). Caffeine alters the temporal dynamics of the visual BOLD response. *Neuroimage* **23**(4): 1402-13.
- Livingstone, M. S. and D. H. Hubel (1984a). Anatomy and physiology of a color system in the primate visual cortex. *J Neurosci* **4**(1): 309-56.
- Livingstone, M. S. and D. H. Hubel (1984b). Specificity of intrinsic connections in primate primary visual cortex. *J Neurosci* **4**(11): 2830-5.

- Lockhart, R. S. (2002). Levels of processing, transfer-appropriate processing, and the concept of robust encoding. *Memory (Hove, England)* **10**(5-6): 397-403.
- Logothetis, N. K. (2002). The neural basis of the blood-oxygen-level-dependent functional magnetic resonance imaging signal. *Philosophical transactions of the Royal Society of London* **357**(1424): 1003-37.
- Logothetis, N. K. (2003). The underpinnings of the BOLD functional magnetic resonance imaging signal. *J Neurosci* **23**(10): 3963-71.
- Logothetis, N. K., J. Pauls, M. Augath, T. Trinath and A. Oeltermann (2001). Neurophysiological investigation of the basis of the fMRI signal. *Nature* **412**(6843): 150-7.
- Logothetis, N. K. and J. Pfeuffer (2004). On the nature of the BOLD fMRI contrast mechanism. *Magnetic resonance imaging* **22**(10): 1517-31.
- Logothetis, N. K. and B. A. Wandell (2004). Interpreting the BOLD signal. *Annual review of physiology* **66**: 735-69.
- London, M. and M. Hausser (2005). Dendritic computation. *Annual review of neuroscience* **28**: 503-32.
- Maier, N., V. Nimmrich and A. Draguhn (2003). Cellular and network mechanisms underlying spontaneous sharp wave-ripple complexes in mouse hippocampal slices. *The Journal of physiology* **550**(Pt 3): 873-87.
- Mallot, H. A. and F. Giannakopoulos (1996). Population networks: a large-scale framework for modelling cortical neural networks. *Biological cybernetics* **75**(6): 441-52.
- Martin, E., P. Joeri, T. Loenneker, D. Ekatodramis, D. Vitacco, J. Hennig and V. L. Marcar (1999). Visual processing in infants and children studied using functional MRI. *Pediatric research* **46**(2): 135-40.
- McClelland, J. L., B. L. McNaughton and R. C. O'Reilly (1995). Why there are complementary learning systems in the hippocampus and neocortex: insights from the successes and failures of connectionist models of learning and memory. *Psychological review* **102**(3): 419-57.
- McGaugh, J. L. (2000). Memory--a century of consolidation. *Science (New York, N.Y)* **287**(5451): 248-51.

- McNaughton, N. and J. Wickens (2003). Hebb, pandemonium and catastrophic hypermnesia: the hippocampus as a suppressor of inappropriate associations. *Cortex; a journal devoted to the study of the nervous system and behavior* **39**(4-5): 1139-63.
- Messenger, J. B. (1971). Two-stage recovery of a response in Sepia. *Nature* **232**(5307): 202-3.
- Meunier, M., J. Bachevalier, M. Mishkin and E. A. Murray (1993). Effects on visual recognition of combined and separate ablations of the entorhinal and perirhinal cortex in rhesus monkeys. *J Neurosci* **13**(12): 5418-32.
- Miyashita, Y., M. Morita, Y. Naya, M. Yoshida and H. Tomita (1998). Backward signal from medial temporal lobe in neural circuit reorganization of primate inferotemporal cortex. *Comptes rendus de l'Academie des sciences* **321**(2-3): 185-92.
- Montaldi, D., T. J. Spencer, N. Roberts and A. R. Mayes (2006). The neural system that mediates familiarity memory. *Hippocampus* **16**(5): 504-20.
- Moscovitch, M., L. Nadel, G. Winocur, A. Gilboa and R. S. Rosenbaum (2006). The cognitive neuroscience of remote episodic, semantic and spatial memory. *Current opinion in neurobiology* **16**(2): 179-90.
- Moser, M. B. and E. I. Moser (1998). Functional differentiation in the hippocampus. *Hippocampus* **8**(6): 608-19.
- Mulligan, N. W. and J. P. Lozito (2006). An asymmetry between memory encoding and retrieval. Revelation, generation, and transfer-appropriate processing. *Psychol Sci* **17**(1): 7-11.
- Nadel, L. and C. Land (2000). Memory traces revisited. *Nature reviews* **1**(3): 209-12.
- Nadel, L., A. Samsonovich, L. Ryan and M. Moscovitch (2000). Multiple trace theory of human memory: computational, neuroimaging, and neuropsychological results. *Hippocampus* **10**(4): 352-68.
- Naveh-Benjamin, M., A. Kilb and T. Fisher (2006). Concurrent task effects on memory encoding and retrieval: further support for an asymmetry. *Memory & cognition* **34**(1): 90-101.
- Naya, Y., M. Yoshida and Y. Miyashita (2003a). Forward processing of long-term associative memory in monkey inferotemporal cortex. *J Neurosci* **23**(7): 2861-71.

- Naya, Y., M. Yoshida, M. Takeda, R. Fujimichi and Y. Miyashita (2003b). Delay-period activities in two subdivisions of monkey inferotemporal cortex during pair association memory task. *The European journal of neuroscience* **18**(10): 2915-8.
- Nobre, A. C., G. N. Sebestyen, D. R. Gitelman, M. M. Mesulam, R. S. Frackowiak and C. D. Frith (1997). Functional localization of the system for visuospatial attention using positron emission tomography. *Brain* **120** (Pt 3): 515-33.
- Ogawa, S., T. M. Lee, A. R. Kay and D. W. Tank (1990). Brain magnetic resonance imaging with contrast dependent on blood oxygenation. *Proceedings of the National Academy of Sciences of the United States of America* **87**(24): 9868-72.
- Oldfield, R. C. (1971). The assessment and analysis of handedness: the Edinburgh inventory. *Neuropsychologia* **9**(1): 97-113.
- Orban, G. A. and R. Vogels (1998). The neuronal machinery involved in successive orientation discrimination. *Progress in neurobiology* **55**(2): 117-47.
- Pammer, K., R. Lavis and P. Cornelissen (2004). Visual encoding mechanisms and their relationship to text presentation preference. *Dyslexia (Chichester, England)* **10**(2): 77-94.
- Polat, U. and A. M. Norcia (1998). Elongated physiological summation pools in the human visual cortex. *Vision research* **38**(23): 3735-41.
- Poldrack, R. A. (2000). Imaging brain plasticity: conceptual and methodological issues--a theoretical review. *Neuroimage* **12**(1): 1-13.
- Preston, A. R. and J. D. Gabrieli (2002). Different functions for different medial temporal lobe structures? *Learning & memory (Cold Spring Harbor, N.Y)* **9**(5): 215-7.
- Qiu, F. T. and R. von der Heydt (2005). Figure and ground in the visual cortex: v2 combines stereoscopic cues with gestalt rules. *Neuron* **47**(1): 155-66.
- Raichle, M. E. (1998). Behind the scenes of functional brain imaging: a historical and physiological perspective. *Proceedings of the National Academy of Sciences of the United States of America* **95**(3): 765-72.
- Ranganath, C., M. K. Johnson and M. D'Esposito (2003). Prefrontal activity associated with working memory and episodic long-term memory. *Neuropsychologia* **41**(3): 378-89.

- Rao, R. P. (2005). Bayesian inference and attentional modulation in the visual cortex. *Neuroreport* **16**(16): 1843-8.
- Robb, W. G. and M. D. Rugg (2002). Electrophysiological dissociation of retrieval orientation and retrieval effort. *Psychonomic bulletin & review* **9**(3): 583-9.
- Rolls, E. T. (2000). Memory systems in the brain. *Annual review of psychology* **51**: 599-630.
- Rosen, B. R., R. L. Buckner and A. M. Dale (1998). Event-related functional MRI: past, present, and future. *Proceedings of the National Academy of Sciences of the United States of America* **95**(3): 773-80.
- Ross, R. S. and H. Eichenbaum (2006). Dynamics of hippocampal and cortical activation during consolidation of a nonspatial memory. *J Neurosci* **26**(18): 4852-9.
- Rossion, B., C. Schiltz and M. Crommelinck (2003). The functionally defined right occipital and fusiform "face areas" discriminate novel from visually familiar faces. *Neuroimage* **19**(3): 877-83.
- Rubin, D. C., S. Hinton and A. Wenzel (1999). The precise time course of retention. *J Exp Psychol Learn Mem Cogn* **25**(5): 1161-1176.
- Rudy, J. W. and P. Matus-Amat (2005). The ventral hippocampus supports a memory representation of context and contextual fear conditioning: implications for a unitary function of the hippocampus. *Behav Neurosci* **119**(1): 154-63.
- Rudy, J. W. and P. Morledge (1994). Ontogeny of contextual fear conditioning in rats: implications for consolidation, infantile amnesia, and hippocampal system function. *Behav Neurosci* **108**: 227-234.
- Rugg, M. D. and E. L. Wilding (2000). Retrieval processing and episodic memory. *Trends Cogn Sci* **4**(3): 108-115.
- Saad, Z. S., K. M. Ropella, E. A. DeYoe and P. A. Bandettini (2003). The spatial extent of the BOLD response. *Neuroimage* **19**(1): 132-44.
- Sakai, K. and Y. Miyashita (1991). Neural organization for the long-term memory of paired associates. *Nature* **354**(6349): 152-5.
- Salmond, C. H., J. Ashburner, F. Vargha-Khadem, A. Connelly, D. G. Gadian and K. J. Friston (2002). Distributional assumptions in voxel-based morphometry. *Neuroimage* **17**(2): 1027-30.

- Sanders, G. D. and J. J. Barlow (1971). Variations in retention performance during long term memory formation. *Nature* **232**(5307): 203-4.
- Save, E., L. Nerad and B. Poucet (2000). Contribution of multiple sensory information to place field stability in hippocampal place cells. *Hippocampus* **10**(1): 64-76.
- Save, E. and B. Poucet (2000a). Hippocampal-parietal cortical interactions in spatial cognition. *Hippocampus* **10**(4): 491-9.
- Save, E. and B. Poucet (2000b). Involvement of the hippocampus and associative parietal cortex in the use of proximal and distal landmarks for navigation. *Behavioural brain research* **109**(2): 195-206.
- Savoy, R. L. (2005). Experimental design in brain activation MRI: cautionary tales. *Brain research bulletin* **67**(5): 361-7.
- Schacter, D. L., R. L. Buckner, W. Koutstaal, A. M. Dale and B. R. Rosen (1997). Late onset of anterior prefrontal activity during true and false recognition: an event-related fMRI study. *Neuroimage* **6**(4): 259-69.
- Schacter, D. L. and E. Tulving (1994). What are the memory systems of 1994? *Memory Systems 1994*. D. L. Schacter and E. Tulving. Cambridge, MIT Press: 1-38.
- Scouten, A., X. Papademetris and R. T. Constable (2006). Spatial resolution, signal-to-noise ratio, and smoothing in multi-subject functional MRI studies. *Neuroimage* **30**(3): 787-93.
- Segev, I. (2006). What do dendrites and their synapses tell the neuron? *Journal of neurophysiology* **95**(3): 1295-7.
- Shannon, C. E. (1948). A mathematical theory of communication. *Bell Sys Tech J* **27**: 379-423, 623-656.
- Shepherd, G. M. (1996). The dendritic spine: a multifunctional integrative unit. *Journal of neurophysiology* **75**(6): 2197-210.
- Shepherd, G. M. and R. K. Brayton (1987). Logic operations are properties of computer-simulated interactions between excitable dendritic spines. *Neuroscience* **21**(1): 151-65.
- Siapas, A. G. and M. A. Wilson (1998). Coordinated interactions between hippocampal ripples and cortical spindles during slow-wave sleep. *Neuron* **21**(5): 1123-8.

- Squire, L. R. and P. Alvarez (1995). Retrograde amnesia and memory consolidation: a neurobiological perspective. *Current opinion in neurobiology* **5**(2): 169-77.
- Stenberg, G., M. Johansson and I. Rosen (2006). Conceptual and perceptual memory: retrieval orientations reflected in event-related potentials. *Acta psychologica* **122**(2): 174-205.
- Stickgold, R., L. Scott, C. Rittenhouse and J. A. Hobson (1999). Sleep-induced changes in associative memory. *Journal of cognitive neuroscience* **11**(2): 182-93.
- Summerfield, C., M. Greene, T. Wager, T. Egner, J. Hirsch and J. Mangels (2006). Neocortical connectivity during episodic memory formation. *PLoS biology* **4**(5): e128.
- Talairach, J. and P. Tournoux (1988). *Co-planar Stereotaxic Atlas of the Human Brain*. New York, Thieme.
- Tanaka, S., M. Honda and N. Sadato (2005). Modality-specific cognitive function of medial and lateral human Brodmann area 6. *J Neurosci* **25**(2): 496-501.
- Tassoni, G., C. A. Lorenzini, E. Baldi, B. Sacchetti and C. Bucherelli (1999). A peculiar pattern of temporal involvement of rat perirhinal cortex in memory processing. *Behav Neurosci* **113**(6): 1161-9.
- Treves, A. and E. T. Rolls (1994). Computational analysis of the role of the hippocampus in memory. *Hippocampus* **4**(3): 374-91.
- Tse, D., R. F. Langston, M. Kakeyama, I. Bethus, P. A. Spooner, E. R. Wood, M. P. Witter and R. G. Morris (2007). Schemas and memory consolidation. *Science (New York, N.Y)* **316**(5821): 76-82.
- Tulving, E. (1983). *Elements of Episodic Memory*. Oxford, Clarendon Press.
- Uncapher, M. R. and M. D. Rugg (2005a). Effects of divided attention on fMRI correlates of memory encoding. *Journal of cognitive neuroscience* **17**(12): 1923-35.
- Uncapher, M. R. and M. D. Rugg (2005b). Encoding and the durability of episodic memory: a functional magnetic resonance imaging study. *J Neurosci* **25**(31): 7260-7.

- Ungerleider, L. G. and M. Mishkin (1982). Two cortical visual systems. *Analysis of Visual Behavior*. D. J. Ingle, M. A. Goodale and R. J. W. Mansfield. Cambridge, MA, MIT Press: 549-586.
- Vaidya, C. J., M. Zhao, J. E. Desmond and J. D. Gabrieli (2002). Evidence for cortical encoding specificity in episodic memory: memory-induced re-activation of picture processing areas. *Neuropsychologia* **40**(12): 2136-43.
- Verzi, D. W. (2004). Modeling activity-dependent synapse restructuring. *Bulletin of mathematical biology* **66**(4): 745-62.
- Verzi, D. W., M. B. Rheuben and S. M. Baer (2005). Impact of time-dependent changes in spine density and spine shape on the input-output properties of a dendritic branch: a computational study. *Journal of neurophysiology* **93**(4): 2073-89.
- Walker, M. P. (2004). Issues surrounding sleep-dependent memory consolidation and plasticity. *Cell Mol Life Sci* **61**(24): 3009-15.
- Walker, M. P. and R. Stickgold (2004). Sleep-dependent learning and memory consolidation. *Neuron* **44**(1): 121-33.
- Wang, H., Y. Hu and J. Z. Tsien (2006). Molecular and systems mechanisms of memory consolidation and storage. *Progress in neurobiology* **79**(3): 123-35.
- Ward, B. D. (1998). 3dDeconvolve Reference Manual. Atlas of Functional Neuroimaging (AFNI) Suite, NIMH.
- Weis, S., P. Klaver, J. Reul, C. E. Elger and G. Fernandez (2004). Neural correlates of successful declarative memory formation and retrieval: the anatomical overlap. *Cortex; a journal devoted to the study of the nervous system and behavior* **40**(1): 200-2.
- Weldon, M. S., H. L. Roediger, 3rd and B. H. Challis (1989). The properties of retrieval cues constrain the picture superiority effect. *Memory & cognition* **17**(1): 95-105.
- Wheeler, M. E. and R. L. Buckner (2003). Functional dissociation among components of remembering: control, perceived oldness, and content. *J Neurosci* **23**(9): 3869-80.
- Wichmann, W. and W. Muller-Forell (2004). Anatomy of the visual system. *European journal of radiology* **49**(1): 8-30.
- Wickelgren, W. A. (1974). Single-trace fragility theory of memory dynamics. *Memory & cognition* **2**: 775-780.

- Winters, B. D. and T. J. Bussey (2005a). Glutamate receptors in perirhinal cortex mediate encoding, retrieval, and consolidation of object recognition memory. *J Neurosci* **25**(17): 4243-51.
- Winters, B. D. and T. J. Bussey (2005b). Removal of cholinergic input to perirhinal cortex disrupts object recognition but not spatial working memory in the rat. *The European journal of neuroscience* **21**(8): 2263-70.
- Winters, B. D. and T. J. Bussey (2005c). Transient inactivation of perirhinal cortex disrupts encoding, retrieval, and consolidation of object recognition memory. *J Neurosci* **25**(1): 52-61.
- Winters, B. D., S. E. Forwood, R. A. Cowell, L. M. Saksida and T. J. Bussey (2004). Double dissociation between the effects of peri-postrhinal cortex and hippocampal lesions on tests of object recognition and spatial memory: heterogeneity of function within the temporal lobe. *J Neurosci* **24**(26): 5901-8.
- Witter, M. P. and E. I. Moser (2006). Spatial representation and the architecture of the entorhinal cortex. *Trends in neurosciences* **29**(12): 671-8.
- Wixted, J. T. (2004). The psychology and neuroscience of forgetting. *Ann Rev Psychol* **55**: 235-269.
- Woodruff, C. C., M. R. Uncapher and M. D. Rugg (2006). Neural correlates of differential retrieval orientation: Sustained and item-related components. *Neuropsychologia* **44**(14): 3000-10.
- Woodruff, M. L. and H. M. Kantor (1983). Fornix lesions, plasma ACTH levels, and shuttle box avoidance in rats. *Behav Neurosci* **97**(6): 897-907.
- Yamaguchi, S., S. Yamagata and S. Kobayashi (2000). Cerebral asymmetry of the "top-down" allocation of attention to global and local features. *J Neurosci* **20**(9): RC72.
- Yovel, G. and N. Kanwisher (2005). The neural basis of the behavioral face-inversion effect. *Curr Biol* **15**(24): 2256-62.
- Yuste, R. and W. Denk (1995). Dendritic spines as basic functional units of neuronal integration. *Nature* **375**(6533): 682-4.
- Zador, A., C. Koch and T. H. Brown (1990). Biophysical model of a Hebbian synapse. *Proceedings of the National Academy of Sciences of the United States of America* **87**(17): 6718-22.

Zhang, F., S. Endo, L. J. Cleary, A. Eskin and J. H. Byrne (1997). Role of transforming growth factor-beta in long-term synaptic facilitation in *Aplysia*. *Science (New York, N.Y)* **275**(5304): 1318-20.

Zola-Morgan, S., L. R. Squire, D. G. Amaral and W. A. Suzuki (1989). Lesions of perirhinal and parahippocampal cortex that spare the amygdala and hippocampal formation produce severe memory impairment. *J Neurosci* **9**(12): 4355-70.

MICHIGAN STATE UNIVERSITY LIBRARIES



3 1293 02956 9492